UNIVERSITÉ LOUIS PASTEUR STRASBOURG

Discipline: Physique

Corrélations des polymères linéaires en volume et aux interfaces

Philippe Beckrich

Thèse soutenue le 19 Septembre 2006

Membres du Jury :

Président :	**J.-F. Joanny**
Rapporteur préalable :	**M. Daoud**
Rapporteur interne :	**N. Rivier**
Examinateur :	**F. Boué**
Examinateur :	**A. E. Likhtman**
Invité :	**I. Ya. Yerukhimovich**
Directeurs de thèse :	**A. Johner et A. N. Semenov**

Correlation Properties of Linear Polymers in the Bulk and near Interfaces

"*Do not fear mistakes. There are none.*"
Miles Davis

Résumé

Les polymères sont des grandes molécules linéaires, ramifiées ou cycliques résultant de l'assemblage covalent ou de l'auto-assemblage d'unités élémentaires appelées monomères. On peut les trouver dans divers états: dilués en solution ou plus condensés en solution semi-diluée, en gel, en phases cristallines ou fondus. Ils comptent typiquement $N \simeq 10^4$ unités et leur extension spatiale est de l'ordre de 100Å. Il existe une grande variété de propriétés macroscopiques et de structures mésoscopiques dans les systèmes constitués de ces macromolécules. Quand les polymères sont assez longs, on observe des propriétés critiques universelles, independantes de la nature chimique de leurs monomères. Ils sont d'un intérêt majeur dans divers domaines de la science et de l'industrie notamment parce qu'ils peuvent médier des interactions sur des échelles mésoscopiques (de 10 a 100Å). On les utilise par exemple pour empêcher la coagulation ou les séparations de phases dans les suspensions de colloïdes (qui tendent à s'aggréger sous l'effet des forces de Van der Waals). La portée des forces effectives que peuvent induire les polymères est la longueur de corrélation ξ (qui définit le blob de concentration). Dans les solutions diluées, les corrélations sont essentiellement intramoléculaires, le long d'une macromolécule. Dans ce cas, ξ est de l'ordre du rayon de giration R_{g}. Dans le régime semi-dilué, atteint quand la concentration moyenne en monomères c_0 devient supérieur à $c^* = N/R\mathrm{g}^d \simeq N^{1-d\nu}b^{-d}$, où d est la dimension de l'espace et ν est l'exposant de Flory, les chaînes se recouvrent et ξ devient indépendant du degré de polymerisation N. La longueur de corrélation décroît alors avec c_0 comme la loi de puissance $\xi \sim c_0^{-\nu/(d\nu-1)}(\sim c_0^{-3/4}$ à trois dimensions). Dans les systèmes très denses, puisque les fluctuations sont faibles, l'approximation du champs moyen s'applique et ξ devient alors la longueur de corrélation d'Edwards, donnée par la relation $\xi^2 = b^2/(12c_0v)$, où b est le segment statistique et v est le volume exclu (l'inverse de la compressibilité du système). Quand ξ decroît au point de devenir microscopique, dans les solutions très concentrées, le rôle de la connectivité des maillons

tend à disparaître: le système peut alors être vu comme un liquide ordinaire de particules de taille $\xi \simeq b$. Ceci est en accord avec l'hypothèse connue sous le nom de théorème de Flory, qui sous-entend que les interactions entre monomères sont complètement écrantées, donc que les corrélations sont très localisées.

Cependant, dans les fondus de longues macromolécules *linéaires*, il reste en fait une corrélation de l'ordre de la taille du polymère , c'est à dire bien au-delà de l'échelle microscopique ξ. Son origine et certains de ses effets sont décrits dans la suite.

Corrélations intramoléculaires

Dans une première partie, on dérive principalement des corrélations intramoléculaires dans les systèmes denses. En utilisant l'approximation Gaussienne, Edwards a montré que dans les solutions concentrées de polymères, les interactions stériques sont écrantées. Il en a déduit une interaction effective entre les monomères. Cette interaction est de l'ordre de $v_{\text{eff}} \simeq v/N$, et depend explicitement de la distribution de masse du système. On a donc effectué des calculs, soit dans la limite des chaînes infinies, soit sous la distribution exponentielle de Flory (de manière à dériver des effets de tailles). La probabilité pour qu'une chaîne soit constituée de N monomères est sous cette distribution

$$P^{(0)}(N) = \mu e^{-\mu N}$$

où μ est le potentiel chimique qui fixe la longueur moyenne des polymères $\langle N \rangle = 1/\mu$. Dans les systèmes denses de concentration moyenne en monomère c_0, les fluctuations sont faibles tant que le paramètre de Ginzburg est assez petit, $G_{\text{z}} = v/(c_0\, b^6) \ll 1$. Dans ce cas, le champs moyen s'applique. De plus le paramètre d'interaction de Fixman dans ce cas précis varie comme $u_{\text{eff}} \sim N^{-1/2}$, il est donc faible pour les chaînes assez longues et peut être traité perturbativement. On évalue dès lors des propriétés intramoléculaires en appliquant la théorie des perturbations, qui donne, au premier ordre, la valeur moyenne d'une quantité physique A perturbée en fonction de moyennes evaluées sur la statistique non-perturbée. Cela s'écrit de manière générale

$$\delta\langle A \rangle \equiv \langle A \rangle - \langle A \rangle_0 \simeq \langle U \rangle_0 \langle A \rangle_0 - \langle UA \rangle_0,$$

où l'indice 0 désigne la statistique non-perturbée.

Corrélations d'orientation le long d'une chaîne d'un fondu

Pour caractériser la persistance de l'orientation le long d'une chaîne, on peut évaluer la corrélation de deux vecteurs tangentiels situés aux abscisses curvilignes n et m avec le premier polynôme de Legendre qui s'écrit

$$P_1(m-n) = \langle \hat{\mathbf{l}}_n \cdot \hat{\mathbf{l}}_m \rangle \quad \text{avec} \quad \hat{\mathbf{l}}_n = \frac{\mathbf{l}_n}{|\mathbf{l}_n|}.$$

Les différents modèles de chaîne isolée prédisent une décroissance exponentielle de cette grandeur avec la distance curviligne entre deux points de la chaîne. La distance de coupure de ces corrélations est la longueur de persistance l_p definie, pour $|m-n|$ assez grand, par $P_1(m-n) \simeq \exp(-|m-n|/l_\mathrm{p})$. Cet important concept de la physique des polymères caractérise la rigidité d'une chaîne. On s'attend notamment à ce qu'une chaîne, dans n'importe quel système de polymères, soit caractérisée par une longueur de persistance. On montre ici que ce n'est pas toujours évident: dans les fondus de longues chaînes flexibles, où les interactions sont écrantées, les corrélations angulaires sont *a priori* négligeables au delà de la longueur de corrélation $\xi = (b^2/(12 c_0\, v))^{1/2}$. Nous avons évalué alors la corrélation entre deux maillons fluctuants d'une chaîne Gaussienne infinie (qui est proportionnelle au premier polynôme de Legendre dans ce cas) perturbée par l'interaction écrantée en calculant

$$P(s) = P(|n-m|) = \frac{1}{b^2} \langle \frac{\partial}{\partial n}\mathbf{r}_n \cdot \frac{\partial}{\partial m}\mathbf{r}_m \rangle = -\frac{1}{2\,b^2}\frac{\partial}{\partial n}\frac{\partial}{\partial m}\langle r^2_{nm}\rangle.$$

Qualitativement, le traitement perturbatif de la longueur d'un segment plus grand qu'un blob, constitué de s unités peut s'écrire $R^2(s) = sb^2(1 - cste\, u_\mathrm{eff})$, ce qui nous conduit a une décroissance en loi de puissance de la corrélation angulaire de la forme $P(s) \sim s^{-3/2}$. Pour un segment plus petit qu'un blob, la perturbation donnerait la longueur du segment de la forme $R^2(s) = sb^2(1 + cste'\, u)$, où $u \sim s^{1/2}$ est désormais le paramètre de Fixman de l'interaction stérique non écrantée. La corrélation angulaire suivrait alors la forme $P(s) = s^{-1/2}$ dans le blob ($s \ll g \equiv$ nombre de monomères dans un blob $= 6\,\xi^2/b^2$). Quantitativement, cette perturbation donne l'expression

$$P(X) = \frac{\sqrt{6}}{2\pi^2 c_0\, b^3}\,\frac{1}{g^{3/2}}\left(\sqrt{\frac{\pi}{X}} - \pi e^X \mathrm{Erfc}(\sqrt{X})\right),$$

avec $g = \xi^2/a^2 = 6\xi^2/b^2$, le nombre de monomères dans un blob de concentration, le paramètre réduit $X = s/g$ et Erfc, la fonction erreur complémentaire.

On retrouve les deux régimes asymptotiques annoncés auparavant puisque

$$P(X) \underset{X\ll 1}{\simeq} \frac{\sqrt{6}}{2\pi^{3/2} c_0\, b^3}\,\frac{1}{g^{3/2}}\,\frac{1}{\sqrt{X}} \qquad \text{dans le blob}$$

$$P(X) \underset{X\gg 1}{\simeq} \frac{\sqrt{6}}{4\pi^{3/2} c_0\, b^3}\,\frac{1}{g^{3/2}}\,\frac{1}{X^{3/2}} \qquad \text{au delà du blob.}$$

Cette décroissance algébrique souligne la difficulté à définir une longueur de persistance dans un fondu. D'autre part, on observe une bonne adéquation entre ces prévisions théoriques et les résutats des simulations Monte-Carlo de J.P. Wittmer dans toutes la gamme de $X = s/g$ accessible. Il émerge également de ce calcul un effet d'orientation de longue portée[1] associé au premier polynôme de Legendre.

Perturbation de la distribution de Flory dans un fondu

Dans cette partie nous évaluons la perturbation induite par le potentiel effectif d'Edwards sur la distribution de masse de Flory. En effet, dans le cadre du champs moyen, pour un système sans interactions, la probabilité qu'une molécule soit un N-mère est

$$P^{(0)}(N) = Z_N^{(0)} \mu e^{-\mu N} = \mu e^{-\mu N}.$$

Les moments de la distribution s'écrivent alors $\langle N^p \rangle^{(0)} = p!/\mu^p = p! \langle N \rangle^{(0)p}$. En considérant désormais les interactions écrantées, la fonction de partition perturbée s'écrit au premier ordre

$$Z_N = \langle e^{-U_{\text{eff}}} \rangle_N \simeq 1 - \langle U_{\text{eff}} \rangle_N$$

où U_{eff} est le volume exclu effectif sommé sur toutes les paires de monomères de la chaîne. Cette expression nous permet de statuer qualitativement une dépendance avec la taille en $N^{-1/2}$ puisque $U_{\text{eff}} \simeq u_{\text{eff}}$. Pour cette distribution précise, le volume exclu effectif devient, dans la limite $\xi \ll R_{\text{g}}$

$$v_{\text{eff}} = \frac{v\xi^2}{1 + q^2\xi^2}(q^2 + \frac{\mu}{a^2}).$$

En ôtant la divergence ultra-violette non physique, on trouve

$$\delta Z_N = Z_N - Z_N^{(0)} = -\langle U_{\text{eff}} \rangle_N \simeq -\frac{c}{\sqrt{N}}\{1 - 2\mu N\} \qquad \text{avec} \qquad c = \frac{1}{8\pi^{3/2}\, c_0\, a^3}\,.$$

[1] De l'ordre de la taille R_{g} pour une chaîne finie.

Il faut d'abord noter que le coefficient c ne dépend pas du volume exclu. Le premier terme suit la loi d'échelle attendue. Le second aussi, mais il mérite plus d'attention: en effet, il n'est plus perturbatif pour $N > \langle N \rangle^2$. Pour mieux comprendre l'origine de ce terme, considérons une chaîne de taille N plongée dans un fondu de polymères identique de taille $\langle N \rangle$. Le paramètre d'interaction pour cette chaîne est de l'ordre de $u \sim N^{1/2}/\langle N \rangle$. On voit bien que la chaîne gonfle si $N > \langle N \rangle^2$. C'est très peu probable dans notre cas puisque notre distribution est coupée exponentiellement par la taille moyenne. Dès lors on peut considérer la distribution de Flory corrigée

$$P(N) \simeq \left(1 - \frac{c}{\sqrt{N}}\{1 - 2\mu N\}\right) \mu e^{-\mu N},$$

et mesurer la manière dont les moments dévient des valeurs de la distribution idéale en évaluant

$$\begin{aligned} \beta_p &= 1 - \frac{\langle N^p \rangle}{p! \langle N \rangle^p} \\ &\simeq \frac{c}{p!} \left(\Gamma(p + 1/2) + p\sqrt{\pi}\Gamma(p+1) - 2\Gamma(p+3/2)\right) \sqrt{\mu} = c\, w_p \sqrt{\mu} \\ &\text{avec} \qquad w_1 = 0, \qquad w_2 = \frac{\sqrt{\pi}}{2}, \qquad w_3 = \frac{9\sqrt{\pi}}{8} \qquad etc... \end{aligned}$$

Là encore, cette expression correspond bien aux mesures effectuées par J. P. Wittmer dans ses simulations de polymères vivants.

Facteur de forme: écart systématique à la formule de Debye.

Le théorème de Flory, qui fait autorité en physique des polymères, prédit la statistique Gaussienne pour une chaîne dans un fondu. Cette affirmation sous-entend l'écrantage total des interactions de volume exclu. Une preuve expérimentale consisterait à mettre en évidence le plateau caractéristique du comportement asymptotique de la formule de Debye, en traçant le facteur de forme en représentation de Kratky ($q^2 F(q)$ en fonction de q). Ce plateau a fait l'objet de nombreuses recherches. Néanmoins il n'a jamais vraiment été montré expérimentalement. Nous montrons dans cette partie que pour des raisons fondamentales, ce plateau ne peut jamais être observé.

Dans cette partie, nous perturbons au premier ordre la fonction de corrélations Gaussienne de deux points séparés par $|i - j|$ unités $G_{|i-j|}(q)$,

avec le potentiel effectif associé à la distribution de Flory. Puis on évalue la correction au facteur de forme qui dans ce système polydisperse s'écrit

$$\begin{aligned}\delta F(q) &= \sum_{N=0}^{\infty} \mu^2 e^{-\mu N} \sum_{i,j=1}^{N} \delta\langle \exp(-i\mathbf{q}\cdot\mathbf{r}_{i,j})\rangle \\ &= \sum_{N=0}^{\infty} \mu^2 e^{-\mu N} \sum_{i,j=1}^{N} \delta G_{|i-j|}(q).\end{aligned}$$

On trouve alors une correction non-monotone comme le montre les figures suivantes. Aux petits vecteurs d'onde, cette correction devient

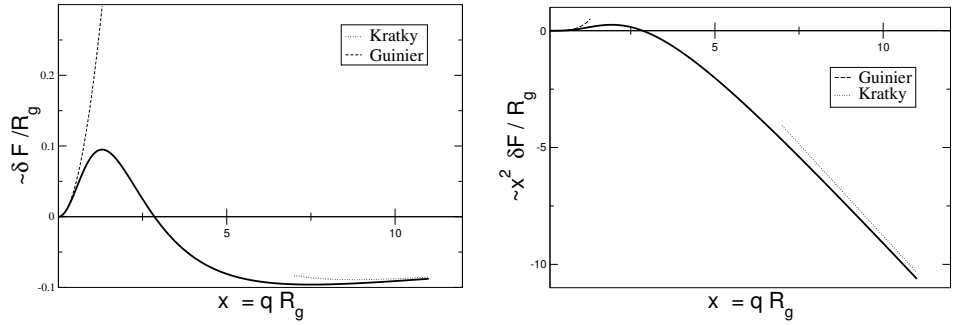

Figure 1: Représentation directe et représentation de Kratky de la correction non-monotone au facteur de forme. Le crossover se situe environ à $qR_{\mathrm{g}}^{(0)} \simeq 5$. On identifie une décroissance linéaire aux grands vecteurs d'onde dans la seconde représentation.

$$\delta F(q) \underset{\frac{qa}{\sqrt{\mu}}\ll 1}{\simeq} \frac{11 R_{\mathrm{g}}^{(0)}}{4\sqrt{3}\pi c_0\, b^{*4}} q^2 R_{\mathrm{g}}^{(0)\,2},$$

avec b^* le segment statistique renormalisé. Elle met en évidence un facteur de gonflement, puisque le rayon de giration s'écrit

$$R_{\mathrm{g}}^2 = R_{\mathrm{g}}^{(0)2} \frac{b^{*2}}{b^2}\left(1 - \frac{11\sqrt{6}}{16\pi c_0\, b^{*3}}\sqrt{\mu}\right).$$

Dans le régime intermédiaire $R_{\mathrm{g}}^{-1} \ll q \ll \xi^{-1}$, la correction s'écrit

$$\delta F(q) \underset{qR_{\mathrm{g}}\gg 1}{\simeq} \frac{12}{q^2 b^{*2}}\left(\frac{3\sqrt{6}}{\pi c_0\, b^{*3}}\sqrt{\mu} - \frac{3q}{8c_0\, b^{*2}}\right).$$

Dans ces deux régimes asymptotiques, les dépendances en taille suivent la loi d'échelle attendue par le traitement perturbatif en $\langle N\rangle^{-1/2}$. Cependant un terme supplémentaire émerge dans le régime intermédiaire qui permet d'écrire le facteur de forme d'une chaîne infinie sous la forme parlante

$$\frac{1}{F(q)} = \frac{q^2 b^{*2}}{12} + \frac{1}{32}\frac{q^3}{c_0} \qquad \text{pour} \quad q\xi \ll 1.$$

Ce terme correctif ne dépend ni du paramètre de volume exclu, ni du segment statistique. Il n'est donc pas spécifique aux systèmes très denses et devrait également apparaître dans le régime semi-dilué. En fait, un terme similaire a été dérivé à l'aide du groupe de renormalisation par L. Schäfer. Ce terme empêche évidemment l'apparition du plateau de Kratky dans une mesure de facteur de forme. Cette correction est en fait un terme d'anticorrélation qui décroît en r^{-2} dans la fonction de corrélation de paire intramoléculaire exprimée dans l'espace direct. On montre par des arguments d'échelle qu'il provient d'interactions résiduelles entre blobs de concentration: en effet, en raisonnant sur la fonction $G(r,s)$, qui mesure la corrélation entre deux points separés par s monomères et sa transformée de Fourier $G_s(q)$, dans un système de chaînes infinies ($N \to \infty$, $\mu \to 0$), le facteur de forme peut s'écrire

$$F(q) = 2\int ds\, G_s(q).$$

En considérant les conformations pour lesquelles la distance $r \ll \sqrt{s}b^*$, un fragment de s monomères d'une chaîne peut être vu comme un collier de blob de taille r contenant $g \sim r^2/b^{*2}$ monomères. La correction à la fonction de corrélation δG est essentiellement due aux interactions directes des blobs qui se recouvrent (ceux aux extrémités du fragment). Le nombre de contacts binaires est alors de l'ordre de g^2/r^3, alors que l'interaction de paire est de l'ordre de $1/gc_0$ menant à un excès d'énergie $U \sim g/c_0\, r^3 \sim 1/rb^{*2}c_0$. Dès lors, pour $\xi \ll r \ll \sqrt{s}\, b^*$,

$$\begin{aligned} G(r,s) &\simeq G^{(0)}(r,s)\,(1-U) \\ &\simeq G^{(0)}(r,s)\left(1 - \frac{const}{rb^{*2}c_0}\right), \end{aligned}$$

Dans l'espace réciproque on obtient alors pour $q \gg \frac{1}{\sqrt{s}b}$

$$\delta G_s(q) = -const\left(\frac{6}{4\pi b^{*2}s}\right)^{\frac{3}{2}} \frac{4\pi}{q^2 b^{*2}c_0}.$$

Comme ce régime est limité par la condition $q \gg \frac{1}{\sqrt{s}b}$, on introduit un cut-off inférieur $s_{\rm cut} \sim 1/(q^2 b^2)$. On en déduit la correction

$$\delta F(q) = -\frac{const}{c_0\, b^{*4}}\,\frac{1}{q}$$

qui correspond à notre terme en q^3 dans $F(q)^{-1}$. Dans cette partie aussi, les résultats numériques et les prévisions analytiques coïncident.

Influence des fluctuations sur des propriétés collectives

Origine des corrélations de longue portée

Dans cette dernière partie, nous traitons des propriétés collectives dans des fondus de polymères *linéaires*. En remarquant que le Hamiltonien de champs moyen (très local) ne générait pas les bonnes fonctions de corrélation de densité dans les systèmes de polymères linéaires sans interaction, nous avons dérivé le premier terme correctif au Hamiltonien. Ce terme répulsif s'écrit pour les polymères vivants

$$H_{\rm lr} = \frac{1}{64\pi c_0^2\, a^4}\int \frac{d\mathbf{q}}{(2\pi)^3}\,\frac{(\mu + q^2a^2)^2}{q}\,\arctan\left(\frac{qa}{2\sqrt{\mu}}\right)\delta c_q \delta c_{-q}.$$

On peut alors corriger le facteur de structure d'un fondu. On obtient

$$S(q) = \left(v + \frac{(\mu + q^2a^2)}{2c_0} + \frac{(\mu + q^2a^2)^2}{64c_0^2 q a^4}\,\frac{2}{\pi}\,\arctan\left(\frac{qa}{2\sqrt{\mu}}\right)\right)^{-1}.$$

Dans l'espace direct, les corrélations de densité deviennent alors

$$\begin{aligned}\mathcal{G}(r) =& \mathcal{G}_{\rm mf}(r) - \frac{3}{16\pi^2\, c_0^2\, v_\mu^2}\,\frac{e^{-2\frac{\sqrt{\mu}}{a}r}}{r^6}\{1 + 2\frac{\sqrt{\mu}}{a}r + \frac{11}{6}\,\frac{\mu}{a^2}r^2 + \frac{\mu^{3/2}}{a^3}r^3 + \frac{3}{8}\frac{\mu^2}{a^4}r^4\}\\ \underset{r\gg\xi}{\simeq}& -\frac{3}{16\pi^2\, c_0^2\, v_\mu^2}\,\frac{e^{-2\frac{\sqrt{\mu}}{a}r}}{r^6}\{1 + 2\frac{\sqrt{\mu}}{a}r + \frac{11}{6}\,\frac{\mu}{a^2}r^2 + \frac{\mu^{3/2}}{a^3}r^3 + \frac{3}{8}\frac{\mu^2}{a^4}r^4\} = \mathcal{G}_{\rm lr}(r).\end{aligned}$$

Dans un système de chaînes infinies ($\mu \to 0$), cette correction devient un terme en q^3 au denominateur (comme dans le facteur de forme) qui génère des corrélations de longue portée en r^{-6}. Nous montrons ensuite que cette

correction revient à retirer l'excès d'énergie libre dû aux conformations cycliques. En effet, elle peut s'écrire

$$\begin{aligned} F_{\rm lr} &\simeq \frac{1}{2}{\rm Tr}\int_0^\infty \frac{dN}{N} e^{-N(\hat{L}+\mu)} \simeq \frac{1}{2}\int d\mathbf{r}\int_0^\infty \frac{dN}{N} G_N(r,r) e^{-\mu N} \\ &= \sum_N Z_N = -F_{\rm ring} \end{aligned}$$

où Z_N est le poids statistique d'un anneau de N monomères.

Effets sur les surfaces et interfaces

Finalement, nous avons décrit certains effets de ces corrélations de longue portée. D'abord, nous avons considéré un modèle simpliste d'interface entre deux solutions denses de polymères avec des solvants différents: dans ce modèle, un monomère peut gagner ou perdre l'énergie U en changeant de solvant. En faisant de la réponse linéaire avec le facteur de structure, on trouve, en plus des variations du profil de concentration issues du champs moyen et confinées dans une fine couche d'épaisseur $\simeq \xi$, des queues algébriques dominées par z^{-3} pour des distances à l'interface vérifiant $\xi \ll z \ll R_{\rm g}$. Puis nous avons évalué la correction à la tension de surface à proximité d'un mur impénétrable. Comme l'effet majeur évalué ici est localisé à des distances bien supérieures à ξ du mur, les conditions aux limites réfléchies s'appliquent indépendamment des interactions spécifiques qui existent entre les monomères et la surface. L'énergie libre dans ce cas provient non seulement des boucles "directes" qui existent aussi en volume, mais également des nouvelles conformations fermées resultant des réflexions sur le mur. Ces nouvelles boucles induisent des répulsions supplémentaires et augmentent la tension de surface (comme le montre la figure suivante). Qualitativement, pour des chaînes très longues, la répulsion entre monomères est de l'ordre de r^{-6}. L'excédent de répulsion des conformations réfléchies proviendrait des monomères contenus dans le volume $R_{\rm g}^3$ et serait donc proportionnel à $(R_{\rm g}^3)^2/R_{\rm g}^6 \sim 1$ ($k_{\rm B}T = 1$ ici). Dès lors on attend une contribution à la tension du surface qui varie avec $\langle N\rangle$ comme $-1/R_{\rm g}^2 \sim -1/\langle N\rangle$. Quantitativement, on peut écrire la contribution à la

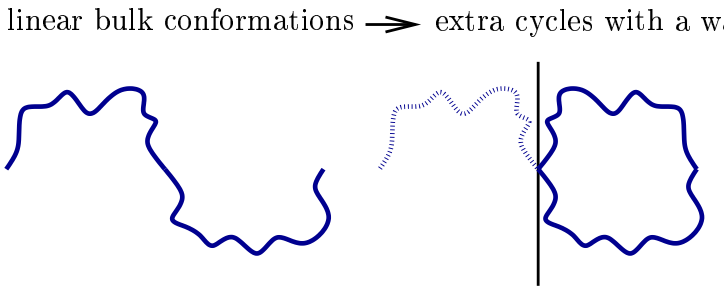

Figure 2: Les boucles qui contribuent aux effets de longue portée près d'un mur sont naturellement les conformations fermées qui existeraient également en volume, mais aussi les conformations linéaires en volume, qui une fois réfléchies donnent des cycles supplémentaires. Ces conformations réfléchies induisent des répulsions supplémentaires qui augmentent la tension de surface.

tension de surface de ces nouvelles corrélations:

$$\begin{aligned}
\gamma_{\rm lr} &\simeq \left(\frac{F_{\rm lr}}{A}\right)_{\rm wall} - \frac{1}{2}\left(\frac{F_{\rm lr}}{A}\right)_{\rm bulk} \\
&\simeq \frac{1}{2}\int_{\xi}^{\infty} dz \int_{g_0}^{\infty} \frac{dN}{N}\{G_{N,\rm wall}(r,r) - G_{N,\rm bulk}(r,r)\}e^{-N\mu} \\
&\simeq \frac{1}{2}\int_{\xi}^{\infty} dz \int_{g_0}^{\infty} \frac{dN}{N} e^{-N\mu}\left(\frac{1}{4\pi N a^2}\right)^{3/2} \exp\left(-\frac{z^2}{Na^2}\right) \\
&= \frac{cste}{g_0 a^2} - \frac{1}{32\pi a^2}\frac{1}{\langle N\rangle}\left\{\log\left(\frac{\langle N\rangle}{g_0}\right) + 1 - C\right\}
\end{aligned}$$

où $g_0 = \xi^2/a^2$ est le nombre de monomères dans un blob de concentration, utilisé ici pour ôter les divergences dues aux petits cycles, et C est la constante d'Euler ($C = \lim_{m\to\infty}\{\sum_{k=1}^{m}\frac{1}{k} - \log(m)\} \simeq 0.577216...$). Cette correction à la tension de surface de champs moyen $\gamma_{\rm mf} \sim a^2 c_0/\xi$ contient donc un terme induit par les fluctuations de l'ordre de ξ^{-2}, provenant du cut-off inférieur et une fonction croissante de la taille moyenne d'une chaîne en $-1/\langle N\rangle$ et $-(1/\langle N\rangle)\log\langle N\rangle$.

Contents

Chapter 1

Introduction

1.1 Motivations

Polymers or macromolecules are large molecules, linear branched or cyclic, resulting from the covalent binding or the self-assembly of elementary molecular units called monomers. They can be dilute in solution, or in more condensed phase as semidilute solutions, melts or crystalline phases. Typically, a macromolecule counts about $N \sim 10^4$ units. Its spatial extension is about 10^2 or 10^3Å, and the lowest length scale involved in polymer physics, known as the statistical segment, is about $b \sim 5$Å. Polymeric systems exhibit a very wide range of complex macroscopic properties and mesoscopic structures. Some of the first important physical phenomena studied were the atypical viscoelasticity properties and the low osmotic pressure of polymers in solutions, that are signatures of their large dimensions. It has extensively been shown [18, 35, 19, 25, 32] that they exhibit universal critical behaviors, when the number of monomers becomes very large, even if polymers are build up of very chemically or physically different units. Thus macromolecules are governed more by statistical averages than by microscopic (chemical) peculiarities. This observation enables then to build general theoretical tools to deal with statics and dynamics of polymers.

Macromolecules are of major interest in different domains of science and industry, because they can mediate steric interactions on mesoscopic scales (typically ~ 10Å). As a starting point, let us discuss some aspects of colloidal suspensions stability. Colloids in solutions tend to coagulate or to demix in different phases, because of Van der Waals attraction [41]. To stabilize a suspension, it is possible to tune the chemical composition of the solution to play with the width of the Stern and Gouy layers, in order to

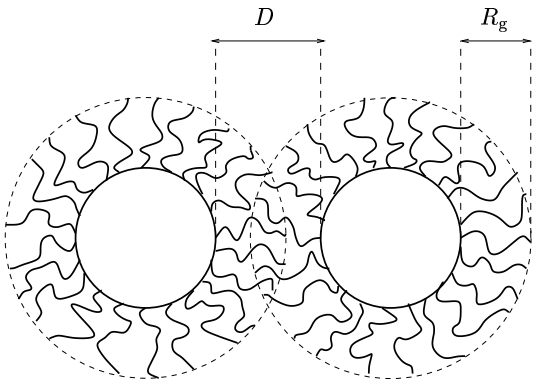

Figure 1.1: It is possible to stabilize colloidal suspensions, grafting or adsorbing polymers on their surfaces. The steric repulsion between monomers generates repulsive forces between colloids on the mesoscopic scale R_g, their spatial extension. These forces are called steric forces.

compensate attractive forces. Closer to the topic of this thesis, steric interactions can also stabilize (or destabilize, increasing the coagulation rate) colloidal suspensions [41]. For instance it is possible to graft (chemisorption) or adsorb (physisorbtion) polymers on colloid surfaces. Choosing a way to stick polymers on colloids, tuning the quality of the solvent (tuning the temperature) or the coverage (mushrooms or extended brushes) of colloids surfaces with polymers, it is possible to generate a wide range of effects. Considering a theta or a good solvent (with excluded volume $v > 0$, so that monomers tend to repel, $R_g \sim N^\nu$, where $\nu = 3/5$ is the Flory critical exponent), the coverage of polymers creates repulsive forces[1] if the distance between two colloid is $D \lesssim 2R_g \sim N^\nu$ (see Fig.1.1)[22, 41]. These ways to prevent solutions of colloids from coagulating are well-known by now, and both biopolymers and synthetic polymers are commonly used in industrial productions (paints, cosmetics, lubricants...).

Attractive polymer-mediated interactions between surfaces also exist. If polymers are grafted on an inert surface, it is possible to create attractions tuning the solvent quality under the theta-point (to induce monomer-monomer attraction). If the chains are adsorbed, even above the θ-point, a bridge may be made by a chain from one surface to another (under the condition of low coverage). Another steric attraction has been also evaluated for colloids in a solution of polymers, the so-called "depletion interaction"

[1] For a brief overview, see [41]

(see Fig.1.2) [2, 44, 33, 36, 40, 20, 21]. Supposing repulsion between units

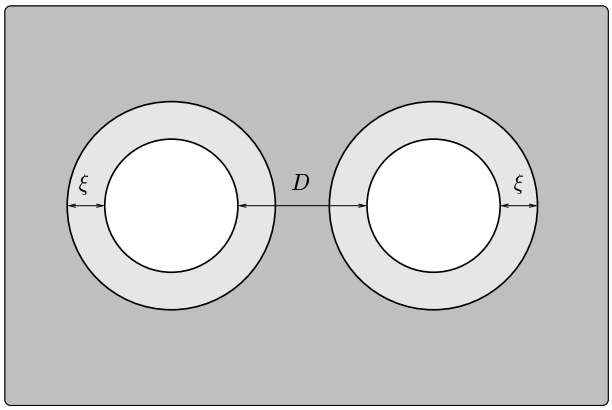

Figure 1.2: Two colloids in a solution of polymers. The shades of grey are qualitatively related to local concentration, they illustrate the depletion layer of width ξ (the correlation length), the impenetrable colloids, and the mean background with monomer density c_0. These two colloids interact *via* attractive forces induced by polymers if the distance D between their surfaces is less than the correlation length $\xi \sim c_0^{-3/4}$.

of polymers and impenetrable colloidal particles, depletion layers of width ξ appear around the spheres. This depletion can be strongly enhanced in the gap between the spheres, driving to attractive forces due to the osmotic pressure exerted on the opposite sides of the particles. ξ is the correlation length (or concentration blob). Typically, ξ is large in polymer solutions because polymer molecules are bulky. And because ξ may be more than microscopic, polymeric solvent might be interesting. From the semidilute limit of overlapping to the melt state (see Fig.1.3), the relevant length scale is not the coil size, but ξ, this correlation length, *i.e.* the range of "collective" correlations. Scaling arguments enable to deduce the dependencies of ξ [19]: indeed for dilute solutions of concentration $c_0 \lesssim c^*$, where $c^* \simeq N/{R_\mathrm{g}}^d \simeq N^{1-d\nu}b^{-d}$ is the overlap concentration of the polymer coils in d dimensions (see Fig.1.3), correlations are essentially intramolecular along the entire chain. Thus $\xi \sim R_\mathrm{g}$. Whereas when $c_0 > c^*$, chains are overlapping and the correlation length does not depend on the degree of polymerization N any more, but decreases with the monomer density. For $c_0 \geq c^*$, ξ should follow the scaling law

$$\xi(c_0) \simeq R_\mathrm{g} \left(\frac{c^*}{c_0}\right)^m \sim N^{\nu+m(1-d\nu)} \qquad \Rightarrow \qquad m = \frac{\nu}{d\nu - 1}. \tag{1.1}$$

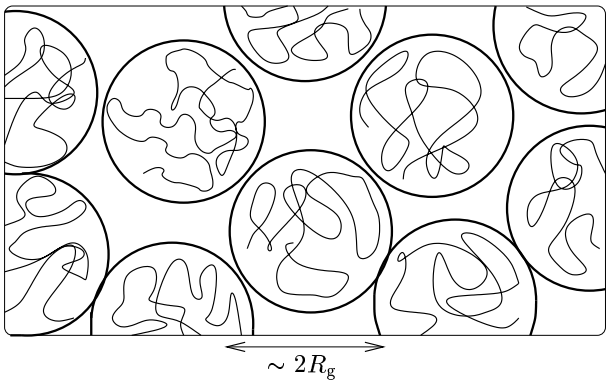

Figure 1.3: Schematic view of the overlap limit: coils start to overlap in d dimensions when $c_0 > c^*$, with $c^* \simeq N/R_{\rm g}^d \simeq N/R_{\rm g}^d \sim N^{1-d\nu}b^{-d}$, where ν is the Flory critical exponent giving $R_{\rm g} \sim N^{\nu}b$ ($\nu \simeq 3/5$ in three dimensions).

To kill the N-dependency in semidilute solutions, m has to be set equal to $\nu/(d\nu - 1) = 3/4$ for $d = 3$. So, the correlation length is comparable to the coil size in the dilute limit, it scales as $c_0^{-3/4}$ in the semidilute regime. In very dense systems now, where fluctuations are small and mean-field applies (see section 1.2.6, 1.2.7), ξ is now Edwards correlation length[2] and scales as $c_0^{-1/2}$. When ξ is decreasing until becoming microscopic, as it is in concentrated solutions of polymers, the role of connectivity tends to vanish (these notions are extensively discussed in the thesis). The polymer matrix can therefore be treated as an ordinary liquid (with particles of size $\sim \xi$). This is what is expected from the mean-field treatment of polymer solutions [32, 19, 35], in agreement with the Flory theorem (see [32] and section 1.2.6).

However, considering polymer melts of long linear chains, a long-range correlation still remains on the mesoscopic coil size, far over ξ. Its origin and some effects are described in details in this thesis. In the beginning, some theoretical concepts are briefly discussed, among them the physical features of the screening of the excluded volume interactions. Then some intramolecular long-range correlation effects are derived. The second part deals with collective properties. The response functions are derived. It is

[2]The scaling law eq.(1.1) with $d = 3$ and $\nu = 1/2$ yields to $\xi \sim c_0$ which is the right scaling in the fluctuating regime of semidilute coils at the θ-point. Eq.(1.1) with $\nu = 1/2$ coincides with the mean-field Edwards correlation length when $d = 4$. In that case, mean-field is always correct.

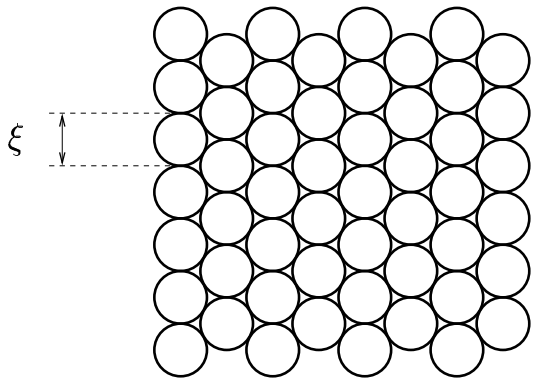

Figure 1.4: Because correlations vanish on the length ξ in dense systems of polymers, one can view concentrated solutions as ordinary liquids.

shown that they are long-range, and that they can induce repulsive forces between colloids, that could eventually stabilize them.

1.2 Mean-Field Methods

This section deals with the background necessary to describe our physical problems. It starts with considerations about mathematical tools related to connectivity of polymer chains, formalized long ago. Then, it introduces some mean-field methods used in this thesis.

1.2.1 Green Functions and Ground State Dominance

Let us consider a system of polymer chains. $\{\mathbf{x_i}\}$ is a set of parameters which describe completely the state of the i^{th} unit [35, 4]. This set of coordinates can be spatial coordinates, as considered here (see Fig.1.5), but also orientations or any other intrinsic parameters of the monomer. To take

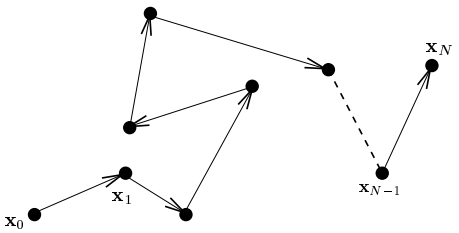

Figure 1.5: A conformation is described by the set of coordinates $\Gamma = \{\mathbf{x}_0, \mathbf{x}_1, ..., \mathbf{x}_N\}$.

into account the connectivity in our physical model, one may consider a polymer conformation as a progressive process. The easiest way to do it is to consider linear memory along a chain [35], as in the Brownian motion analysis. It means that the statistical weight of a conformation of a chain therefore reads

$$\rho(\Gamma) = g(\mathbf{x}_1, \mathbf{x}_2)g(\mathbf{x}_2, \mathbf{x}_3)...g(\mathbf{x}_{N-1}, \mathbf{x}_N). \tag{1.2}$$

This conformation distribution is characteristic of ideal chains (by definition, units of ideal chains do not interact if they are separated by a long curvilinear distance measured along the chain). The Green function or two-point correlation function of an N-chain is the partition function with fixed coordinates for the ends, obtained integrating all the intermediate coordinates. It is:

$$G_N(\mathbf{x}_1, \mathbf{x}_N) = \int \rho(\Gamma) d\mathbf{x}_2 ... d\mathbf{x}_{N-1} \tag{1.3}$$

The linear memory in the chain leads to the recursive relation

$$G_{N+1}(\mathbf{x}_1, \mathbf{x}_{N+1}) = \int G_N(\mathbf{x}_1, \mathbf{x}_N) g(\mathbf{x}_N, \mathbf{x}_{N+1}) d\mathbf{x}_N \tag{1.4}$$

which makes emerge the statistical kernel $\hat{g}$ defined as:

$$\hat{g}: \qquad \hat{g}\psi(\mathbf{x}) = \int g(\mathbf{x}', \mathbf{x})\psi(\mathbf{x}')d\mathbf{x}'. \tag{1.5}$$

Let us widen this formalism to the case of a chain in an external field $\varphi(\mathbf{x})$. In this context[3], the function associated to the transfer operator becomes

$$Q(\mathbf{x}', \mathbf{x}) = \exp(-\varphi(\mathbf{x}))g(\mathbf{x}', \mathbf{x}). \tag{1.6}$$

One can expand this operator [19] with its eigenfunctions ψ_m and eigenvalues $\Lambda_m = e^{-\epsilon_m}$. For a N chain, it gives [4]:

$$G_N(\mathbf{x}, \mathbf{x}') = \sum_m \psi_m(\mathbf{x})\psi_m(\mathbf{x}')e^{-N\epsilon_m} \tag{1.7}$$

Considering very long chains ($N \gg 1$), the term with the largest eigenvalue $\Lambda_0 = e^{-\epsilon_0}$ may dominate this last series. Ensuring that the second eigenvalue verifies $\exp(-N(\epsilon_1 - \epsilon_0)) \ll 1$ one can neglect higher terms and use the Ground State Dominance Approximation, which gives:

$$G_N(\mathbf{x}, \mathbf{x}') \simeq \psi_0(\mathbf{x})\psi_0(\mathbf{x}')e^{-N\epsilon_0}. \tag{1.8}$$

In this case, the concentration is simply proportional to $\psi_0^2(\mathbf{x})\, e^{\varphi(\mathbf{x})}$ (depending on the chosen normalization).

1.2.2 The Gaussian Kernel and the Lifshitz-Edwards Equation

To generate the Gaussian Kernel, one just has to remember that there is no orientational memory in ideal flexible chains, so that the associated kernel $g(\mathbf{x}, \mathbf{x}')$ is just a function of $|\mathbf{x} - \mathbf{x}'|$, $g(\mathbf{x}, \mathbf{x}') = \tilde{g}(|\mathbf{x} - \mathbf{x}'|)$ whose relevant characteristic is:

$$b^2 = \int x^2 \tilde{g}(x) d^3\mathbf{x}, \tag{1.9}$$

[3] The convention is here $k_B T = 1$.

[4] The discrete notation is taken for convenience, ϵ_m are increasingly ordered, and the eigenfunctions ψ_m are normalized: $\int \psi_m^2(\mathbf{x})\, e^{\varphi(\mathbf{x})} d\mathbf{x} = 1$.

b being the statistical segment. Therefore, defining the i^{th} bond vector of a chain as $\mathbf{u}_i = \mathbf{x_i} - \mathbf{x_{i-1}}$, $\{\mathbf{u}_i\}$ are independent random variables verifying $\langle \mathbf{u}_i.\mathbf{u}_j \rangle = b^2\delta_{i,j}$ and as an application of the central-limit theorem when $N \gg 1$, the distribution of the end-to-end distance $\mathbf{r} = \sum_i \mathbf{u}_i$ is,

$$G_N(\mathbf{r}) = (\frac{d}{2\pi N b^2})^{d/2} \exp\left(-\frac{d\,\mathbf{r}^2}{2Nb^2}\right), \tag{1.10}$$

with d the space dimension. This expression highlights the entropic elasticity involving the *"spring"* constant $\frac{d}{Nb^2}$. At this point, one can also immediately identify the *path-integral* formalism deriving from equation (1.10) for the Gaussian model using continuous variables and writing the action of a conformation $\mathbf{r}(N)$ as:

$$H(\mathbf{r}(N)) = \int_0^N \left(\frac{d}{2b^2}\left(\frac{\partial \mathbf{r}}{\partial n}\right)^2 + \varphi(\mathbf{r}(n)) + \frac{d}{2}\ln\left(\frac{2\pi b^2}{d}\right)\right) dn \tag{1.11}$$

The last term in the integral is a normalization term that can be omitted if the statistical segment is a constant in the system. This formulation involving path-integrals enables many analogies with quantum mechanics.

In the continuum limit, the Gaussian kernel $\hat{g}$ acts like a Laplace operator. Actually, a Fourier Transform, $\mathbf{k}$ standing for the wave-vector, immediately shows that because of the convolution theorem:

$$(\hat{g}\psi)_{\mathbf{k}} = g_{\mathbf{k}}\psi_{\mathbf{k}} = \exp(-k^2\frac{b^2}{2d})\psi_{\mathbf{k}} = [\exp(\frac{b^2}{2d}\nabla^2)]_{\mathbf{k}}\psi_{\mathbf{k}} \tag{1.12}$$

such that $\hat{g} = \exp(\frac{b^2}{2d}\nabla^2)$. So $\hat{Q} = \exp(\frac{b^2}{2d}\nabla^2 - \varphi(\mathbf{r}))$. Because of continuous variables, $\hat{Q}$ should be close to unity so that $\hat{Q} \simeq 1 - \varphi(\mathbf{r}) + \frac{b^2}{2d}\nabla^2$ and because of the definition of the transfer operator, $G_{N+1} = G_N + \frac{\delta G_N}{\delta N}\delta N$, one obtains the Lifshitz-Edwards equation

$$\frac{\partial}{\partial N}G_N = \frac{b^2}{2d}\nabla^2 G_N - \varphi(\mathbf{r})G_N \tag{1.13}$$

that is Schrödinger-like. Please note that the length $a^2 = \frac{b^2}{2d}$ appears naturally. One can identify Edwards operator:

$$\hat{L} = -a^2\nabla^2 + \varphi \tag{1.14}$$

Formally, it comes down to solving the system

$$\begin{aligned} \frac{\partial}{\partial N}G_N &= -\hat{L}G_N \\ G_0(\mathbf{x}, \mathbf{x}') &= \delta(\mathbf{x} - \mathbf{x}'). \end{aligned} \tag{1.15}$$

It is also possible to associate the operator $\hat{G}_N = e^{-N\hat{L}}$ to the two-points correlation function.

1.2.3 Response Functions of Noninteracting Chains

Let us consider firstly a solution of N_p ideal chains of N units, with mean density of units c_0. Applying a perturbation, $w(\mathbf{r})$ is the excess potential energy of a monomer due to this perturbation. If this perturbation is small enough, the response remains linear and reads:

$$\delta c(\mathbf{r}) = -\int d\mathbf{r}' \mathcal{G}(\mathbf{r}-\mathbf{r}')w(\mathbf{r}'), \tag{1.16}$$

or in the reciprocal space, because of the convolution:

$$\delta c(\mathbf{q}) = -S(\mathbf{q})w(\mathbf{q}), \tag{1.17}$$

with the response function S measuring the density correlations. In the reciprocal space, it reads:

$$S(\mathbf{q}) = \frac{1}{V}\langle c(\mathbf{q})c(-\mathbf{q})\rangle, \quad q \neq 0 \tag{1.18}$$

with $c(\mathbf{q}) = \int d\mathbf{r} \sum_{\alpha=1}^{N_p}\sum_{i=1}^{N} e^{-i\mathbf{q}\cdot\mathbf{r}}\delta(\mathbf{r}-\mathbf{R}_{i,\alpha})$. Actually, this function is taken at equilibrium (before the perturbation)[5].

As there are no inter-chain contribution to correlations, because chains do not interact, the correlations $S(q)$ are proportional to the intramolecular correlations $F^{(0)}$, known as the form factor. For a monodisperse system of ideal N-chains this response function reads:

$$S^{(0)}(q) = \frac{c_0}{N}\sum_{i,j=1}^{N}\langle e^{i\mathbf{q}\cdot\mathbf{r}}\rangle_0 = \frac{2c_0}{N}\sum_{n=1}^{N}\sum_{s=1}^{n} e^{-sq^2a^2} = c_0 N f_\mathrm{D}(q^2{R_\mathrm{g}}^2), \tag{1.19}$$

with $f_\mathrm{D}(x) = \frac{2}{x^2}(x-1+e^{-x})$, the Debye function and $R_\mathrm{g} = N^{1/2}a$ the radius of gyration (see appendix A) measuring the spatial extension of the macromolecule. The index 0 indicates averages done on Gaussian distributions. In the asymptotic limit $qR_\mathrm{g} \to \infty$, the collective correlation function is given by the simple formula

$$S^{(0)}(q) = \frac{2c_0}{q^2a^2}. \tag{1.20}$$

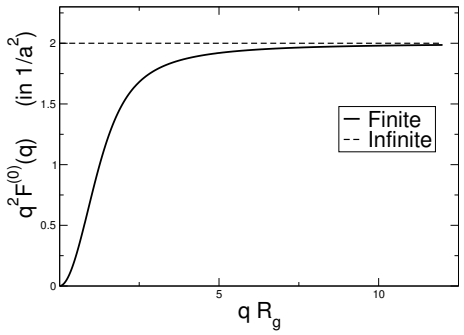

Figure 1.6: Shape of the Debye function, in the Kratky representation. Because of the general definition of the form factor, the small-q regime gives the radius of gyration. At large-q, the Kratky plateau is a signature of the Hausdorff dimension of the Gaussian coil ($d_{\mathrm{H}} = 2$).

which are also the correlations for infinite chains at any q since $R_{\mathrm{g}} \to \infty$. At thermodynamical equilibrium, the compressibility $1/S^{(0)}(q \to 0)$ diverges to infinity as the mass N of a macromolecule. In a system of ideal infinite chains, fluctuations are long-range: the correlation length $\xi = \infty$.

1.2.4 Excluded Volume Interaction

To be more realistic, interactions between units that are not strictly connected have to be considered. For instance, steric constraints, molecular (Van der Waals) interactions and other complicated specific interactions have to be treated, involving too many parameters. Nevertheless, considering large length scales, the details of these potentials will not be involved [65] and these effects can be adsorbed, in the first approximation, into a single parameter v defining the strength of the pairwise contact potential. Therefore, the interaction energy reads:

$$U = \frac{1}{2} v \sum_n \sum_m \delta(\mathbf{R}_n - \mathbf{R}_m) = \frac{1}{2} v \sum_n \sum_m \int d\mathbf{r} \delta(\mathbf{r} - \mathbf{R}_n) \delta(\mathbf{r} - \mathbf{R}_m), \quad (1.21)$$

the sum counting all the units of the system. One just has to be conscious that this first-order term is enough only when the three-body interactions are negligible. It is absolutely not sufficient too close to the theta point, when $v \to 0$ and the three-body interactions are dominant.

[5] The response functions are averaged for equilibrium conformations and δc is already a statistical mean value $\langle \delta c \rangle$ but to lighten the text, these brackets are omitted.

As we want to reach macroscopic properties, one can resort to a "coarse-graining", integrating these microscopic variables on the intermediate scale Λ. The new variable is a smooth local concentration identified as an averaging of the microscopic density $c_{\mathrm{m}} = \sum_n \delta(\mathbf{r} - \mathbf{R}_n)$:

$$c(\mathbf{r}) = \langle c_{\mathrm{m}}(\mathbf{r}) \rangle = \frac{1}{\Lambda^d} \sum_m \int_\Lambda d\mathbf{r}' \delta(\mathbf{r} + \mathbf{r}' - \mathbf{R}_m). \tag{1.22}$$

Looking at equations (1.21) and (1.22), the mean-field approximation consists in substituting $\langle c_{\mathrm{m}} \rangle^2 \leftarrow \langle c_{\mathrm{m}}^2 \rangle$. In this approximation, the energy reads now

$$U = \frac{1}{2} v \int c^2(\mathbf{r}) d\mathbf{r} \tag{1.23}$$

Thus the (self-consistent) molecular field felt by a monomer is $U_{\mathrm{mol}} = \frac{\delta U[c(\mathbf{r})]}{\delta c} = v c(\mathbf{r})$. In this thesis, only good solvents are considered, ensuring $v > 0$. In the Ground State Dominance[6], $c = \psi^2$, and one can write the Hamiltonian [7] of a polymer solution as:

$$H[\psi] = \int \{ a^2 (\nabla \psi)^2 + \frac{1}{2} v \psi^4 \} d\mathbf{r}. \tag{1.24}$$

Strictly speaking, Landau-Ginzburg theory enables here to recognize ψ as the order parameter of the problem [19]. This last equation can be formulated in c [35]:

$$H[c] = \int \{ \frac{a^2}{4} \frac{(\nabla c)^2}{c} + \frac{1}{2} v c^2 \} d\mathbf{r}. \tag{1.25}$$

The first term comes from the conformational entropy. It tends to smooth out ψ and as a consequence, the density. The self-consistent term is called excluded volume or steric interaction. It is to be noted that these formulations of the mean-field Hamiltonian imply only polynomial and gradients of ψ or c, therefore very local terms. These expressions cannot appreciate large scales. In other words, this Hamiltonian does not distinguish, for instance, a linear from a ring conformation. This is the central point of chapter 4.

1.2.5 The Fixman Parameter

Let us consider a bulk solution of polymers made up of N monomers in a d-dimensional space. The polymer concentration (number of chains per unit volume) is c_p and the monomer concentration is $c_0 = N c_p$. In the light of

[6] without any external field

[7] the index 0 is omitted in this approximation

the excluded volume interaction, a virial expansion of the osmotic pressure in the mean-field approximation would include the sum of the translational term and the potential contribution [35, 19], saying

$$\begin{aligned}\Pi &= \frac{c_0}{N} + \frac{1}{2}\, v\, c_0^2 + O(c_0^3) \\ &= c_p + \frac{1}{2}\, v\, N^2\, c_p^2. + O(c_0^3).\end{aligned} \tag{1.26}$$

The translational term is obviously negligible for the semidilute regime of overlapping coils $c \gg c^* \sim N/R^d$, or for long enough chains. From eq.(1.26), it is possible to give a criterion able to confirm whether the excluded volume is just a perturbation for the chains without excluded volume (Gaussian chains) or if it is strong enough to swell them. Introducing the Gaussian radius of gyration $R_{\mathrm{g}}^2 = Na^2 = Nb^2/6$, a relevant non-dimensional quantity would read

$$\begin{aligned}\frac{\Pi}{c_p} &= 1 + \frac{1}{2}\, v\, N^2\, c_p \\ &= 1 + \frac{1}{2} v\, N^{2-d/2}\, c_p\, R_{\mathrm{g}}^d\, a^{-d}.\end{aligned} \tag{1.27}$$

Thus the Fixman interaction parameter, measuring the effective strength of the interaction for a complete chain reads

$$u \simeq v\, N^{2-d/2}\, a^{-d}. \tag{1.28}$$

For $d = 3$, this parameter, u is diverging as $N^{1/2}$, confirming that the excluded volume is clearly not a perturbation. Nevertheless, considering the screening of v in dense systems, the effective potential may become perturbative (see section 2.1 and chapter 3).

1.2.6 Screening and the Flory Theorem

Firstly, a soft argument, typically "mean-field" to confirm the screening of the steric interaction. Let us consider the repulsive potential felt by a monomer. It reads $U_{\mathrm{mol}} = v(c_0 + \delta c)$. So that fluctuations are ruling the statistics. In a dilute (very fluctuating) solution, this field is strong. But in a concentrated solution, the fluctuations are far weaker, and the excluded volume interactions tend to zero, leading to Gaussian statistics. This is usually the justification of the Flory conjecture, often called the "Flory theorem", that stipulates that a chain in a very dense system is ideal (follows Gaussian statistics). To describe more quantitatively screening

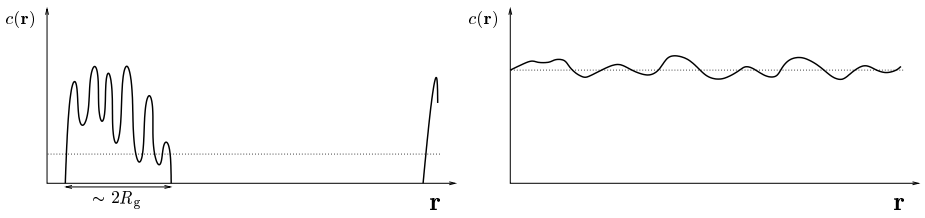

Figure 1.7: Schematic visualization of density fluctuations in a dilute and in a dense systems of polymers.

in concentrated solutions, one can use the Random Phase Approximation (RPA) for dense polymer systems. As Pines and Nozières noticed[53], there are many ways to derive it, and *"seemingly different results are related"*. One of the simplest self-consistent method to derive it in our context [35, 19, 24, 25, 71] is the following: let us consider a dense system of chains (with density c_0). Applying a weak external field w, which could create a small deviation δc, linear response and mean-field considerations enable to write in the reciprocal space:

$$\delta c(\mathbf{q}) = -S^{(0)}(\mathbf{q})(w(\mathbf{q}) + v\delta c(\mathbf{q})) \tag{1.29}$$

which gives self-consistently the new response function as a function of the ideal one, through the classical RPA relation:

$$\frac{1}{S(\mathbf{q})} = v + \frac{1}{S^{(0)}(\mathbf{q})} = v + \frac{1}{c_0 F^{(0)}(\mathbf{q})} \tag{1.30}$$

Equation (1.30) can be rewritten as :

$$\begin{aligned} S(\mathbf{q}) = S^{(0)}(\mathbf{q}) - S^{(0)}(\mathbf{q})vS^{(0)}(\mathbf{q}) + S^{(0)}(\mathbf{q})vS^{(0)}(\mathbf{q})vS^{(0)}(\mathbf{q}) \\ - S^{(0)}(\mathbf{q})vS^{(0)}(\mathbf{q})vS^{(0)}(\mathbf{q})vS^{(0)}(\mathbf{q}) + ... \end{aligned} \tag{1.31}$$

highlighting the *simple tree* approximation featured in this reasoning [24] (see Fig.1.8).

The first part of this work will deal with single-molecule properties. Therefore, to take into account correlation holes that screen the repulsion of monomers in a chain, consider a labeled chain (whose units are referred to as "black" monomers, with density c_b small) and treat other chains as a background (referred to as "white", with density c_w almost c_0). The effective interactions between the "black" monomers are screened due to the presence of neighboring "white" chains. To see this, one just has to rewrite the

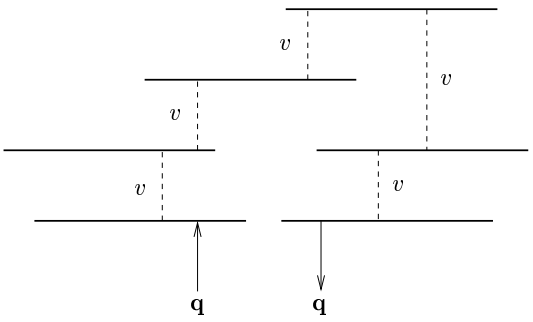

Figure 1.8: Example of a simple tree taken into account by RPA.

equation of linear response theory for this new system, taking into account the new correlations [19, 25, 63], the steric interaction and a perturbative potential w acting only on black monomers:

$$\begin{aligned} \delta c_b(\mathbf{q}) &= -c_b F^{(0)}(\mathbf{q})(v(\delta c_b(\mathbf{q}) + \delta c_w(\mathbf{q})) + w) \\ \delta c_w(\mathbf{q}) &= -c_w F^{(0)}(\mathbf{q}) v(\delta c_w(\mathbf{q}) + \delta c_b(\mathbf{q})). \end{aligned} \tag{1.32}$$

Solving this system leads to

$$\delta c_w(\mathbf{q}) = -c_w \frac{F^{(0)}(\mathbf{q})}{1 + c_w\, v\, F^{(0)}(\mathbf{q})} v \delta c_b(\mathbf{q}) \tag{1.33}$$

and, as $c_w \simeq c_0$, it gives the effective interaction v_{eff} between black monomers as

$$v_{\text{eff}}(\mathbf{q}) = v - v^2 S(\mathbf{q}) \tag{1.34}$$

If chains are infinite, this last expression is simply:

$$v_{\text{eff}}(\mathbf{q}) = \frac{v q^2 \xi^2}{1 + q^2 \xi^2} \qquad \text{with } \xi^2 = \frac{b^2}{12 c_0 v} \tag{1.35}$$

and the correlations estimated *via* RPA give the classical Ornstein-Zernike correlation form:

$$S(q) = \frac{1}{v} \frac{1}{1 + q^2 \xi^2}, \tag{1.36}$$

ξ being the mean-field correlation length. The inverse Fourier transform of $S(q)$ in 3 dimensions reads

$$\mathcal{G}(r) = \langle \delta c(r) \delta c(0) \rangle = \frac{3 c_0}{\pi b^2 r} e^{-r/\xi}, \tag{1.37}$$

showing that correlations vanish over ξ. With eq.(1.35), the effective interaction in real space therefore reads [25]

$$v_{\text{eff}}(r) = v\left(\delta(r) - \frac{1}{4\pi r\xi^2}e^{-r/\xi}\right). \tag{1.38}$$

In this special case (infinite chains), the weak attractive term screens the δ-repulsion, giving $\int v_{\text{eff}}(r)d\mathbf{r} = v_{\text{eff}}(q=0) = 0$. Scanning on scales larger than ξ, the system seems incompressible, the effective potential of infinite chains becomes:

$$v_{\text{eff}}(\mathbf{q}) = \frac{q^2b^2}{12c_0}. \tag{1.39}$$

which is the incompressible limit of eq.(1.35) when $v = \frac{1}{c_0}\frac{\partial\Pi}{\partial c_0}$ diverges to infinity. So, this effective potential, at the light of the *simple tree* approximation expresses correctly the main idea: correlation holes imply that interactions are mediated (and naturally screened) by surrounding chains. It also confirms the *a priori* ordinary liquid behavior of dense polymer systems.

1.2.7 The Ginzburg Criterion

To test the validity of these methods, one has to check that correlations are always small after a mean-field treatment [17, 48, 25]. Formally, one has to check that $\langle\delta c(r)\delta c(0)\rangle \ll c_0^2$ everywhere in the system. Noticing that

$$\langle\mathcal{G}(r)\rangle = \frac{1}{\xi^d}\int\mathcal{G}(r)d^d\mathbf{r} = \frac{1}{\xi^d}S(q=0) = \frac{1}{v\xi^d} \tag{1.40}$$

one always has the possibility to validate approximations, verifying that $\frac{1}{v\xi^d} \ll c_0^2$, *i.e.* the Ginzburg parameter $G_{\text{z}} \equiv \frac{1}{v\xi^d}\frac{1}{c_0^2}$ is small:

$$G_{\text{z}}^2 = \frac{v^{d-2}}{c_0^{4-d}\,b^{2d}} \ll 1. \tag{1.41}$$

Please note that for $d = 2$, G_{z} does not depend on v, which shows that this case needs nearly always renormalization rather than mean-field treatments [63]. Obviously, eq.(1.41) is only valid for $c_0\,v \lesssim 1$. At this point, one can wonder in which context these mean-field methods could apply for semiflexible polymers. A good schematic model to describe them is shown in Fig.1.9 [35, 4]. Generally, orientational correlations hold on a typical curvilinear length scale called the persistent length l_{p}. In this view, the end-to-end distance R_{e} scales as $R_{\text{e}} \sim L\,l_{\text{K}}$ where L is the curvilinear length of the

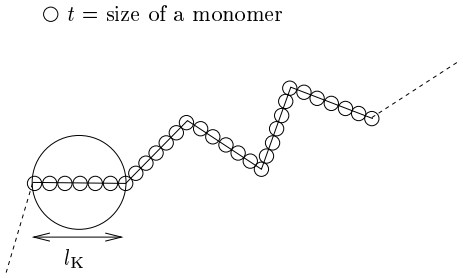

Figure 1.9: Model of a semiflexible polymer: because of persistence, the macromolecule may be seen as a chain of effective rods of length l_K with l_K/t units per segment. t is the typical size of a unit, or the thickness of the chain.

macromolecule, $L = Nt$ and l_K is the Kuhn effective segment. This relation infers Gaussian statistics for long enough chains of $N\,d/l_K$ rods of length l_K. In the persistent model relevant for semiflexible macromolecule, the Kuhn segment is twice as long as the persistence length [35] $l_K = 2\,l_p$. Therefore the scaling ideas below may be expressed indifferently in terms of l_K or l_p. Ratios d/l_K or d/l_p measure the rigidity of the chain. We are dealing with a solution of $c_0\ t/l_K \sim c_0\ t/l_p$ persistent units, of step-size l_p (instead of t if the chain would be flexible). The virial coefficient v of such rods scales (as in the Onsager theory of liquid crystals) as $v \sim l_p^2\ t$. According to eq.(1.41), the Ginzburg criterion reads by now $1/c_0\ l_p^3 \ll 1$ or, with the volume density $\Phi = c_0 t^3$ [47]

$$G_z^2 = \frac{t^3}{\Phi\ l_p^3} \ll 1. \tag{1.42}$$

The mean-field correlation length (which reads $\xi^2 \simeq b^2/(c_0\,v)$ for flexible chains) reads by now

$$\xi^2 \simeq \frac{l_p\,t}{\Phi}. \tag{1.43}$$

Of course, these methods apply only when $G_z \ll 1$ and $l_p \ll \xi$, giving the domain of validity as a function of the rigidity which reads

$$\left(\frac{t}{l_p}\right)^3 \ll \Phi \ll \frac{t}{l_p}. \tag{1.44}$$

The same upper bound also indicates the isotropic/nematic transition [47, 35].

1.2.8 Surface Tension in the Mean-Field Approximation

The aim here is to evaluate the surface tension of a dense solution of infinite polymers near a repulsive wall, for a bulk mean concentration c_0, in the mean-field approximation (see Fig.1.10). Thermodynamics give the excess

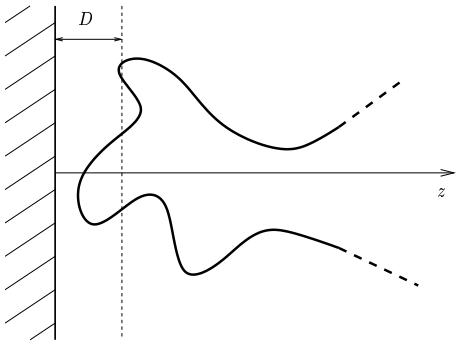

Figure 1.10: One conformation of a polymer in a solution near a repulsive wall. The range D of the repulsion is inversely proportional to the potential strength.

mean-field free energy created by the surface, saying the part of the grand potential due to the surface [48] as $\Omega_{\rm surf} = \int \gamma dA = \Omega + \int \Pi dV = \min_{\{\psi\}} \mathcal{H}[\psi]$). As for infinite chains, ground state dominance applies and since in the bulk, the osmotic pressure of semidilute solution reads $\Pi = \frac{1}{2} v c_0^2$ (the translational entropy is negligible), the Hamiltonian which has to be minimized reads

$$\mathcal{H}[\psi] = \int d\mathbf{r} \left\{ a^2 \left(\frac{d\psi}{dz} \right)^2 + \frac{v}{2} \psi^4 - \epsilon \psi^2 + \Pi + h_{\rm s}\, \delta(z) \psi^2 \right\}, \tag{1.45}$$

where $h_{\rm s}$ is the surface potential strength and $\epsilon = v c_0$ is the bulk chemical potential, necessary to ensure $\psi(z \to \infty) = \sqrt{c_0}$ [19]. The last term is the short-range wall contribution to the energy. This equation may be simplified, and drives to

$$\mathcal{H}[\psi] = \int d\mathbf{r} \left\{ a^2 \left(\frac{d\psi}{dz} \right)^2 + \frac{v}{2} \{ \psi^2 - c_0 \}^2 + h_{\rm s}\, \delta(z) \psi^2 \right\}. \tag{1.46}$$

The mean-field approximation amounts to performing the variational minimization of this functional. Thus, the effect of a wall, weakly absorbing or desorbing, is essentially to impose the boundary condition [19, 13, 20, 21]

$$\frac{1}{\psi} \frac{d\psi}{dz} \bigg|_{z \simeq 0} = \frac{h_{\rm s}}{a^2} = \frac{1}{D} \tag{1.47}$$

with $|D|$, known as the extrapolation length [19], tunes the amplitude of the potential. D is positive when repulsion dominates the integral of the potential (and $D<0$ otherwise) and the differential equation for the order parameter $\psi=\sqrt{c_0}f$ is

$$\left(\frac{df}{dx}\right)^2 = c_0^2\frac{1}{4\xi^2}\{1-f^2\}^2. \tag{1.48}$$

Dealing with depletion (effective repulsion), the order parameter is therefore increasing until $\sqrt{c_0}$ as

$$\psi(z) = \sqrt{c_0}\tanh\left(\frac{z+z_0}{2\xi}\right) \tag{1.49}$$

$$\text{with} \qquad \tanh\left(\frac{z_0}{2\xi}\right) = \sqrt{1+(\xi/D)^2}-\xi/D.$$

The width of the interface scales obviously as ξ. Over several ξ, the density profile has reached its bulk value, $\psi^2=c_0$. Supposing now a very strong repulsion, such that $D\ll\xi$ and $z_0\to 0$, the wall contribution to the surface tension is $\frac{a^2}{D}\psi^2(0)\simeq\frac{a^2}{D}c_0\frac{D^2}{4\xi^2}\to 0$. Therefore, for infinite chains, the minimization of the ψ^4-functional $\mathcal{H}$ [34] leads to the surface tension

$$\begin{aligned}\gamma_{\rm mf} &= \int_0^\infty dz\left\{a^2\left(\frac{d\psi}{dz}\right)^2+\frac{v}{2}(\psi^2-c_0)^2\right\}\\ &= 2*\int_0^\infty dz\frac{v}{2}(\psi^2-c_0)^2 = \frac{a^2c_0}{\xi}\left(\frac{2}{3}\right)\\ &\Rightarrow \qquad \gamma_{\rm mf}=\frac{2}{3}\frac{a^2c_0}{\xi}.\end{aligned} \tag{1.50}$$

To conclude, mean-field methods enable to establish a depletion on the scale ξ. That mean-field correlation length diminishes when the concentration is increased. So, from this point of view, interfacial effects are confined in a layer of width ξ, and the surface tension scales as $\frac{a^2c_0}{\xi}$ [19, 44]. To take into account fluctuations, let us consider for instance the correction due to capillary waves: following the equipartition theorem ($k_{\rm B}T$ per mode), the correction is proportional to the number of modes. The system is liquid-like on scales larger than the correlation length, allowing only wave-lengths larger than ξ. The correction to the surface tension is thus dominated by the short modes scaling as $\gamma_{\rm fluct}\sim q_{\rm cut}^2\sim\xi^{-2}$, the square of the cut-off wave number. Note that $\gamma_{\rm fluct}/\gamma_{\rm mf}\simeq G_{\rm z}$, where $G_{\rm z}$ is the Ginzburg parameter defined in eq.(1.41).

1.2.9 The Flory Exponential Distribution

Consider an A-B bifunctional (linear) polymerization process (for instance a polyesterification involving an acid group -COOH and an alcool group -OH) at equilibrium. For a macromolecule, beginning from the first end which

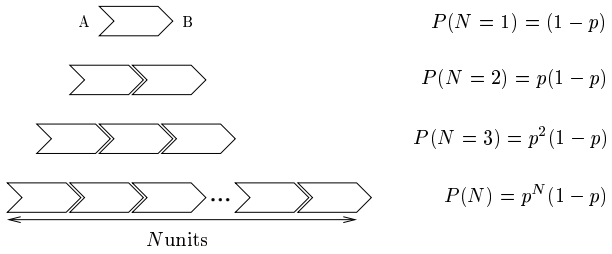

Figure 1.11: $1-p$ is the probability that the B-group is unreacted and p, the probability that the monomer has reacted from its B-side. It leads to a geometric distribution of N-mers $P(N)=p^{N-1}(1-p)$.

is an unreacted A-function, the probability that the adjacent B-group is also unreacted is $(1-p)$, and the probability that this group is reacted is p. This simple consideration leads to a geometric distribution of N-mers [32] $P(N)=p^{N-1}(1-p)$ (see Fig.1.11). That probability p is *a priori* very difficult to determine and depends on many parameters. Nevertheless, using a mean-field view, if the average size $\langle N\rangle=\frac{1}{\mu}$ is known, the probability that a monomer to be a chain-end is $1-p=\frac{1}{\langle N\rangle}=\mu$. Moreover, if $\langle N\rangle\gg 1$, the distribution becomes:

$$P(N)=\mu(1-\mu)^{N-1}\simeq\mu e^{-\mu N} \tag{1.51}$$

This distribution, known as the Flory distribution, is relevant for equilibrium (living) polymers [15, 68], and it tends to simplify the derivation of size-effects. It is a way to legitimate the Grand-Canonical formalism (where $e^{-\mu}$ is the fugacity of a monomer) extensively used in this thesis. Just notice that the monomer density c_0 is a constant, and the concentration in N-mers is $\phi_N=c_0\mu^2e^{-\mu N}$. Infinite chains correspond to the $\mu\to 0$ limit.

As an example, let us define the intramolecular form factor under that distribution

$$F(q)=\sum_{N=0}^{\infty}\mu^2\exp(-\mu N)\sum_{i=1}^{N}\sum_{j=1}^{N}\langle\exp(-i\mathbf{q}\cdot\mathbf{r}_{i,j})\rangle, \tag{1.52}$$

which ensures the relation $S(q) = c_0 F(q)$. In a system of non interacting gaussian macromolecules, it is easy to evaluate this form factor, as the correlations between two points of a chain, separated by s monomers with the wavevector $\mathbf{q}$ reads

$$G_s(q) = \int d\mathbf{r}\, e^{-i\mathbf{q}\cdot\mathbf{r}} G_s(r) = \langle e^{-i\mathbf{q}\cdot\mathbf{r}_s}\rangle_0 = e^{-q^2 s a^2}. \tag{1.53}$$

Using the general theorems of Laplace transforms, the form factor reads:

$$F^{(0)}(q) = \frac{2}{\mu}\ \frac{1}{1+q^2a^2/\mu}. \tag{1.54}$$

In the small-q regime, $qR_{\mathrm{g}} \ll 1$, the radius of gyration is estimable via the Guinier relation (see appendix A), which reads for a *polydisperse* system [35, 24, 37]

$$F(q) \underset{qR_{\mathrm{g}}^{(0)}\ll 1}{\simeq} \frac{\langle N^2\rangle}{\langle N\rangle}\left(1 - \frac{q^2 R_{\mathrm{g,Z}}^{(0)\,2}}{3}\right). \tag{1.55}$$

Please note the Z-averaging [24] in the definition of $R_{\mathrm{g,Z}}$

$$R_{\mathrm{g,Z}}^2 = \frac{\sum_N N^2 \phi_N R_{\mathrm{g}}^2(N)}{\sum_N N^2 \phi_N}, \tag{1.56}$$

$R_{\mathrm{g}}(N)$ being the radius of gyration in the monodisperse case. As the Flory distribution gives $\langle N^p\rangle = \Gamma(p+1)/\mu^p$, one has $R_{\mathrm{g,Z}}^{(0)\,2} = 3a^2/\mu$. In the Kratky regime, when q^{-1} is between the coil and the monomer size, one recovers the classical result for infinite chains

$$F^{(0)}(q) \underset{qR_{\mathrm{g}}^{(0)}\gg 1}{\simeq} \frac{2}{q^2a^2}, \tag{1.57}$$

(indicated by the dashed line in Fig.1.6) which expresses the fractal dimension of the Gaussian coil (see appendix A).

Chapter 2

Corrections to some Intramolecular Properties

In this chapter, we derive the corrections of some intramolecular quantities characteristic of a chain in a melt. It offers an opportunity to introduce some general tools of statistical physics and to deal with approximations extensively used in this thesis. Some orientation effects for a chain in the melt and the partition function of living polymers under the shielded interactions are discussed below.

2.1 Orientational Correlations along an Infinite Chain in a Melt

2.1.1 Introduction

To measure the persistence of the orientation along a chain, one may try to evaluate the correlation between two tangential unit vectors *via* the first Legendre polynomial given by the formula

$$P_1(m-n) = \langle \hat{\mathbf{l}}_n \cdot \hat{\mathbf{l}}_m \rangle \quad \text{with} \quad \hat{\mathbf{l}}_n = \frac{\mathbf{l}_n}{|\mathbf{l}_n|}. \tag{2.1}$$

The fact that in the different exactly-solved models of single chain[32] (the wormlike chain, the freely-rotating chain *etc*...) these correlations are predicted to decrease exponentially with the curvilinear length $|m-n|$ between two points makes emerge the persistence length l_{p} (see Fig.2.1). The persistence length is the curvilinear scale on which orientation correlations are

exponentially cut, *i.e.*

$$P_1(m-n) \simeq e^{-|m-n|/l_{\rm p}}. \tag{2.2}$$

It is an important concept in polymer physics which characterizes the rigidity of a chain. It may be experimentally measured, as mentioned in section 3.1 and in appendix A. So far, in any polymeric system, a chain is expected to be characterized by a persistence length. This notion implies in particular

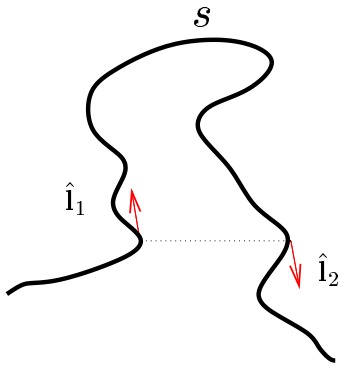

Figure 2.1: The persistence length expresses the fact that the correlations between the unit tangential vectors $\hat{\mathbf{l}}_1$and $\hat{\mathbf{l}}_2$ are exponentially cut $P_1(s) = \langle \hat{\mathbf{l}}_1 \cdot \hat{\mathbf{l}}_2 \rangle \simeq e^{-s/l_{\rm p}}$.

that, for long enough macromolecules ($L \gg l_{\rm p}$), it is possible to consider coarse-grained units larger than some $l_{\rm p}$, and to treat a chain as a model of independent bonds (see the discussion in section 1.2.7 for more details).

Here, we consider polymer melts of very long flexible chains, where the interactions are screened on the correlation length ξ, and where chains are supposed to be Gaussian[32]. One does not expect any persistence of the angular correlations over at most the correlation length $\xi \sim b$. We demonstrate here that this statement is in fact incorrect. The notion of persistence length may fall down: indeed it is shown in the next sections that the screened potential of Eq.(1.35), treated perturbatively, induces algebraically decreasing correlations under and over the correlation blob size ξ. These correlation could easily be misinterpreted as an exponential decrease in numerical data which only sweep a partial range of length, for instance. We then show that there is a very good agreement between the analytical results and the numerical simulations (performed by J. P. Wittmer).

2.1.2 Perturbative Treatment

We want here to apply first order perturbations to the angular correlations eq.(2.1). Our state of reference follows Gaussian statistics. It is well-known in statistical physics that a quantity under a perturbation U [48] reads at first order in U

$$\delta\langle A\rangle \equiv \langle A\rangle - \langle A\rangle_0 \simeq \langle U\rangle_0\langle A\rangle_0 - \langle UA\rangle_0, \tag{2.3}$$

the index 0 indicating that the averages are done on the unperturbed statistics. To apply it, we should check that the perturbation ($U = U_{\text{eff}} \equiv$ the pairwise effective potential summed over the entire chain) is small. A qualitative argument is the following [63]: consider a polymer coil I located near the origin in the region $r \leq R$, where R is its size. The concentration of its monomers in that region is $c_I = N/R^3$, and the concentration of monomers belonging to other chains is $c_0 - c_I$, with c_0 the mean concentration. Dealing with dense systems, the probability for two neighboring monomers to belong to the same chain is small, or in this case $c_I \ll c_0$ or $c_0 R^3/N \gg 1$. Next we consider the polymer I and another polymer J, and we deal with their simultaneous distributions, all other chains being invisible. The probability density[1] $\rho(r)$ that the chain J is located near r while the chain I is near the origin enables to define the effective interaction between coils

$$\frac{\rho(r)}{\rho(\infty)} = e^{-U(r)}. \tag{2.4}$$

As any other chain is equivalent to J, that probability reads in fact

$$\frac{\rho(r)}{\rho(\infty)} \simeq \frac{c_0 - c_I}{c_0} \simeq 1 - U(r). \tag{2.5}$$

And since chains are nearly Gaussian, $R^2 \simeq Na^2$ and $U(r) \simeq 1/(c_0\sqrt{N})$ in the region $r \leq R$. For long chains, $N \gg 1$, the interaction of two coils is thus weak. The same approach holds if we consider two halves of a chain or the interaction summed over the entire chain. Therefore the perturbative treatment is allowed[2].

We are considering a system of *a priori* Gaussian chains. Each segment thus follows the Gaussian kernel described in chapter 1.2. Particularly the distribution of a single bond is Gaussian and reads

$$G(\mathbf{l}_1) = \left(\frac{6}{4\,\pi\,b^2}\right)^{3/2} \exp\left(-\frac{6\,\mathbf{l}_1{}^2}{4\,b^2}\right). \tag{2.6}$$

[1] More or less the pair correlation function of the centers of mass.

[2] The same considerations involving the Fixman parameter are given in chapter 3.

Let us first consider the bond-bond correlation function $C_1(r) = \langle \mathbf{l}_1(0)\mathbf{l}_2(r)\rangle/b^2$

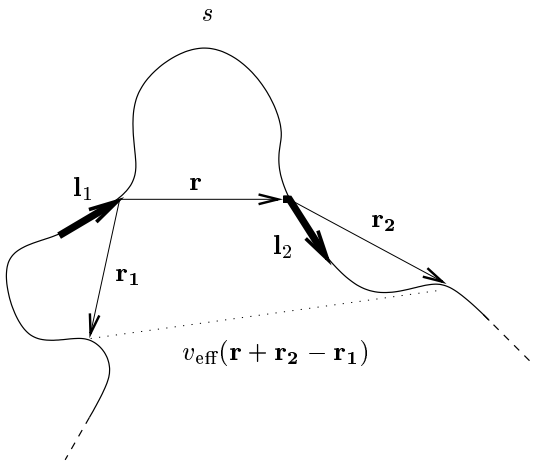

Figure 2.2: This figure indicates the notations used. Choosing the bonds out of the s-segment induces that only the interactions out of the s-segment gives non trivial contribution.

between two points from the same chain[3] [4] separated by the distance r. Following eq.(2.3) and notations of Fig.2.2, and noticing that without any interactions, the bonds of a Gaussian chains are strictly independent (in such a way that only the second term of eq.(2.3) is not null), the perturbation reads

$$C_1(r) = -\sum_{s_1=0}^{\infty}\sum_{s_2=0}^{\infty}\int d\mathbf{r_1}d\mathbf{r_2}G(\mathbf{l_1})G(\mathbf{l_2})\frac{\mathbf{l_1}\cdot\mathbf{l_2}}{b^2} \\ v_{\text{eff}}(\mathbf{r_2}+\mathbf{r}-\mathbf{r_1})G_{s_1}(\mathbf{r_1}+\mathbf{l_1})G_{s_2}(\mathbf{r_2}-\mathbf{l_2}). \tag{2.7}$$

It is convenient to use this potential in the reciprocal space. Noticing that

$$G(q) = \int d\mathbf{l}\,G(\mathbf{l})\,e^{-i\mathbf{q}\cdot\mathbf{l}} = e^{-q^2a^2} \qquad \text{and} \qquad \nabla_{\mathbf{q}}G(q) = -i\int d\mathbf{l}\mathbf{l}G(\mathbf{l})\,e^{-i\mathbf{q}\cdot\mathbf{l}}\,, \tag{2.8}$$

[3]Strictly speaking, this function does not measure the angular correlations between two tangential unit vectors $\langle\hat{\mathbf{l}}_1\cdot\hat{\mathbf{l}}_2\rangle$. Nevertheless, it can be shown in this framework that $\langle\hat{\mathbf{l}}_1(0)\cdot\hat{\mathbf{l}}_2(r)\rangle = \frac{8}{3\pi}C_1(r)$ and $P_1(s) = \frac{8}{3\pi}P(s)$ (see eqs(2.10,2.12)).

[4]Positions of $\mathbf{l}_1$ and $\mathbf{l}_2$ and $\mathbf{r}$ are well-chosen on Fig.2.2. The definition of the vectors is quite important here. The head of $\mathbf{l}_1$ is at the origin and the tail of $\mathbf{l}_2$ is at a distance r.

the correlations between the two points reads now

$$\begin{aligned} C_1(r) &= \int \frac{d\mathbf{q}}{(2\pi)^3} v_{\text{eff}}(q)\, \frac{1}{b^2}\, \nabla_{\mathbf{q}} G(q)\, \nabla_{\mathbf{q}} G(q)\, \left(\int_0^\infty G_{s_1}(q) ds_1 \right)^2 e^{i\mathbf{q}\cdot\mathbf{r}} \\ &= \int \frac{d\mathbf{q}}{(2\pi)^3}\, \frac{4}{q^2 b^2} v_{\text{eff}}(q) e^{i\mathbf{q}\cdot\mathbf{r}} = \int \frac{d\mathbf{q}}{(2\pi)^3}\, C_1(q) e^{i\mathbf{q}\cdot\mathbf{r}} \\ &\Rightarrow \qquad C_1(r) = \frac{v}{\pi\, b^2\, r} e^{-r/\xi}. \end{aligned} \tag{2.9}$$

As expected from the previous discussion, these correlations are screened on the scale ξ. Let us now focus on the initial aim: assessing $P(s)$. As the s-segment is not implied in the perturbation of $C_1(r)$, the constraint which consists in putting the two points on the same chain, and putting a s-strand between them simply reads

$$P(s) = \int C_1(r) G_s(r) d\mathbf{r} = \int C_1(q) G_s(q) \frac{d\mathbf{q}}{(2\pi)^3}. \tag{2.10}$$

Once more this integral is easier to assess using Laplace transforms. It leads to

$$P(\tau) = \int_0^\infty P(s) e^{-s\tau} ds = \frac{6v}{\pi^2\, b^4} \int_{-\infty}^{+\infty} \frac{q^2}{q^2 + \xi^{-2}} \frac{1}{q^2 + \tau/a^2} dq\,. \tag{2.11}$$

This formula explicitly makes appear two contributions, from two separated scales, the s-strand size $\sim \sqrt{a^2/\tau}$ and the correlation length $\xi \ll \sqrt{a^2/\tau}$. This integral is thus easy to assess, and after inversion of the Laplace Transform, the correlations read

$$P(X) = \frac{\sqrt{6}}{2\pi^2 c_0\, b^3} \frac{1}{g^{3/2}} \left(\sqrt{\frac{\pi}{X}} - \pi e^X \text{Erfc}(\sqrt{X}) \right), \tag{2.12}$$

with $g = \xi^2/a^2$, the number of monomer in a correlation blob, the reduced parameter $X = s/g$ and Erfc the complementary error function. Asymptotically, we find that these correlations behave as

$$\begin{aligned} P(X) &\underset{X \ll 1}{\simeq} \frac{\sqrt{6}}{2\pi^{3/2} c_0\, b^3} \frac{1}{g^{3/2}} \frac{1}{\sqrt{X}} && \text{inside the blob} \\ P(X) &\underset{X \gg 1}{\simeq} \frac{\sqrt{6}}{4\pi^{3/2} c_0\, b^3} \frac{1}{g^{3/2}} \frac{1}{X^{3/2}} && \text{over the blob.} \end{aligned} \tag{2.13}$$

Figure 2.3 presents a comparison between this result and numerical simulations performed by J. P. Wittmer. In his simulations, he developed a

method which consists in allowing monomers to overlap on a lattice with an energetic penalty ε. This approach makes the correlation length ξ a tunable parameter[5]. The agreement with the analytical formula is striking. It

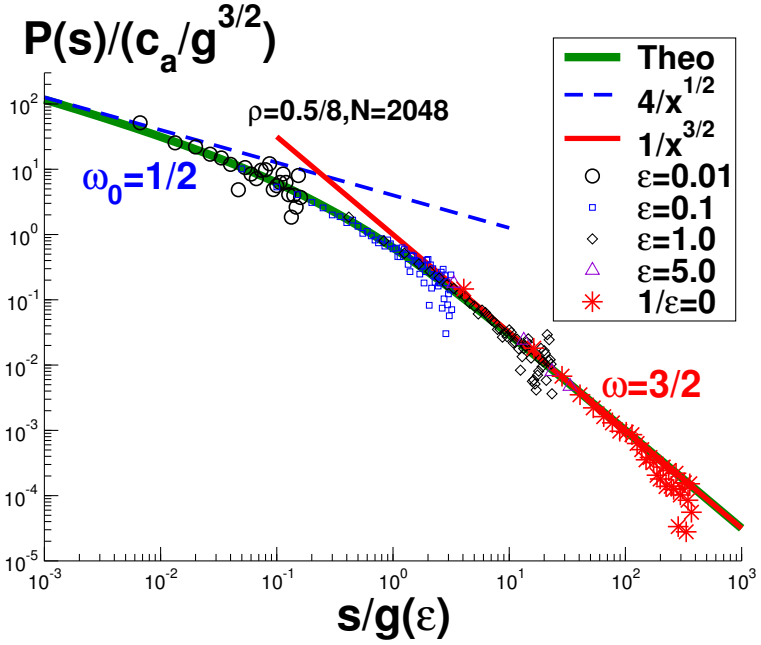

Figure 2.3: Comparison of the predictions eqs(2.12,2.12) with numerical simulations. Here $C_a = \sqrt{6}/(4\pi^{3/2} c_0 b^3)$. The curve noted "Theo" is the theoretical prediction. The agreement is verified on many order of magnitude. The both regimes inside and over the blob are explicitly identified with the right power laws.

highlights the fact that correlations decrease algebraically as $s^{-3/2}$. It also underlines the difficulty of defining a persistence length in dense systems of polymers.

For a better comprehension, let us justify these two regimes (under and over the blob) with qualitative arguments. The correlation function $P(s)$ is in fact related to the end-to-end distance of the internal segment *via* the relation

$$P(s) = \frac{1}{b^2} \langle \frac{\partial}{\partial n} \mathbf{r}_n \cdot \frac{\partial}{\partial m} \mathbf{r}_m \rangle = -\frac{1}{2\,b^2} \frac{\partial}{\partial n} \frac{\partial}{\partial m} \langle r_{nm}^2 \rangle. \tag{2.14}$$

The theory of screening implies on the first hand that the excluded vol-

[5]More details in forthcoming papers of J. P.Wittmer.

ume between two monomers separated by $s \gg g$ units is screened. Because of the perturbative treatment, it is expected (and shown in appendix C) that the correction to the ideal end-to-end distance of an s-segment reads $R^2(s) \simeq sb^2(1-1/\sqrt{s}) \simeq sb^2(1-U_{\text{eff}})$ (omitting the correction proportional to s). Therefore, following eq.(2.14), one expects $P(s) \sim s^{-3/2}$ for $s \gg g$ (substituting the result of eq.(C.5) leads to the correct prefactor in $P(s)$). On the other hand this theory also underlies that the excluded volume interactions are not screened inside a blob, when $s \ll g$, therefore U_{eff} is now the Fixman parameter (see section 1.2.5), which scales as $\sqrt{s}$. Hence we expect a perturbative correction to the end-to-end distance of the s-segment in the blob $R^2(s) \simeq sb^2(1+\sqrt{s})$, and eq.(2.14) leads to the algebraic decrease inside the blob as $P(s) \sim s^{-1/2}$.

As a conclusion, let us discuss the result eq.(2.9): at first sight, the formula obtained for an infinite chain implies that the orientation effect measured by $C_1(r)$ is local in direct space. Nevertheless, this point deserves more attention. In equation (2.9), a $1/(q^4b^4)$ factor clearly comes from integrations of propagators on infinite chains leading to $C_1(q=0) = 4v\xi^2/b^2$. The same procedure for finite chains would remove those singularities from the origin of the reciprocal space, and would give $C_1(q=0) = 0$. The integral of $C_1(r)$ vanishes for finite chains of any size, hence it should vanish also for infinite chains. Our approach hides an extra negative tail in $C_1(r)$ of zero amplitude and *infinite range*, thus non-local[6]. It is also to be mentioned that for the second Legendre polynomial $P_2(s)$ the integral of the corresponding function $C_2(q=0) = 0$ for infinite chains. It is a consequence of higher powers of q (q^4) in the representation of P_2 in **q**-space. The orientation effects measured by P_2 are local in geometrical space: they compete with any other local orientation effects.

[6]For finite chains, this orientation effect would be explicitly non-local: it would range on scales $\sim R_{\text{g}}$ with a finite amplitude decreasing with the chain length.

2.2 Correction to the Flory Distribution in a Melt

We want to know here how the screened interactions in the melt may affect the molecular weight distribution of living polymers (see section1.2.9 or [32, 15]). The deviation from that ideal distribution has already been evaluated in the dilute case in [71]. Here, the state of reference is the ideal chain in a melt of concentration of monomer c_0 (the interactions are supposed to be totally shielded). The statistical weight of an N-chain with the end-to-end distance r is given by the Gaussian kernel eq.(1.10) and the single-chain partition function is simply $Z_N^{(0)} = \int d\mathbf{r}\, G_N(r) = 1$. Then Cates showed [15, 68] that at the mean-field level, living chains follow the Flory distribution and the probability for a chain to be a N-mer is

$$P^{(0)}(N) = Z_N^{(0)} \mu e^{-\mu N} = \mu e^{-\mu N} \tag{2.15}$$

giving all the moments by the simple formula $\langle N^p \rangle^{(0)} = p!/\mu^p = p! \langle N \rangle^{(0)p}$. However, it is possible to assess the corrections to the probability induced by the effective potential U_{eff} derived *via* RPA. As already mentioned in the previous section, this potential is weak and can be treated perturbatively. The single N-chain partition function reads then, at first order

$$Z_N = \langle e^{-U_{\text{eff}}} \rangle_N \simeq 1 - \langle U_{\text{eff}} \rangle_N \tag{2.16}$$

where the brackets indicate Gaussian averaging, and U_{eff} is the sum of the pairwise screened interactions v_{eff} over the entire chain. At this point, it is important to remember that this effective potential explicitly depends on the distribution (see section 1.2.6 and [71, 70])

$$\frac{1}{v_{\text{eff}}} = \frac{1}{v} + c_0 F^{(0)}(q) \tag{2.17}$$

where $F^{(0)}$ is the intramolecular correlation function of ideal living polymers in $\mathbf{q}$-space (see eq.1.54 and section 3.2.1 for a small discussion). Therefore, when the mean-field correlation length is far smaller than the coil size $\xi = a/(\sqrt{2c_0 v}) \ll a/\sqrt{\mu}$, this potential reads[71]

$$v_{\text{eff}} = \frac{v\xi^2}{1 + q^2\xi^2}(q^2 + \frac{\mu}{a^2}). \tag{2.18}$$

With the notations of Fig.(2.4), the correction to the partition function reads

$$\langle U_{\text{eff}} \rangle_N = \sum_{s=0}^{N} (N - s) \int v_{\text{eff}}(q) G_s(q) \frac{d\mathbf{q}}{(2\pi)^3} \tag{2.19}$$

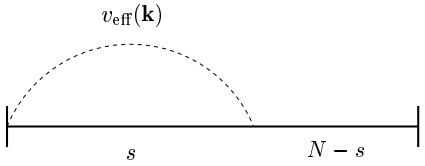

Figure 2.4: In an ideal N-chain there are $(N-s)$ equivalent pairs separated by s units.

or, defining the Laplace transform $\langle U_{\rm eff}\rangle_\tau = \int_0^\infty dN \langle U_{\rm eff}\rangle_N e^{-\tau N}$

$$\begin{aligned}\langle U_{\rm eff}\rangle_\tau &= \frac{1}{2\pi^2}\,\frac{v}{\tau^2 a^2}\int_0^\infty \frac{q^2}{q^2+\tau/a^2}\,\frac{q^2+\mu/a^2}{q^2+\xi^{-2}}\,dq \\ &= \frac{1}{4\pi^2}\,\frac{v}{\tau^2 a^2}\int_{-\infty}^\infty f(\tau,q)\,dq.\end{aligned} \tag{2.20}$$

It is first to be noted an unphysical ultraviolet divergence since $f(\tau,q)\simeq 1$ when q is large. Moreover that divergence is $\propto 1/\tau^2$ in Laplace space, thus $\propto N$, and would not change the physics of the problem. Removing that divergence, two residues contribute to that integral: the first singularity $i\xi^{-1}$ leads to a correction also $\propto N$ which is Edwards renormalization of the statistical segment discussed in appendices C and D. The interesting singularity is $i\sqrt{\tau}/a^2$ which leads to

$$\langle U_{\rm eff}\rangle_\tau \simeq -\frac{1}{8\pi\, c_0\, a^3}\left\{\frac{\mu}{\tau^{3/2}}-\frac{1}{\tau^{1/2}}\right\} \tag{2.21}$$

or in N-space

$$\begin{aligned}\delta Z_N = Z_N - Z_N^{(0)} = -\langle U_{\rm eff}\rangle_N \simeq -\frac{c}{\sqrt{N}}\{1-2\mu N\} \\ \text{with}\qquad c=\frac{1}{8\pi^{3/2}\, c_0\, a^3}\,.\end{aligned} \tag{2.22}$$

This equation gives the first corrections to the partition function. The first term of the correction scales as expected from a perturbative treatment of $U_{\rm eff}$ (see previous section). The second term scales as well in fact, taking $N=\langle N\rangle$, but it is worth more comments. This term is not perturbative any more when $N\simeq\langle N\rangle^2$. Indeed, considering an N-chain plunged in a melt of $\langle N\rangle$-chains, the effective excluded volume scales now as $v_{\rm eff}\simeq v/\langle N\rangle$ and the Fixman parameter now scales as [19] $u\simeq N^{1/2}/\langle N\rangle$. It shows explicitly that the N-chain would swell if $N\gtrsim\langle N\rangle^2$. Thus our mean-field approach

would fail (it is not the case here, the probability of such a large molecule is weak). It is also to be noted that this term is related to the γ critical exponent[18, 19] for swollen chains.

Therefore, with that correction, the corrected molecular-weight distribution is expected to read

$$P(N) \simeq \left(1 - \frac{c}{\sqrt{N}}\{1 - 2\mu N\}\right) \mu e^{-\mu N}. \tag{2.23}$$

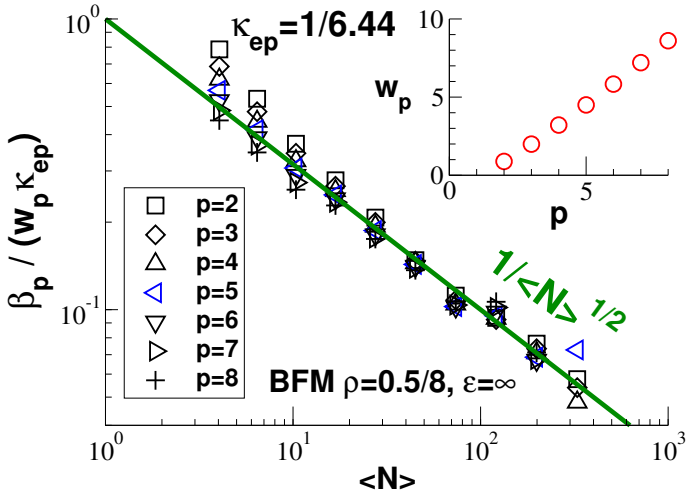

Figure 2.5: This figure shows the non-exponentiality of different size-moments for different mean size in simulations of dense systems of living polymer, performed by J. P. Wittmer. Using notations of eq.(2.24), it shows $\beta_p/(cw_p)$ *versus* $\langle N\rangle = 1/\mu$. It decreases as $\mu^{1/2}$, as predicted by eq.(2.24).

At this point, it is possible to define the non-exponentiality parameter β_p as the function which measures how the moments deviate from the ideal Flory distribution as

$$\begin{aligned}\beta_p &= 1 - \frac{\langle N^p\rangle}{p!\langle N\rangle^p} \\ &\simeq \frac{c}{p!}\left(\Gamma(p+1/2) + p\sqrt{\pi}\Gamma(p+1) - 2\Gamma(p+3/2)\right)\sqrt{\mu} = c\,w_p\sqrt{\mu} \qquad (2.24)\\ \text{with} \quad & w_1 = 0, \quad w_2 = \frac{\sqrt{\pi}}{2}, \quad w_3 = \frac{9\sqrt{\pi}}{8} \quad etc...\end{aligned}$$

which yields a decrease as $\sqrt{\mu}$ expected from the qualitative arguments for perturbations (see previous section). Some values of these deviations have been measured in numerical simulations of living polymers performed by J. P. Wittmer[7] (see Fig.2.5) and fit well to the theoretical prediction.

[7]For more details about these numerical simulations, see forthcoming papers of J. P. Wittmer.

Chapter 3

Form Factor in Dense Polymer Systems: Systematic Deviation from the Debye Formula

In this section, the intramolecular form factor $F(q)$ in dense polymer systems is discussed theoretically and confirmed by numerical simulations (performed by J. P. Wittmer). Following Flory's hypothesis (see section 1.2.6), chains in the melt should adopt Gaussian configurations and their form factor is supposed to be given by Debye's formula (eq.1.19). At striking variance to this, here is derived a noticeable (up to 20%) non-monotonic deviation which can be traced back to the incompressibility of dense polymer solutions beyond a local scale. The Kratky plot ($q^2F(q)$ *versus* wave-vector q) does not exhibit the plateau expected for Gaussian chains in the intermediate q-range (Fig.1.6). One rather finds a significant decrease according to the correction $\delta(F^{-1}(q)) = (q^3/32c_0)$ that only depends on the concentration c_0 of the solution, but not on the statistical segment or the interaction strength. Hence it is to be expected, that it survives renormalization procedure. We explicitly checked, that the numerical result obtained by Schäfer for infinite chains in the semidilute limit *via* renormalization techniques boils down to the above formula. The non-analyticity of the above q^3 correction is linked to the existence of long-range correlations for collective density fluctuations that survive screening (more discussed in section 4). In both Guinier regime (low-q range) and Kratky regime, finite-chain size effects are found to decay with chain length N as $1/\sqrt{N}$.

3.1 Introduction

Following Flory's ideality hypothesis [32], one expects a macromolecule of size N, in a melt (disordered polymeric dense phase) to follow Gaussian statistics [19, 25, 35, 56]. The official justification of this mean-field result is that density fluctuations are small, hence negligible. Early Small Angle Neutron Scattering experiments [37, 54] have been set up to check this central conjecture of polymer physics. The standard technique measures the scattering function $S(q)$ (q being the wave-vector) of a mixture of deuterated (fraction f) and hydrogenated (fraction $1-f$) otherwise identical polymers. The results are rationalized [10, 56] *via* the formula

$$S(q) \propto f(1-f)F(q). \tag{3.1}$$

to extract the form factor (single chain scattering function) $F(q)$. This formula neglects a χ Flory parameter between the two species (see [57] or [56, 37] and appendix B for arguments implying RPA). To reveal the asymptotic behavior of the form factor for a Gaussian chain $F^{(0)}(q) \sim 12/q^2b^2$, one usually plots $q^2F(q)$ versus q (called "Kratky plot"). The aim would be to show the existence of the "Kratky plateau" in the intermediate range of wave-vectors $\frac{2\pi}{R_\mathrm{g}} \lesssim q \lesssim \frac{2\pi}{b}$ ("Kratky regime") where R_g is the radius of gyration of the macromolecule and b is the (effective) statistical segment length [25]. In contrast to the low-q "Guinier regime" ($q \lesssim \frac{2\pi}{R_\mathrm{g}}$), clean scattering measurements can be performed in the Kratky regime[1] suggesting the measurement of b from the height of the Kratky plateau (see Fig.1.6).

Surprisingly, this plateau appears to be experimentally elusive as already pointed out by Benoît [37]: "Clearly, Kratky plots have to be interpreted with care". For typical experiments, the available q-range is $5 \cdot 10^{-3}\text{Å}^{-1} < q < 0.6\text{Å}^{-1}$. Kratky plots are quickly increasing at high q [54, 37], because of the rod-like effect starting at $q \sim \frac{1}{l_\mathrm{p}}$, when the beam is scanning scales comparable with the persistence length l_p (this regime is in fact used to assess l_p [12])[2]. Sometimes these curves can also quickly decrease, this is usually attributed to the fact that the chain cannot be considered as infinitely thin. The finite cross section of the chain tends to switch off the signal [54, 37, 12] as $\exp\left(-\frac{q^2R_\mathrm{c}^2}{2}\right)$, where R_c is the radius of gyration of the cross section (in CS_2, a good solvent for dilute polystyrene, $R_\mathrm{c}^2 = 9.5\text{Å}^2$ [55]). Rawiso *et al.* [54, 37] have also shown that sometimes

[1] Unwanted inhomogeneities (dusts or bubbles) scatter at low-q, also polydispersity effects are most important there.

[2] See also appendix A.

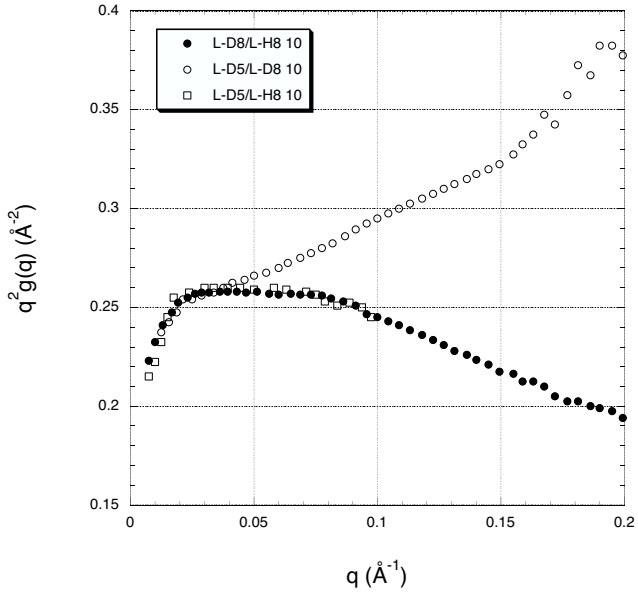

Figure 3.1: Scattering function of Polystyrene (PS) in the melt: the black circles describe the scattering D8-PS in H8-PS. The white circles are representing the scattering function of PS with deuterated phenyl-groups D5H3 with D8-PS, putting forward the behavior of the backbone of PS. The white squares shows the scattering function generated by the only lateral phenyl-groups.

these two effects can compensate. To illustrate this last statement, let us mention some experimental results of Combet, Boué and Rawiso [54, 55, 37]. They plotted the form factor of atactic polystyrene (PS) using the common deuterium labeling (see Fig.3.1). The black circles of figure 3.1 represent the form factor of an entire PS, using fully deuterated (8 D's instead of H's per monomer, noted D8, see Fig.3.2) and fully hydrogenated (H8) polymers. This curve lets appear a kind of plateau confirming *a priori* the Flory conjecture. This plateau even extends outside the intermediate regime to higher q-values. Then, they exploited the chemistry of PS (see Fig.3.2). They observed the effect of the only backbone, using blends of fully deuterated (D8) and partially (D5H3) labeled PS (it is possible to mark only the phenyl-groups). The resulting form factor is the curve with the white circles. They found what is expected for a thin macromolecule (see appendix A). When q^{-1} becomes of the order of the persistence length l_{p} (here ~ 10Å [12]), the Kratky representation of the form factor exhibits a linear increase. That

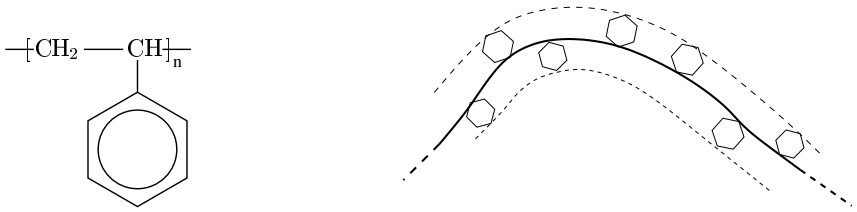

Figure 3.2: The formula of PS: it is possible to label only the phenyl-groups, and therefore quench the effective thickness according to the labeling.

plot suggests a misinterpretation of the first curve in terms of the Flory theorem. And finally to confirm their results, they observed the scattering function generated by the only phenyl-groups, masking the backbone using D5H3 and H8-PS (white squares on Fig.3.1). This curve naturally superimposes the first one. These results confirm the first idea: this plateau is in fact due to the compensation of the rod-like behavior by the effect of the effective thickness perceptible in that range of wave-vectors.

Indeed, up to now *no* scattering experiment has been performed on a sample allowing for a test over a wide enough range[3] of q and there exists *no* clear experimental evidence of the Kratky plateau expected for Gaussian chains. As we will show in this section, there are fundamental reasons why this plateau may actually *never* be observed, even for samples containing very long and flexible polymers. Recently, long-range correlations, induced by fluctuations, have been theoretically derived [63, 67, 64, 52] and numerically tested [67, 16] for two [63, 16] and three-dimensional dense polymer systems. The conceptually simpler part of these effects is related to the correlation hole [19] and happens to dominate the non-Gaussian deviations to the form factor[4] described here. This is derived in the following section 3.2. There we first recapitulate the general perturbation approach (section 3.2.1), discuss then the intramolecular correlations in Flory size-distributed polymers (section3.2.2) and obtain finally the form factor of monodisperse polymer melts by inverse Laplace transformation of the polydisperse case

[3]Obviously, these operational problems may be overcome in the future by using very long *and* flexible polymers provided labeled and unlabeled chains do not demix, $\chi N < 2$ with χ the Flory parameter (for a demonstration and further discussions, see appendix B). For a blend of hydrogenated and fully deuterated polystyrene at 453K, $\chi = 1.5 \cdot 10^{-4}$ [6]. Dilution is expected to upgrade the experimental conditions; this point is discussed in B.3.

[4]A more subtle effect arises from the non-mean-field treatment [64, 52]) of the bath of linear chains (with strictly no cycles) surrounding the chain under consideration. This can be shown to be negligible.

(section 3.2.3).

3.2 Analytical Results

3.2.1 The Mean-Field Approach

It has been shown in section 1.2.6 that at the mean-field level [25], the excluded volume interaction is entropically screened in dense polymeric melts. Edwards and de Gennes [25, 19, 28, 29, 24] developed the self-consistent mean-field method (see section1.2.6) to derive this screened mean (molecular) field. The most important result they obtained is eq.(1.30). It is also shown in section1.2.6 that the interactions between labeled monomers are screened by the background of unlabeled monomers, and linear response gave the screened effective potential of eq.(1.34). To apply these formulas, the form factor $F^{(0)}(q)$ has to be properly averaged over the relevant size-distribution of the chains [24]. From now on, we will consider a dense system of long chains with exponentially decaying number density $\phi_N = c_0\,\mu^2 e^{-\mu N}$ for polymer chains of length N with $\mu \equiv 1/\langle N\rangle$ being the chemical potential. This so-called Flory distribution is relevant to living polymers (noted EP for equilibrium polymers) systems (see section 1.2.9 and of course [15, 68]). Hence, eq.(1.34) yields (using eqs(1.52) and (1.54)) [71]

$$v_{\rm eff}(q) \;= \frac{v\xi_\mu^2}{1+q^2\xi_\mu^2}(q^2+\frac{\mu}{a^2}) \underset{R_{\rm g}\gg\xi}{\approx} \frac{v\xi^2}{1+q^2\xi^2}(q^2+\frac{\mu}{a^2}). \qquad (3.2)$$

Here a is the characteristic length of the monomer ($a^2 \equiv b^2/6$) and $\xi_\mu = \sqrt{\frac{a^2}{2c_0 v+\mu}} \underset{R_{\rm g}\gg\xi}{\approx} \sqrt{a^2/2c_0 v}$ is the mean-field correlation length. When chains are infinitely long ($\mu \to 0$) we recover the classical result by Edwards [25] ignoring finite-size effects. If we further restrict ourselves to length scales larger than ξ ($q\xi \ll 1$) eq.(3.2) simplifies to $v_{\rm eff}(q) \approx q^2a^2/2c_0$ which does not depend on the bare excluded volume v and corresponds to the incompressible melt limit. For very large scales ($qR_{\rm g} \ll 1$) one obtains the contact interaction associated to the volume $v^* \equiv v_{\rm eff}(q \to 0)$, such that $v^*/v = \mu\xi^2/a^2 \sim \xi^2/R_{\rm g}^2$ (far weaker than the initial one given in the direct space by $v(\mathbf{r}) = v\delta(\mathbf{r})$). The interaction v^* is relevant to the swelling of a long chain immersed in the polydisperse bath [19]. The screened excluded volume interaction eq.(3.2) taken at scale $R_{\rm g}$ is weak and decays with chain length as $1/\langle N\rangle$. The associated perturbation parameter u in d-dimensional space depends on chain length as $u \simeq v^*N^2/R_{\rm g}^d \sim \langle N\rangle^{1-d/2}$ and the screened

excluded volume potential is, hence, perturbative in three dimensions (see [19] and 1.2.5). So, for a quantity $\langle A \rangle$, if the system is only perturbed by a potential U, the first order correction reads [48]

$$\delta\langle A \rangle \equiv \langle A \rangle - \langle A \rangle_0 \simeq \langle U \rangle_0 \langle A \rangle_0 - \langle UA \rangle_0 \tag{3.3}$$

where the index 0 indicates that the averaging is made on the statistical ensemble before the perturbation (here the Gaussian ensemble.) Thus, one can perturb the two-point Gaussian correlation function for two points separated by s monomers

$$G_s^{(0)}(q) = \langle \exp(-i\mathbf{q} \cdot \mathbf{r}_s) \rangle_0 = \exp\left(-sq^2a^2\right) \tag{3.4}$$

with the molecular field eq(3.2). In this type of calculations, there are only

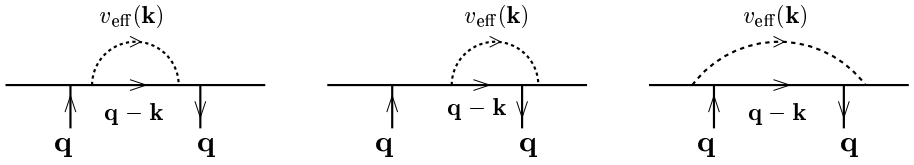

Figure 3.3: Non-zero contributions to the first-order perturbations.

three non-zero contributions [26] (see diagrams on Fig.3.3). Knowing this correlation, it is possible to derive many single-molecule properties.

3.2.2 Intramolecular Correlations for Flory Size-Distributed Polymers

The intramolecular correlation function is investigated through its Fourier transform, the form factor. Let us consider a polydisperse system with a Flory-type size-distribution. In this case, the form factor reads as in eq.(1.52) with $\mathbf{q}$ the scattering vector. If the chains followed Gaussian statistics (as suggested by the Flory's hypothesis), one should find using eq.(3.4) the same result as in eq.(1.54), $F^{(0)}(q) = 2/(\mu + q^2a^2)$. The ideal chain form factor for Flory size-distributed polymers is represented in the Figures 3.11, 3.12 and 3.13 where it is compared to the computational results on equilibrium ("living") polymers discussed below in section 3.3, due to J.P. Wittmer. In the small-q regime, $qR_{\text{g}} \ll 1$ and for a polydisperse system, we can measure R_{g} *via* the Guinier relation [35, 24, 37] as mentioned in the end of section1.2.9, in eqs (1.55,1.56). In order to understand more deeply how the corrections are evaluated, let us give some details about the

construction of the first (top-left) diagram of Fig.3.3 with the screened potential $v_{\text{eff}}(\mathbf{r}) = \int v_{\text{eff}}(q) e^{i\mathbf{q}\cdot\mathbf{r}} d^3\mathbf{q}/(2\pi)^3$. Following the general definition of the form factor for the Flory distribution eq.(1.52), perturbations drive to evaluate

$$\begin{aligned}\delta F(q) &= \sum_{N=0}^{\infty} \mu^2 e^{-\mu N} \sum_{i,j=1}^{N} \delta\langle \exp(-i\mathbf{q}\cdot\mathbf{r}_{i,j})\rangle \\ &= \sum_{N=0}^{\infty} \mu^2 e^{-\mu N} \sum_{i,j=1}^{N} \delta G_{|i-j|}(q).\end{aligned} \tag{3.5}$$

It comes down to evaluating $\delta G_{|i-j|}(q)$. For the top-left diagrams, it is exactly equation (D.1) in appendix D. And, as in appendix D, because of this special distribution, one enjoys the properties of Laplace transforms. So, the same procedure applied to each diagram, yields, after summation of all the contributions,

$$\begin{aligned}\delta F(q) = F(q) - F^{(0)}(q) =& \frac{v}{4\pi^2 a^2(\mu + q^2a^2)^2} \int_{\mathbb{R}} dk \frac{k^2\xi^2}{1+k^2\xi^2} \\ & \frac{(2\mu + (q^2+k^2)a^2)^2}{\mu + k^2a^2} \left(\frac{2}{\mu + (q^2+k^2)a^2} - \frac{1}{2kqa^2} \ln\left(\frac{\mu + (q+k)^2a^2}{\mu + (q-k)^2a^2} \right) \right).\end{aligned} \tag{3.6}$$

The contributions to this integral come from three poles, one at $k = i\xi^{-1}$, this high-k contribution renormalizes the statistical segment, one at $k = i\sqrt{q^2 + \frac{\mu}{a^2}}$, one at $k = i\sqrt{\frac{\mu}{a^2}}$ and from the logarithmic branch cut. Absorbing the high-k pole contributions in the renormalized statistical segment b^* [25], and using b^* instead of b in the definition of $F^{(0)}(q)$ (see appendices C and D), one finds (in the limit $q\xi < 1$) as a function of $Q = qR_{\text{g}}^{(0)} = 3qa/\sqrt{\mu}$

$$\delta F(Q)/c = \frac{\sqrt{3}}{Q^2} \left(\frac{1}{(1+\frac{Q^2}{3})^{3/2}} - 1 \right) - \frac{1}{Q} \arctan\left(\frac{Q}{2\sqrt{3}} \right) + \frac{1}{\sqrt{3}} \frac{2+Q^2}{(1+\frac{Q^2}{3})^2}. \tag{3.7}$$

We have introduced here the factor $c = 9R_{\text{g}}^{(0)}/(\pi c_0 b^{*4})$ to write the deviation in a form which should scale with respect to chain length. The statistical segment length b^* is given by:

$$b^{*2} = b^2 \left(1 + \frac{12v\xi}{\pi b^4} \right). \tag{3.8}$$

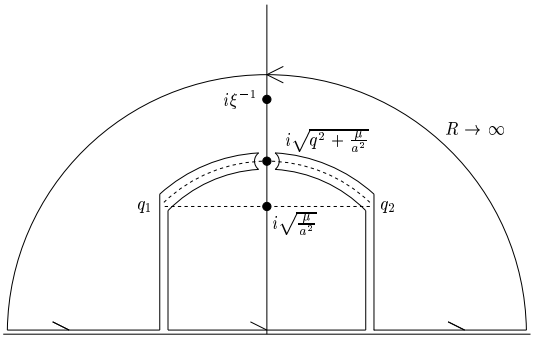

Figure 3.4: A possible contour in the $\mathbb{C}$ plane. The dashed line depicts the logarithmic branch-cut, which is an arc of the circle of radius $r = \sqrt{\mu + q^2 a^2}$ between $q_1 = re^{i(\pi-\alpha)}$ and $q_2 = re^{i\alpha}$, with $\alpha = \arctan(\sqrt{\mu/q^2a^2})$. The other singularities are single poles at $k = i\xi^{-1}$, $k = i\sqrt{\mu/a^2}$ and at $k = i\sqrt{q^2 + \mu/a^2}$. This contour is very similar to Fig.4.1.

As may be seen from the plot of eq.(3.7) in Fig.3.5, the deviation from ideality is positive for small wave-vectors (with a pronounced maximum at $Q \approx 1$). It becomes negative when the internal coil structure is probed ($Q \gg 2$). Asymptotically, eq.(3.7) gives

$$\delta F(q) \underset{\frac{qa}{\sqrt{\mu}} \ll 1}{\simeq} \frac{11 R_{\rm g}^{(0)}}{4\sqrt{3}\pi c_0\, b^{*4}} q^2 R_{\rm g}^{(0)\,2}, \tag{3.9}$$

(one dashed line in Fig.3.5) which highlights the average swelling factor of the molecule in the melt:

$$R_{\rm g}^2 = R_{\rm g}^{(0)2}\, \frac{b^{*2}}{b^2} \left(1 - \frac{11\sqrt{6}}{16\pi c_0\, b^{*3}} \sqrt{\mu} \right) \tag{3.10}$$

(comparable to a logarithmic term in the two-dimensional case [63, 50]). This is a sign of swelling, because $R_{\rm g} = \langle N \rangle^{1/2} f(\sqrt{\langle N \rangle})$, with f, an increasing function, showing that the apparent swelling exponent ν for finite $\langle N \rangle$ is slightly larger than $1/2$. It is interesting to compare it with the (Z-averaged) end-to-end distance, easily available because it involves only double differentiation with respect to $\mathbf{q}$ of the top-left diagram of Fig.3.3 (check also the end of C):

$$R_{\rm e}^2 = R_{\rm e}^{(0)2}\, \frac{b^{*2}}{b^2} \left(1 - \frac{10\sqrt{6}}{16\,\pi c_0\, b^{*3}} \sqrt{\mu} \right). \tag{3.11}$$

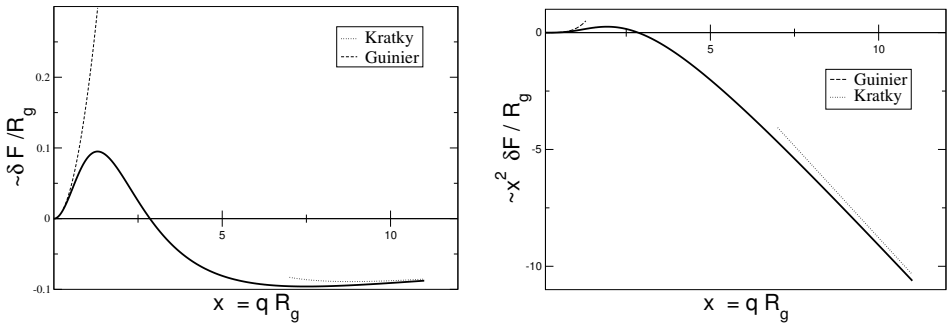

Figure 3.5: Direct and Kratky-like representation of the correction to the form factor. The crossover is at $qR_{\rm g}^{(0)} \simeq 5$. In the Kratky plot, one should eventually identify a hump at the crossover, and a decrease instead of the Kratky plateau to confirm this correction.

The naively defined size-dependent effective statistical segment of an N-chain (from $R_{\rm e}^2 = b_{\rm eff}^2 N$) therefore is:

$$b_{\rm eff}^2 = b^{*2}\left(1 - \frac{\text{const}}{c_0\, b^{*3}\sqrt{N}}\right) \tag{3.12}$$

The size-dependencies in eqs (3.10,3.11) follow the same scaling, but the numerical factors are different. Although internal segments carry a smaller correction ([67] and appendix C), the size-dependent contact potential $\mu/2c_0$ in eq. 3.2 counterbalances this effect and makes the correction to eq.(3.11) a little smaller than the one in eq.(3.10).

The asymptotic behavior of eq.(3.7) in the Kratky regime gives

$$\delta F(q) \underset{qR_{\rm g}\gg 1}{\simeq} \frac{12}{q^2 b^{*2}}\left(\frac{3\sqrt{6}}{\pi c_0\, b^{*3}}\sqrt{\mu} - \frac{3q}{8c_0\, b^{*2}}\right), \tag{3.13}$$

which is also represented in Fig.3.5. The first term in this equation is a size-dependent shift of the Kratky plateau, and the second one, independent of the size, makes the essential difference with the Flory prediction. Hence, the corrections induced by the screened potential are non-monotonic.

Eq.(3.6) is not restricted to $q\xi < 1$, it is applicable over the entire q-range in the case of weakly fluctuating dense polymers[5] (mean-field excluded

[5]The full cumbersome expression leading to eq.(3.7) is not given here.

volume regime) as simulated from soft monomers (allowed to overlap with some small penalty) [66]. In the case of strong excluded volume and less dense solutions (critical semidilute regime, not explicitly considered here) the results are valid at scales larger than ξ provided the statistical segment is properly renormalized. Quantitatively, the Ginzburg parameter measuring the importance of density fluctuations reads $G_z^2 = v/(c_0\, b^6)$. For persistent chains $l_\mathrm{p} > t$, t being the thickness of the chain, density fluctuations are negligible provided $G_z^2 \sim 1/(\Phi\, l_\mathrm{p}^3/t^3) \ll 1$, with $\Phi = c_0\, t^3$, the monomer volume fraction. The above makes sense if $\xi \gg l_\mathrm{p}$, which requires $\Phi < t/l_p$. This criterion also indicates the isotropic/nematic transition [35, 47]. In summary, mean-field applies provided $\left(\frac{t}{l_\mathrm{p}}\right)^3 < \Phi < \frac{t}{l_\mathrm{p}}$. More details about these arguments are given in section 1.2.7.

3.2.3 Monodisperse Polymer Melts in Three Dimensions

It is possible to relate the form factor of the polydisperse system (Flory distribution) to the form factor $F_N(q)$ of a monodisperse system. Following eqs(1.52,3.5),

$$F(q) = \frac{\sum_{N=0}^{\infty} \phi_N N F_N(q)}{\sum_{N=0}^{\infty} \phi_N N} = \sum_{N=0}^{\infty} \mu^2 \exp(-\mu N) N F_N(q) \tag{3.14}$$

the deviations of the form factors of monodisperse and polydisperse systems are related by the inverse Laplace transformation $\delta F_N(q) = \frac{1}{N}\mathcal{L}^{-1}\left(\frac{1}{\mu^2}\delta F(q)\right)$, $\mathcal{L}$ being the Laplace transform operator. Using our result eq.(3.7) for polydisperse systems this yields:

$$\begin{aligned} \delta F_N(Q)/c \;&\simeq\; \frac{2}{\sqrt{\pi}Q^2}e^{-Q^2} + \frac{5}{\sqrt{\pi}Q^2} - \left(\frac{2}{\sqrt{\pi}Q} + \frac{7}{\sqrt{\pi}Q^3}\right) D(Q) \\ &+\; \frac{4}{\sqrt{\pi}Q^3}\int_0^1 \left(\frac{2}{\alpha^3} D\left(\frac{\alpha Q}{2}\right) - \frac{Q}{\alpha^2}\right) d\alpha, \end{aligned} \tag{3.15}$$

where $Q = qR_{\mathrm{g},N}^{(0)}$ with $R_{\mathrm{g},N}^{(0)} = \sqrt{N}a$, the radius of gyration in the ideal monodisperse case and $D(x)$ is the Dawson function, whose definition is $D(x) = e^{-x^2}\int_0^x e^{t^2} dt$ [1]. Eq.(3.15), shown in Fig.3.6, is accurate up to the finite size corrections to the interaction potential as these have been calculated for the Flory distribution, eq.(3.2) (see appendix C.2 for a small discussion). However, on small length scales, this influence is weakened, and

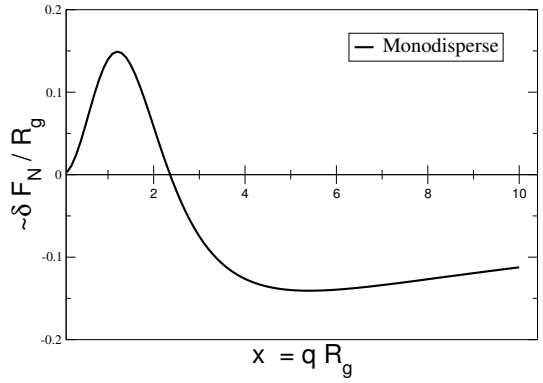

Figure 3.6: Direct representation of the correction to the form factor in a monodisperse system. The shape is similar to that in the polydisperse case (Fig.3.5). Polydispersity merely affects the Guinier regime.

in this limit, it gives:

$$F(q) \underset{qR_g \gg 1}{\simeq} \frac{12}{q^2 b^{*2}} \left(1 + \frac{6\sqrt{6}}{\pi^{3/2} c_0 \, b^{*3}} \frac{1}{\sqrt{N}} - \frac{3q}{8 c_0 b^{*2}} \right). \tag{3.16}$$

Taking $\langle N \rangle = 1/\mu$, eq.(3.13) deviates from eq.(3.16) only by the numerical coefficient in front of $1/\sqrt{N}$. The difference is $\sim 10\%$.

3.2.4 Infinite Chain Limit and Scaling Arguments

It is worthwhile to discuss the infinite chain limit, $\mu \to 0$, that puts forward most clearly the essential differences with an ideal chain (the differences between monodisperse and polydisperse systems are inessential in this limit). We can write the form factor of an infinite chain ($R_g \to \infty$) at scales larger than ξ as:

$$F(q) \simeq \frac{12}{q^2 b^{*2}} \frac{1}{\left(1 + \frac{3}{8} \frac{q b^*}{c_0 \, b^{*3}} \right)}. \tag{3.17}$$

Following standard notations [16, 57, 58], we may rewrite eq.(3.17) in the form:

$$\frac{1}{F(q)} = \frac{q^2 b^{*2}}{12} + \frac{1}{32} \frac{q^3}{c_0}. \tag{3.18}$$

The correction term obtained in the one-loop approximation eq.(3.18) depends neither on the excluded volume parameter v nor on the statistical

segment. Hence, it is expected to hold even in the strongly fluctuating semidilute regime and it is of interest to compare our results with the recent renormalization group calculations of L. Schäfer [57]. There, the skeleton diagrams for the renormalization of interaction and statistical segment have also been performed within the one-loop approximation. From the above, it is expected that both results are identical. After careful insertions (eq.(18.23), p. 389 of Ref. [57]) a q^3/c_0 correction can be extracted with the universal amplitude 0.03124... The fact that this numerical amplitude is so close to our $1/32 = 0.03125$ comforts both our and Schäfer's result.

This corrected form factor may also be written as a function of the Ginzburg number

$$\frac{12}{F(q)} \simeq q^2 b^{*2} + const\,\frac{q^3}{c_0} \simeq q^2 b^{*2}(1 + const\, q\xi\, G_z), \tag{3.19}$$

where *const* designates different constant prefactors. This last formula may be adapted to the semidilute case[6]: in a good solvent, a chain may be seen as an ideal necklace of N/g ($\to \infty$) swollen blobs of size ξ^2 [19]. In each blob, the chain is swollen following the scaling law $\xi = g^\nu b$, where ν is the critical exponent of swelling. As mentioned in the introduction, the correlation length is related to the concentration *via* the relation $c_0 \sim \xi^{1/\nu - d}$. Thus when $G_z \simeq 1$, taking into account the residual interactions between blobs yields to the scaling law

$$\frac{12}{F(q)} = \frac{q^2\xi^2}{g} + const\,\frac{q^3}{c_0} \simeq \frac{q^2\xi^2}{g}(1 + const\, q\xi). \tag{3.20}$$

The essential difference with the preceding formula is featured in the dominant term.

It is possible to perform an inverse Fourier transform of the form factor, eq.(3.17) using the contour shown on Fig.3.7. It gives not only the Coulomb-like term from the singularity at the origin, but also another long-range contribution arising from the branch cut:

$$G_{\text{intra}}(r) = \frac{12}{b^{*2}}\frac{1}{4\pi r} - \frac{9}{4}\frac{1}{c_0 b^{*4}}\frac{1}{\pi^2 r^2} \qquad \text{for} \qquad b^* \ll r \ll \frac{b^*}{\sqrt{\mu}}. \tag{3.21}$$

The correction is never dominant in real space. But both contributions are different in nature. In the collective structure factor [64, 52] $S^{-1}(q) \sim v + c_2 q^2 + c_3 q^3$, the leading singularity of eq.(3.17) is shifted away from the origin and the corresponding contribution is screened on the length scale ξ in real space[7]. The branch cut (from the q^3 term) still contributes a

[6] This point was raised by M. Daoud during the defence.

[7] These correlations are derived in chapter 4

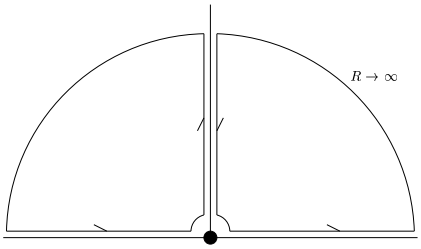

Figure 3.7: One of the possible contour to inverse the form factor. The Coulomb-like term emerges from the singularity at the origin while the correction comes from the branch-cut along the imaginary axis.

power law, namely an anti-correlation term decreasing as r^{-6}, that has been identified as a fluctuation-induced Anti-Casimir effect [64, 52] (or as the $n-1=-1$ Goldstone mode in the polymer-magnet analogy [51]). The average number of particles from the same molecule in a sphere of radius R, $\mathcal{N}(R) = \int G_{\rm intra}(r) d^3\mathbf{r}$ is decreased (compared to a Gaussian coil) because of the sign of the correction. Nevertheless, the differential (apparent) Hausdorff dimension [8] $d_{\rm H}$ as defined by $d_{\rm H} = \mathrm{d}\log\mathcal{N}(R)/\mathrm{d}\log R$ is increased.

The fluctuation corrections presented in eqs(3.17,3.18,3.21) can be interpreted with the following argument, involving $G(r,s)$, the correlation function of two points separated by s monomers

$$G(r,s) = \int \frac{d\mathbf{q}}{(2\pi)^3} G_s(q) e^{i\mathbf{q}\cdot\mathbf{r}}. \tag{3.22}$$

For infinite chains $N \to \infty$, $\mu \to 0$, the form factor is

$$F(q) = 2\int ds\, G_s(q). \tag{3.23}$$

For large s, the distribution G is nearly Gaussian, but with the renormalized statistical segment eq.(3.8)

$$G(r,s) \simeq G^{(0)}(r,s) = \left(\frac{6}{4\pi b^* s}\right)^{3/2} \exp\left(-\frac{6r^2}{4b^{*2}s}\right) \qquad \text{for } s \to \infty. \tag{3.24}$$

The difference $\delta G(r,s) \equiv G(r,s) - G^{(0)}(r,s)$ is discussed below in the limit of large and small geometrical separation r between monomers. A highly stretched s-fragment ($r \gg b^*\sqrt{s}$) can be viewed as a string of Pincus blobs, each blob of $g \sim s^2b^2/r^2$ units (gr^2 scales as the stretched segment s^2b^2). Different blobs do not overlap in this limit, therefore the effective statistical

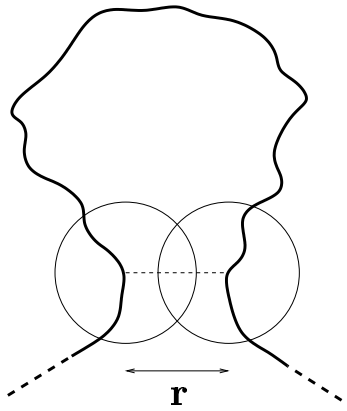

Figure 3.8: For small end-to-end distances $r \ll \sqrt{s}b^*$, monomers of terminal blobs with $g \sim r^2/b^{*2}$ interact.

segment of the blob, $b_{\rm eff}$ comes as a result of interactions of units inside the blob see (eq.3.12 and appendix C)

$$b_{\rm eff}^2 = b^{*2}\left(1 - \frac{const}{c_0\, b^{*3}\sqrt{g}}\right) \tag{3.25}$$

where *const* is a universal numerical constant. The elastic energy of stretching the s-segment is therefore

$$W_{\rm el}(r) = \frac{6r^2}{4b_{\rm eff}^2 s} \simeq \frac{6r^2}{4b^{*2}s}\left(1 + \frac{const}{c_0\, b^{*4}}\frac{r}{s}\right).$$

Thus, when $r \gg \sqrt{s}b^*$

$$G(r,s) \simeq G^{(0)}(r,s)\exp\left(-const\frac{r^3}{c_0\, b^{*6}s^2}\right). \tag{3.26}$$

The faster decay of G as compared to $G^{(0)}$ leads to higher scattering (positive $\delta F(q)$) at small q.

On smaller length scales, $r \ll \sqrt{s}b^*$, it is convenient to consider the s-fragment as a chain of blobs of size r, with $g \sim r^2/b^{*2}$. This is sketched in Fig.3.8. The correction δG here is essentially due to the direct interaction of the overlapping blobs or radius r around the two correlated monomers. The number of binary contacts is proportional to g^2/r^3, while the pairwise interaction between monomers scales like $1/gc_0$ (see eq 3.2), giving [63] $U \sim$

$g/c_0\, r^3 \sim 1/r b^{*2} c_0$. Therefore, for $\xi \ll r \ll \sqrt{s}\, b^*$,

$$\begin{aligned} G(r,s) &\simeq G^{(0)}(r,s)\,(1-U) \\ &\simeq G^{(0)}(r,s)\left(1 - \frac{const}{r b^{*2} c_0}\right), \end{aligned} \tag{3.27}$$

which qualitatively explains eq.(3.21). For $q \gg \frac{1}{\sqrt{s}b}$, we get:

$$\delta G_s(q) = -const \left(\frac{6}{4\pi b^{*2} s}\right)^{\frac{3}{2}} \frac{4\pi}{q^2 b^{*2} c_0}. \tag{3.28}$$

This regime is limited by the condition $q\xi \ll 1$. Thus the low-q correction is positive and it increases with q, while the high-q correction $\delta G_s(q)$ is negative and is also increasing with q, implying an intermediate decline. This non-monotonic behavior of $\delta G_s(q)$ translates in a non-monotonic dependence of $\delta F(q)$ for finite N (Figures 3.5, 3.6). And finally, using eqs (3.23,3.28), with the condition $q \gg \frac{1}{\sqrt{s}b}$ providing a lower cut-off $s_{\rm cut} \sim 1/(q^2 b^2)$, it is instant that

$$\delta F(q) = -\frac{const}{\phi\, b^{*4}} \frac{1}{q} \qquad \text{for } q \ll \xi^{-1}. \tag{3.29}$$

To underline the origin of this "non-analytical" term $1/q$, let us give some details of an easy calculation of the correction to the correlation function for the infinite chain. The top-left diagram in Fig.3.3 is the only diagram producing this term. With notations shown in Fig.3.9 we can write the corresponding analytical expression:

$$\begin{aligned} \delta F(q) = -\sum_{\substack{n-m,m-l \\ t-n}} \int d\mathbf{k}\, v_{\rm eff}(\mathbf{k}) \exp(-\mathbf{k}^2 (m-l) a^2) \\ \exp(-(\mathbf{q}+\mathbf{k})^2 (n-m) a^2) \exp(-\mathbf{k}^2 (n-t) a^2). \end{aligned} \tag{3.30}$$

Here $e^{-\mathbf{k}^2 (m-l) a^2}$ is the correlation function of the chain between monomers l and m. In the interaction, we will leave only the k^2-dependent part. After summation (integration) over $m-l$ and $n-t$ we get:

$$\delta F(q) = -\frac{v\xi^2}{a^4} \sum_{n-m=0}^{\infty} \int \exp(-(\mathbf{q}+\mathbf{k})^2 (m-n) a^2) d(\cos\theta) dk. \tag{3.31}$$

Then, after integration over $n-m$ we get:

$$\delta F(q) = -\frac{v\xi^2}{|q| a^6} \int_{-1}^{1} \frac{d(\cos\theta)}{\sqrt{1-\cos^2\theta}} \simeq -\frac{1}{c_0 b^{*3}} \frac{1}{|q| b^*} \tag{3.32}$$

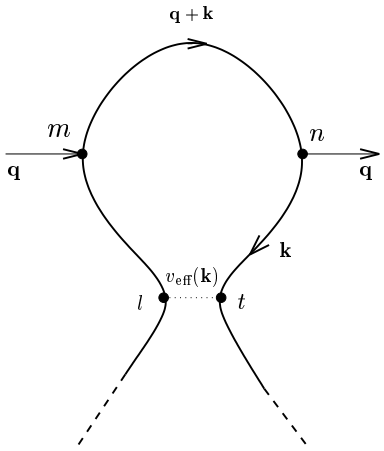

Figure 3.9: Diagram producing the non-analytical term for an infinite chain. The mixing of the wave-vectors is pinned in the (m, n) segment. The summation is first done on (n, t) and (m, l).

which is similar to eq. (3.28). It should be emphasized that for a finite chain, the finite summation over $m-l$ and $n-t$ produces extra terms, and these "odd" terms exist only for $qR_{\rm g} < 1$.

3.2.5 Domain of validity of the results

Let us precise the domain of validity of our results[8]: our perturbation approach, developped at low $G_{\rm z}$, leads us to quantities depending on the renormalized statistical segment b^* as shown, for instance, in equations (3.9,3.10,3.11,3.13). Our results has to be understood as a double expansion in the parameter $G_{\rm z}$ and in the parameter $q\xi \sim \xi/R_{\rm g}$. The only dependence in $G_{\rm z}$ comes from this renormalized statistical segment (see also appendix C)

$$b^{*2} = b^2 \left(1 + \frac{\sqrt{12}}{\pi} G_{\rm z} \right). \tag{3.33}$$

It is therefore possible to extend this last formula to higher Ginzburg parameter: the renormalized statistical segment would then read

$$b^{*2} = b^2 \left(1 + \sum_n \alpha_n {G_{\rm z}}^n \right), \tag{3.34}$$

[8]This question was raised by A. E. Likhtman and J.-F. Joanny during the defence.

but the generic formula (3.12), as well as all other quantities expressed as functions of this relevant parameter remain unchanged. So, noticing that this renormalized segment b^*, oppositely to b, may be experimentally determined, our results should be valid even for Ginzburg number of order unity.

3.3 Computational Results

This section retranscribes nearly exactly computational considerations, numerical results and analyses which are to be attributed to J. P. Wittmer. They tend to confirm the predictions of the previous sections. Please note that, in that part, the density is not noted c_0, but ρ (as in the figures) and quantities are expressed in lattice units.

The previous section contains non-trivial results due to *generic* physics which should apply to all polymer melts containing *long* and preferentially *flexible* chains. We have put these predictions to a test by means of extensive lattice Monte Carlo simulations [5] of linear polymer melts having either a quenched and monodisperse or an annealed size-distribution. For the latter "equilibrium polymers" (EP) one expects (from standard linear aggregation theory) a Flory distribution if the scission energy E is constant (assuming especially chain length independence) [15, 68]. (Apart from this finite scission energy for EP all our systems are perfectly athermal. We set $k_BT = 1$ and all length scales will be given below in units of the lattice constant.) We sketch first the algorithm used and the samples obtained and discuss then the intramolecular correlations as measured by computing the single chain form factor $F(q)$.

3.3.1 Algorithm and some Technical Details

For both system classes we compare data obtained with the three dimensional bond-fluctuation model (BFM) [14] where each monomer occupies the eight sites of an unit cell of a simple cubic lattice. For details concerning the BFM see Refs. [14, 5, 68]. For all configurations we use cubic periodic simulation boxes of linear size $L = 256$ containing 2^{20} monomers. These large systems are needed to suppress finite size effects, especially for EP [68]. The monomer number relates to a number density $\rho = 1/16$ where half of the lattice sites are occupied (volume fraction 0.5). It has been shown that this "melt density" is characterized by a small excluded volume correlation length ξ of order of the monomer size [14, 5], by a low (dimensionless) compressibility, $S(q \to 0)/\rho = 1/v\rho = 0.24$, as may be seen from the bold line ($f = 1$) indicated in the main panel of Figure 3.10, and an effective statistical segment length, $b^* \approx 3.24$ [67][9] The chain monomers are connected by (at most two saturated) bonds. Adjacent monomers are permanently linked

[9] b^* may be best obtained from the intramolecular (mean-squared) distance $\langle R^2(s)\rangle$ averaged over all monomer pairs $(n, m = n + s)$. As suggested by eq(3.12) one plots

together for monodisperse systems (if only local moves through phase space are considered). Equilibrium polymers on the other hand have a finite and constant scission energy E attributed to each bond (independent of density, chain length and position of the bond) which has to be paid whenever the bond between two monomers is broken. Standard Metropolis Monte Carlo is used to break and recombine the chains. Branching and formation of closed rings are explicitly forbidden and only linear chains are present. The delicate question of "detailed balance", *i.e.* microscopic reversibility, of the scission-recombination step is dealt with in Ref. [39].

The monodisperse systems have been equilibrated and sampled using a mix of local, slithering snake and double pivot moves [5]. This allowed us to generate ensembles containing about 10^3 independent configurations with chain length up to $N = 4096$ monomers. We have sampled EP systems with scission energies[10] up to $E = 15$, the largest energy corresponding to a mean chain length $\langle N \rangle \approx 5500$. (Other mean chain lengths are given in the Figures 3.11 and 3.13.) It has been verified (as shown in Refs. [68, 39]) that the size-distribution obtained by our EP systems is indeed close to the Flory distribution studied in the analytical approach presented in the previous section[11]. For EP only local hopping moves are needed in order to

---

$y = \langle R^2(s) \rangle / s$ as a function of $x = 1/\sqrt{s}$ which allows the one-parameter fit:

$$y = b^* \left(1 + \frac{\sqrt{24/\pi^3}}{\rho {b^*}^3} x \right).$$

[10]The scission energy E is related to μ [15, 68] *via* $\mu \simeq \rho^{-1/2} e^{-E/2}$ in the Mean-Field approximation, which *a priori* applies in dense systems.

[11]In fact, consistency of our approach suggests that the self-interaction of the chains should *alter* the concentration of large EP. Instead of a perfect Flory distribution, one expects for dense solutions (additional corrections arise in the dilute and the semidilute regimes [68])

$$\rho_N \propto \exp(-\mu N) \left(1 - \frac{c}{\sqrt{N}} (1 - 2\mu N) \right)$$

with the (small) coefficient $c = \frac{1}{8\pi^{3/2} \rho a^{*3}} \approx 1/6.44$. We have checked numerically that this is indeed true by computing the non-exponentiality cumulant β_p for different moments p. Although the effect is small one confirms readily that

$$\beta_p \equiv 1 - \frac{\langle N^p \rangle}{p! \langle N \rangle^p} \Rightarrow \frac{w_p c}{\sqrt{\langle N \rangle}} \text{ for } \langle N \rangle \gg 10$$

where the coefficients w_p can be obtained from the size-distribution (see eq.2.24). It should be pointed out that Figure 3.14 can be significantly improved if we take as reference $F^{(0)}(q)$ not eq 1.54 (perfect Flory distribution) but the one corresponding to the slightly modified distribution. Details will be presented elsewhere [66].

sample independent configurations since the breaking and recombination of chains reduce the relaxation times dramatically, at least for large scission-recombination attempt frequencies[12]. In fact, all EP systems presented here have been sampled within four months while the sample of monodisperse $N = 4096$ configurations alone required about two years on the same XEON processor. EP are therefore very interesting from the computational point of view, allowing for an efficient test of theoretical predictions which also apply to monodisperse systems.

[12]The equilibration criterion is not the diffusion of a typical chain over its radius of gyration but rather the diffusion time of a small segment $\lambda \ll N$ which has just about the time to diffuse over its radius $\sim \lambda^{1/2}$ before it breaks or recombines [15]. It should be emphasized that due to the permanent recombination events a data structure based on a topologically ordered intra chain interactions is not appropriate and straight-forward pointer lists between connected monomers are required [68]. The attempt frequency should not by taken too large to avoid useless immediate recombination of the same monomers and some time must be given for the monomers to diffuse over a couple of monomer diameters between scission-recombination attempts [39]

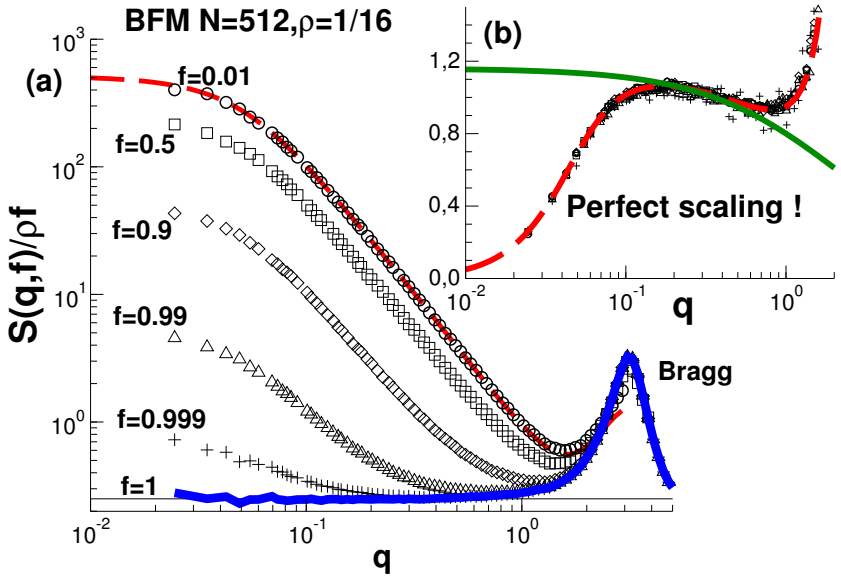

Figure 3.10: The response function $S(q,f)$ of a fraction f of marked monodisperse chains of chain length $N = 512$. The remaining $1-f$ chains are considered to be not "visible" for the scattering. (The simulation box of linear size $L = 256$ contains 2048 chains in total.) The main figure **(a)** presents $S(q,f)$ directly as computed from $S(q,f)/\rho f = \left\langle \frac{1}{n}\left(\sum_i \cos(\mathbf{q}\cdot\mathbf{r}_i)\right)^2 + \left(\sum_i \mathbf{q}\cdot\mathbf{r}_i\right)^2 \right\rangle$ where the sums run over all $n = L^3\rho f$ marked monomers and the wave-vectors are commensurate with the cubic box. Also included is the form factor $F(q)$ (dashed line) from eq.(3.35) which corresponds to the $S(q,f)/\rho f \stackrel{f\to 0}{\Rightarrow} F(q)$ limit (but compares already perfectly with the $f = 0.01$ data set). The so-called "total structure factor" $S(q,f=1)$ (bold line at bottom) is the Fourier transformed monomer pair-correlation function of *all* monomers. The inset **(b)** presents a Kratky representation of $S(q,f)$ as suggested by eq.(3.1) where $q^2(S(q,f) - f^2 S(q,f=1))/\rho f(1-f)$ [56, 57] is plotted. The form factor $F(q)$ is again indicated by the dashed line. All data sets collapse perfectly which provides a striking confirmation of eq.(3.1). Also indicated is the infinite chain asymptote eq.(3.17) (bold line).

3.3.2 Form Factor

It is well known that the intramolecular single chain form factor of monodisperse polymer chains may be computed using

$$F_N(q) \equiv \frac{1}{N} \left\langle \left(\sum_{i=1}^{N} \cos(\mathbf{q} \cdot \mathbf{r}_i) \right)^2 + \left(\sum_{i=1}^{N} \sin(\mathbf{q} \cdot \mathbf{r}_i) \right)^2 \right\rangle, \tag{3.35}$$

the average being taken over all chains and configurations available. The form factor obtained for the largest available monodisperse chain systems currently available is represented in the Figures3.13, 3.15 and 3.16. It should be emphasized that the correct generalization of eq.(3.35) to polydisperse systems compatible with eqs(1.52) and (3.14) is the average with weight $N\rho_N$ over $F_N(q)$. In practice, one computes simply the ensemble averaged sum over $(\sum_{i=1}^{N} \sin(\mathbf{q} \cdot \mathbf{r}_i))^2 + (\sum_{i=1}^{N} \cos(\mathbf{q} \cdot \mathbf{r}_i))^2$ contributions for each chain and divides by the total number of monomers.

Figure 3.11 presents the (unscaled) form factors obtained for four different scission energies for our BFM EP model at $\rho = 1/16$. The three different q-regimes are indicated. Details of the size-distribution must matter most in the Guinier regime which probes the total coil size. Non-universal contributions to the form factor arise at large wave-vectors (Bragg regime). Obviously, the larger E the wider the intermediate Kratky regime (see the dashed line indicating eq.(1.57)) where chain length, polydispersity and local physics should not contribute much to the deviations of the form factor from ideality. A very similar plot (not shown) has been obtained for monodisperse polymers. Not surprisingly, it demonstrates that the form factors of both system classes become indistinguishable for large wave-vectors.

The natural scaling attempt for the form factor of EP is presented in Figure 3.12 for a broad range of scission energies.

We plot $F(Q)/F(0)$ as a function of $Q = qR_g$ where both $F(q \to 0) = \langle N^2 \rangle / \langle N \rangle$ and the (Z-averaged) gyration radius R_g have been measured directly for each E. Note that the strong variation of $F(0)$ and R_g with E showing that the successful scaling collapse is significant. Obviously, this scaling does not hold in the Bragg regime ($q \approx 1$) where $F(q)$ increases rapidly, as one expects. The bold line represents the ideal chain form factor, eq.(1.54), where the identification of the coefficients, $F(0) \to 2/\mu$ and ${R_g}^2 \to 3a^2/\mu$, is suggested by the Guinier limit, eq.(1.55). Hence, the perfect fit for $q \ll 1/R_g$ is imposed, but the agreement remains nice even for much larger wave-vectors. A careful inspection of the Figure reveals, however, that eq.(1.54) overestimates systematically the data in the Kratky regime. (The corresponding plot for monodisperse chains is again very similar.)

This can be seen more clearly in the Kratky representation given in Figure 3.13 in linear coordinates. We present here the systems with the longest masses currently available for both monodisperse ($N = 4096$) and EP systems ($E = 14$ and $E = 15$). The non-monotonous behavior is in striking conflict with Flory's hypothesis. The difference between the ideal Gaussian behavior (thin line) and the data becomes up to 20%. Note that for the large (average) chain masses given here *all* systems are identical for $q \geq 0.1$ (but obviously not on larger scales). The infinite chain prediction, eq.(3.18) (or equivalently eq.(3.17)), gives a lower envelope for the data which fits reasonably — despite its simplicity — in the finite wave-vector range $0.1 < q < 0.4$.

The form factor difference $\delta F(q) = F(q) - F^{(0)}(q)$ is further investigated in the Figures 3.14 and 3.15 for equilibrium and monodisperse systems respectively. These plots highlight the deviations in the Guinier regime. In both cases the ideal chain form factor $F^{(0)}(q)$ is computed assuming the same effective statistical segment length $b^* = a^*\sqrt{6}$, i.e. the reference chain size is $R_g^{(0)} = a^* N^{1/2}$. In the first case the reference $F^{(0)}(q)$ is the ideal chain form factor for Flory-distributed chains, eq.(1.54), in the second the Debye function $F^{(0)}(q) = N f_D(Q^2)$ with $f_D(x) = (\exp(-x) - 1 + x)2/x^2$ [25]. As suggested by eq.(3.7) and eq.(3.15) respectively we plot $\delta F(q)/c$ *vs.* $Q = qR_g^{(0)}$, i.e. the axes have been chosen such that the data should scale for different (mean) chain length. We obtain indeed a reasonable scaling considering that our chains are not large enough to suppress (for the Q-range represented) the deviations $\delta F(q)$ due to local physics. The scaling shows implicitly that the corrections with respect to the infinite chain limit decay as the inverse gyration radius, $1/c \sim 1/\sqrt{N}$, as predicted by eqs(3.13) and (3.16). (Both plots appear to improve systematically with increasing chain length and, clearly, high precision form factors for much larger chains must be considered in future studies to demonstrate the scaling numerically.) Also the functional agreement with theory is qualitatively satisfactory in both cases, for equilibrium polymers it is even quantitative for small wave-vectors. For monodisperse chains we find numerically a much more pronounced hump in the Guinier as the one predicted by eq.(3.15) (bold). This is very likely due to the chosen interaction potential eq.(3.2) for Flory-distributed chains which is not accurate enough for the description of the Guinier regime of monodisperse chains.

It should be pointed out that the success of the representation of the non-Gaussian deviations chosen in the Figures 3.14 and 3.15 does depend strongly on the accurate estimation of the statistical segment length b^* of

the ideal reference chains. A variation of a few percents breaks the scaling and leads to qualitatively different curves. Since such a precision is normally not available (neither in simulation nor in experiment) it is interesting to find a more robust representation of the form factor deviations which does not rely on b^* and allows to detect the theoretical key predictions for long chains (notably eq.(3.18)) more readily. Such a representation is given in Figure 3.16 for monodisperse chains (a virtually indistinguishable plot has been obtained for EP). The reference chain size is set here by the *measured* radius of gyration $R_g(N)$ (replacing the above $R_g^{(0)}$) which is used for rescaling the axis and, more importantly, to compute the Debye function $F^{(0)}(q)$. The general scaling idea is motivated by Figure 3.12, the scaling of the vertical axis is suggested by eq.(3.18) which predicts the difference of the inverse form factors to be proportional to N^0q^3. Without additional parameters (R_g is known to high precision) we confirm the scaling of

$$m(Q) \equiv \left(\frac{N}{F(q)} - \frac{N}{F^{(0)}(q)} \right) \rho/\rho^* \tag{3.36}$$

as a function of $Q = qR_g$ with $\rho^* \equiv N/{R_g}^3$ being the overlap density. Importantly, our simulations allow us to verify for $Q \gg 5$ the fundamentally novel Q^3 behavior of the master curve predicted by eq.(3.18) and this over more than an order of magnitude!

In this representation we do *not* find a change of sign for the form factor difference ($\delta F(q)$ is always negative) and all regimes can be given on the same plot in logarithmic coordinates. In the Guinier regime we find now $m(Q) \propto Q^4$ which is readily explained in terms of a standard expansion in Q^2. (The first two terms in Q^0 and Q^2 must vanish by construction because of the definition of radius of gyration, eq.(1.55) [25].) Finally, we stress that the scaling of Figure 3.16 is not fundamentally different from the one attempted in Figures 3.14 and 3.15. Noting $F(q)F^{(0)}(q) \approx (Nf_D(Q))^2$, it is equivalent to $-\delta F(Q)/c \approx m(Q)f_D(Q)^2$ with $c \approx N^2/(\rho {R_g}^3)$. (Compared with eqs(3.7) and (3.15), $R_g^{(0)}$ has been replaced by the measured R_g.) This scaling has been verified to hold (not shown) but we do not recommend it, since it does not yield simple power law regimes.

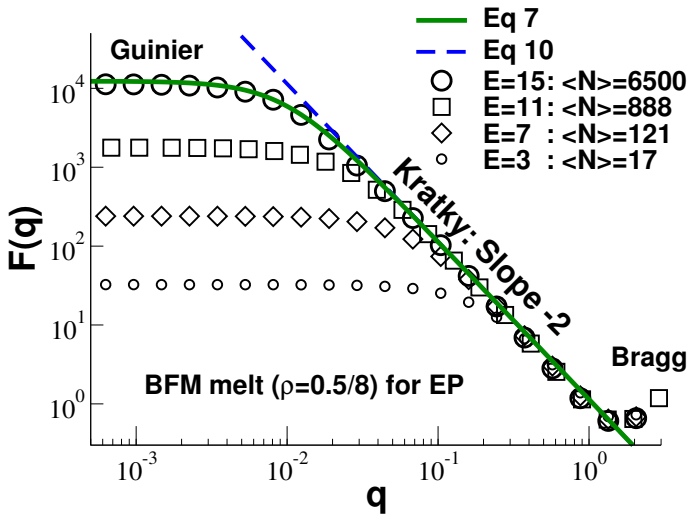

Figure 3.11: The ideal chain form factor for Flory size-distributed polymers, eq 1.54, is indicated by the solid line (Noted Eq 7 on Fig.3.11). In the Kratky regime between the total chain and monomer sizes the form factor expresses the fractal dimension of the Gaussian coil, eq 1.57 (dashed line, noted Eq 10). Experimentally, this is the most important regime since it is, for instance, not affected by the (a priori unknown) polydispersity. The form factors of equilibrium polymers (EP) of various scission energies E obtained numerically are indicated together with the corresponding mean chain length $\langle N \rangle$. The form factor of polydisperse polymer systems is obtained by computing for each chain $(\sum_i \sin(\mathbf{q} \cdot \mathbf{r}_i))^2 + (\sum_i \cos(\mathbf{q} \cdot \mathbf{r}_i))^2$, summing over all chains (irrespective of their length) and dividing by the total number of particles. The computational data reveals an additional regime at wavevectors corresponding to the monomer structure ("Bragg regime") which is not treated by our theory. All data have been obtained for a number density $\rho = 0.5/8$ of the three dimensional bond-fluctuation model (BFM).

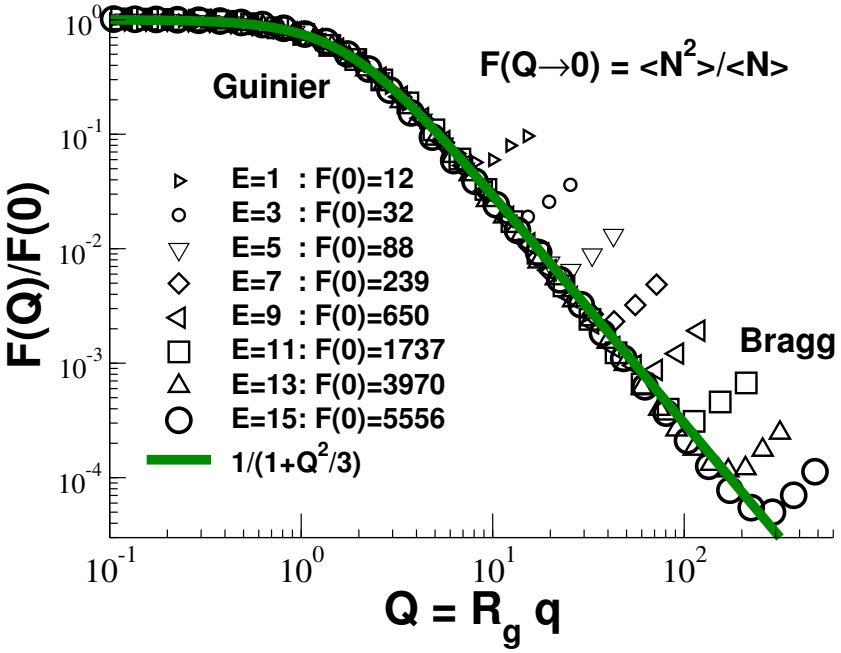

Figure 3.12: Successful scaling of the form factors of EP obtained from our BFM simulations for various scission energies E as indicated: $F(Q)/F(0)$ is plotted *vs.* the reduced wave-vector $Q = R_{\rm g}q$. Note that both scales $F(Q \to 0) = \langle N^2 \rangle / \langle N \rangle$ (values indicated) and the (Z-avaraged) gyration radius $R_{\rm g}$ have been directly measured for each sample. Obviously, the scaling breaks down due to local physics for large wave-vectors (Bragg regime). The bold line represents the prediction for ideal Flory-distributed polymers, eq.(1.54), with parameters chosen in agreement with the Guinier limit, eq.(1.55). Importantly, in the intermediate Kratky regime small, albeit systematic, deviations are visible which will be further investigated below.

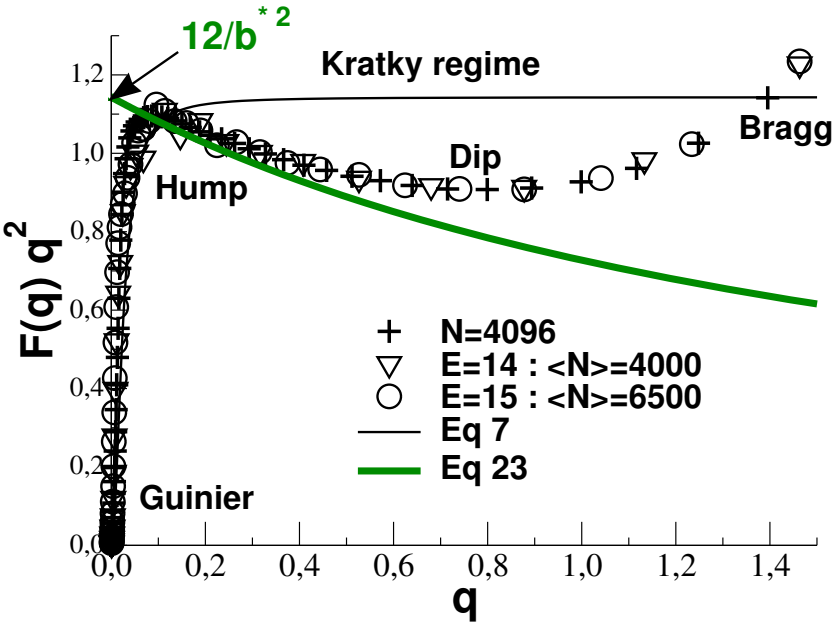

Figure 3.13: Kratky representation of the intramolecular form factor $F(q)q^2$ *vs.* wave-vector q for monodisperse (crosses) and equilibrium polymers. The *non-monotonous* behavior predicted by the theory is clearly demonstrated. The ideal chain form factor, eq.(1.54) (thin line, noted Eq 7), overpredicts the dip of the form factor at $q \approx 0.7$ by about 20%. The bold line (noted Eq 23) indicates the prediction for infinite chains, eq.(3.18), which should hold for both system classes for infinitely long chains. For this reason we have chosen the largest chains currently available.

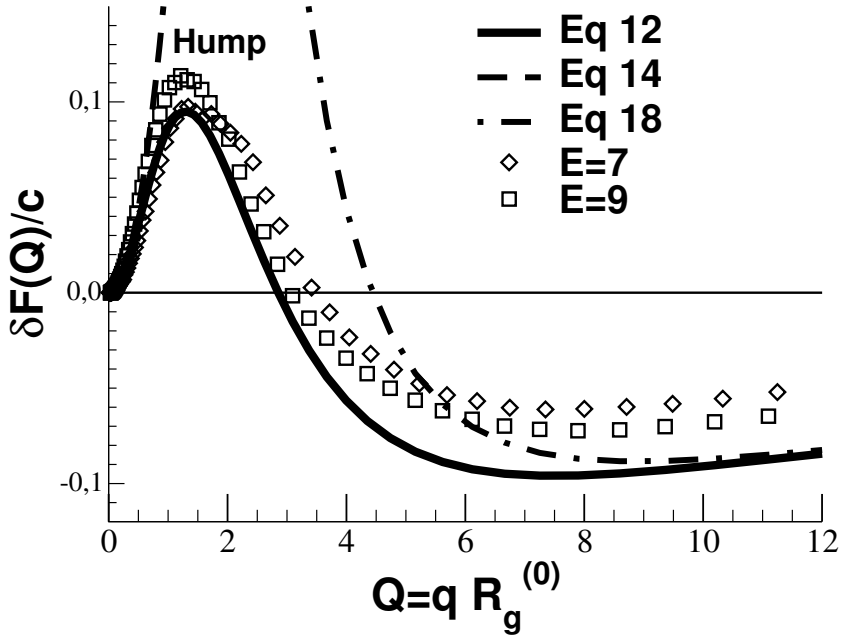

Figure 3.14: Correction $\delta F(Q) = F(Q) - F^{(0)}(Q)$ to the form factor as a function of $Q = qR_{\mathrm{g}}^{(0)}$ (using ${R_{\mathrm{g}}^{(0)}}^2 = 3a^{*2}/\mu$) as predicted by eq.(3.7) (noted Eq 12) for Flory-distributed polymers. The deviation is positive for small wave-vectors (Guinier regime) and becomes negative at about $Q \approx 3$. The scaling factor $c = 9R_{\mathrm{g}}^{(0)}/\pi\rho b^{*4}$ should allow a data collapse irrespective of the mean chain size — provided that the chains are sufficiently long to suppress additional physics in the Bragg regime. Also included are eq.(3.9) and 3.13 (respectiveley Eq 14 and Eq 18 on the graph) for the asymptotic behavior in the Guinier and the Kratky regimes respectively. The data from our BFM simulations (given here for two scission energies where high precision data are available) agree quantitatively (especially for small Q) with eq.(3.7). (Note that the chains are too short to allow a better fit for large Q.) The reference form factor $F^{(0)}(Q)$ has been computed from eq.(1.54) supposing a perfect Flory distribution.

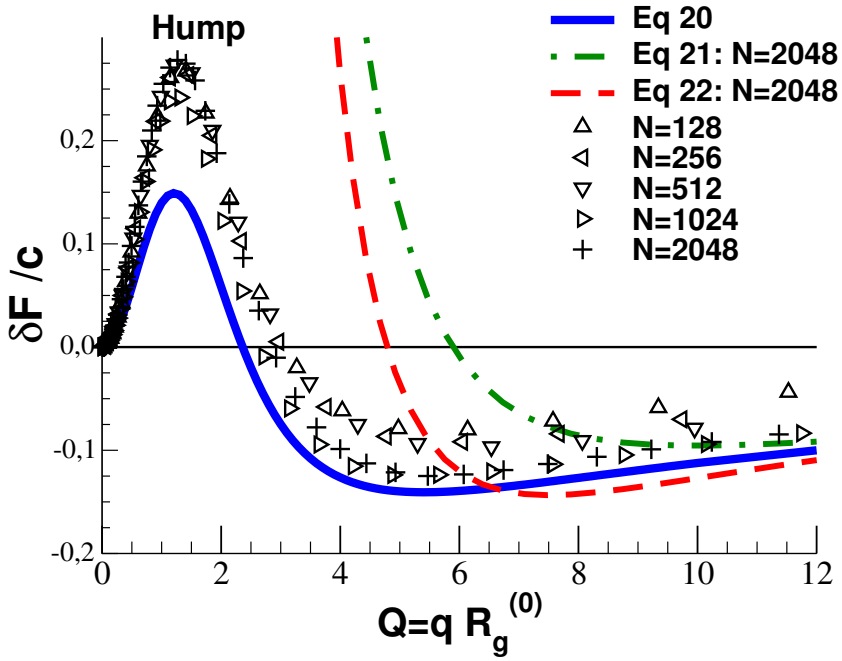

Figure 3.15: Deviation to the ideal form factor in a monodisperse system, eq.(3.15) (noted Eq 20 on the graph). The shape is similar to that in the polydisperse case (Figure 3.14) since polydispersity merely affects the Guinier regime. Also indicated are the asymptotic behavior in the Kratky regime, eq.(3.16) (noted Eq 21), and the prediction for infinite chains, eq.(3.17) (noted Eq 22). The simulation data scales roughly, especially in the Guinier limit (hump), while for larger q deviations are visible which may be attibuted to local physics. The agreement with eq.(3.15) is only qualitative here since a much more proncounced non-monotonic behavior is seen in the simulation. This is due to use of the *polydisperse* chain perturbation potential, eq.(3.2) — an approximation which must become insufficient for low wave-vectors where the coil size matters.

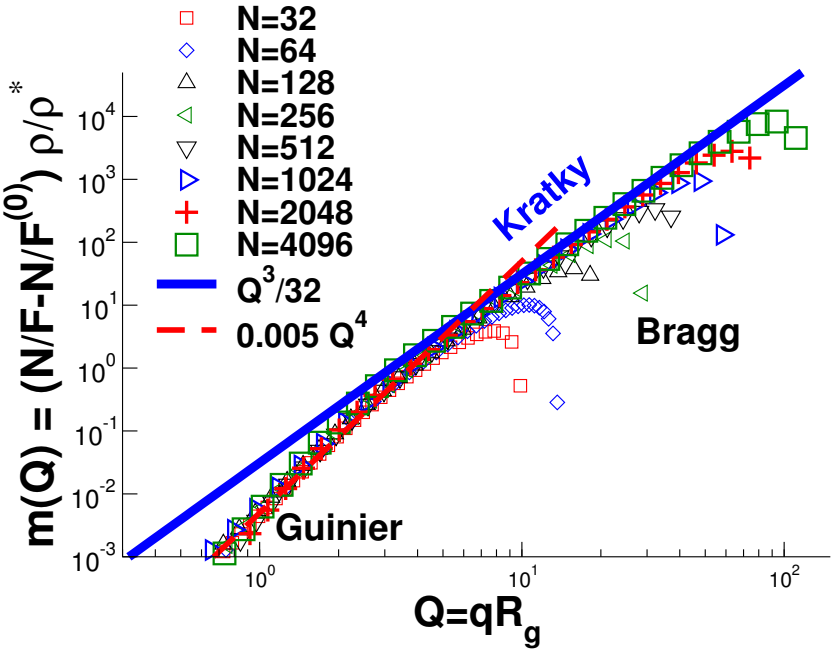

Figure 3.16: Scaling attempt of the non-Gaussian deviations of the form factor of monodisperse polymers in the melt in terms of the *measured* radius of gyration R_g (instead of $R_g^{(0)}$). As suggested by eq 3.18, the difference $1/F(q) - 1/F^{(0)}(q)$ of the measured and the ideal chain Debye form factor has been rescaled by the factor $N\rho/\rho^*$ and plotted as a function of $Q = qR_g$. We obtain perfect data collapse for all chain lengths included. (Obviously, data points in the Bragg limit $q \approx 1$ do not scale.) The difference $-\delta F(q)$ is positive in all regimes and no change of sign occurs in this representation. Note that the power law slope, $m(Q) = Q^3/32$, predicted by eq.(3.18), can be seen over more then one order of magnitude. In the Guinier regime, the difference increases more rapidly, $m(Q) \propto Q^4$ (dashed line), as one expects from a standard analytic expansion in Q^2.

3.4 Conclusion

We have shown in this chapter that even for infinitely long and flexible polymer chains no Kratky plateau should be expected in the form factor measured from a dense solution or melt (see Figure 3.13). We rather predict a non-monotonic correction to the ideal chain scattering crossing from positive in the Guinier regime to negative in the Kratky regime (Figures 3.14 and 3.15). The former regime merely depends on the radius of gyration and the correction corresponds to some deswelling of the coil. In the latter regime the form factor ultimately matches that of an infinite chain $\frac{1}{F(q)} = \frac{q^2 b^{*2}}{12} + \frac{1}{32}\frac{q^3}{\rho}$ for $q\xi \ll 1$ (Figure 3.16).

The q^3-correction depends neither on the interaction nor on the statistical segment, it must hence be generally valid, even in the critical semidilute regime. We checked explicitly that the one-loop correction obtained by Schäfer in the strongly fluctuating semidilute regime by numerical integration of renormalization group equations takes the same form with the amplitude $0.03124\ldots$ within 0.03% of our 1/32.

It is to be noted that for infinite chains, the above correction is not an analytic function of q^2 as one would naively anticipate. For finite chains the correction remains a function of even powers of q. The intriguing q^3-correction for infinite chains formally arises from dilation invariance of the diagrams. Established theoretical methods [33, 59] may implicitly *assume analytical* properties of scattering functions and non-analytical terms discussed here could be easily overlooked.

These theoretical results are nicely confirmed by our Monte Carlo simulations of long flexible polymer melts. The agreement is particularly good for equilibrium polymers (Figure 3.14) and satisfactory for all systems with large (mean) chain length $N \gg 1000$ (Figures 3.13). It should be emphasized that all fits presented are parameter free since the only model dependent parameter b^* has been independently obtained from the internal distances of chain segments. Since a sufficiently accurate value of b^* may not be available in general our simulation suggest as a simple and robust way to detect (also experimentally) the universal q^3-correction the scaling representation of the (inverse) form factor difference in terms of the *measured* radius of gyration given in Figure 3.16. We expect that data for *any* polymer sample — containing long and flexible linear chains with moderate polydispersity — should collapse with good accuracy on the *same* master curve. Strong polydispersity (such as one finds in EP) should merely change its behavior in a small regime around $Q = qR_g \approx 1$.

Measuring the form factor is a well accepted method to determine the statistical segment length. We already mentioned in the Introduction that there is no clear evidence of a true Kratky plateau from experiments and further showed that a plateau is actually not to be expected from the theory on general grounds. We are lacking an operational definition of the statistical segment length, even for very long flexible "thin" chains. One way out would be in principle to fit a large q-range, from the Guinier regime — as far it can be cleanly measured on a sample with controlled polydispersity — to the onset of the persistent length effect, with the corrected formula $F^{(0)}(q) + \delta F(q)$. However, if the size-distribution is not known precisely (as it will be normally the case) we recommend to determine b^* instead by means of the infinite chain asymptote, eq.(3.17), as can be seen Figure 3.13.

At this point one may wonder whether eq.(3.1), (the precise form of this equation being given in the caption of Figure 3.10) routinely used to rationalize the scattering of a mixture of deuterated and hydrogenated chains is accurate enough to extract the form factor, including the corrections. From a theoretical point of view, for "ideal" labeling of the chains, which does not introduce additional interactions between labeled and unlabeled chains, there is no question that this can be done. Practically however, there is a danger that experimental noise in subtracted terms in eq.(3.1) will mask corrections discussed in our paper. The strongest support comes here from numerical results presented in Figure 3.10. We have computed the response function $S(q, f)$ for a melt of monodisperse chains for chain length $N = 512$ and different fractions f of labeled chains. The main panel **(a)** gives $S(q, f)/f\rho$ and the form factor $F(q)$ as a function of the wave-vector. The inset **(b)** presents a Kratky representation of the rescaled structure factor: For a surprisingly large range of f the data scales if the standard experimental procedure is followed and the scattering of the background density fluctuations $f^2 S(q, f = 1)$ has been properly subtracted [56, 57]. The rescaled response function is identical to $F(q)$ and shows precisely the non-monotonic behavior, eq.(3.16), and the asymptotic infinite chain limit, eq.(3.17) (bold line in inset), predicted by our theory. This confirms that eq.(3.1) allows indeed to extract the correct form factor and should encourage experimentalists to revisit this old, but rather pivotal question of polymer science.

Chapter 4

Fluctuation-induced Effects on Collective Properties

As we already mentioned, the starting point of the debate concerning the range of correlations in solution (from semidilute to melts) is more or less related to the problem of the stability of objects in polymer matrices or solutions. In dense solutions of polymers confined between two plates separated by the distance D[1], with $a \ll D \ll R_g$, it is expected that interfacial effects (depletion near walls) [44] do not hold over the correlation length ξ ($\xi \simeq$ monomer size in melts) [19]. So a weak attraction per unit surface appears between the plates, due to confinement, which vanishes as $e^{-z/\xi}$. Therefore in a melt, no forces can appear on larger scales than ξ. In the late eighties, assuming independence between the "Bulk Phase" and the "Surface Phase" [3], scaling laws were derived which lead to an excess of surface energy only due to the microscopic layer near surfaces. This energy is not a function of the separation between the walls, and does not induce long-range interactions. Even if the derivation was not rigorous, these arguments and this conclusion were supposed to close the controversial discussion. Nevertheless, in the mid-nineties, a first paper [60] derived long-range interactions *via* chain ends: developing a generalization of the ground state dominance approach for finite chains (taking into account higher contributions), two correction terms to the free energy of this approximation were derived, one of order $1/N$ and the other of order $1/N^{3/2}$, with N the degree of polymerization. Those chain-end effects lead to long-range interactions between plates which are the strongest in the theta conditions ($v \to 0$), for the overlapping density which characterizes the semidilute regime, *i.e.* $c^* \sim N^{-1/2}$,

[1] The simplest view of the problem.

and which could under certain conditions stabilize a system of colloidal particles. These chain-end effects are extensively described in [62, 60, 9, 45, 61].

In this part, different long-range correlations are derived for dense systems of linear polymers, which hold even for infinite chains or in the Grand-Canonical Ensemble[2]. These effects are loosely related to those described in chapter 3. As a first step, it is tempting to assess the collective correlations through the RPA relation eq.(1.30). For instance, in a dense system of infinite chains, the form factor has to be corrected by a universal term as shown in eq.(3.18). One finds

$$S(q) = \left(v + \frac{q^2 a^2}{2c_0} + \frac{1}{32}\frac{q^3}{c_0^2} \right)^{-1} \tag{4.1}$$

putting forward a q^3-correction. Such a correction in fact exists, but it has to be treated more carefully (the amplitude of the q^3 is overestimated in eq.(4.1)). The method used here to derive these correlations consists in trying to generate the right response functions for the fictitious ideal system [64]. It is established in the first coming section. In the second section, it is shown that these long-range correlations are related to the lowest order fluctuation corrections to the mean-field treatment [17] (integrating fluctuations on their Gaussian distributions). It is also possible to identify this part to the extra cyclic conformations taken into account by the non-corrected mean-field Hamiltonian. Then the effects of such correlations are investigated, considering the fluctuation-induced repulsion between two (colloidal) spheres. This part is extensively inspired by the founder works published in [64].

4.1 Density Correlations in Linear Polymer Melts

The aim here is to evaluate the density fluctuations in a melt of linear chains, evaluating the response function in the reciprocal space, which formally comes down to assessing

$$S(q) = \frac{1}{V}\left\langle c_{\mathbf{q}}\, c_{-\mathbf{q}} \right\rangle = \frac{1}{V}\frac{\int c_{\mathbf{q}} c_{-\mathbf{q}} \exp(-H[c]) D[c]}{\int \exp(-H[c]) D[c]}, \tag{4.2}$$

V being the volume of the system. We know from the first chapter that in a system of chains that do not interact, the response function is $S_{\mathrm{id}}(\mathbf{q}) =$

[2] In those cases, the Ground State Correction does not exist

$c_0F(\mathbf{q})$. Because[3] in the case of infinite chains, a quadratic approximation of the Hamiltonian with excluded volume and small fluctuations $\delta c = c(r) - c_0 \ll c_0$, which reads,

$$H[c] \simeq \int \left(\frac{a^2}{4c_0} (\nabla \delta c)^2 + \frac{v}{2} (\delta c)^2 \right) d\mathbf{r} \tag{4.3}$$

was enough to generate the precited RPA result, saying

$$S(q) = \frac{2c_0}{q^2 a^2 + 2c_0 v} \tag{4.4}$$

and because this RPA result gives the right response function for noninteracting infinite chains, in the limit $v \to 0$, people tend to think that the conformational (local) part of the free energy was the only contribution to the correlations of a solution of ideal polymers. In fact, it has been shown in [64] that it is not. That conformational free energy has to be corrected with long-range interactions. Let us derive these interactions in the (Grand-Canonical) case of living polymers. So following the mean-field equation (1.25), one can write the *a priori* only mean-field terms which describe a dense system of noninteracting chains, under Flory distribution:

$$H_{\text{id}}^{(0)}[c] = \frac{a^2}{4} \int \frac{(\nabla c)^2}{c} d\mathbf{r} + \mu \int \left(\sqrt{c} - \sqrt{c_0} \right)^2 d\mathbf{r}. \tag{4.5}$$

The first term is the classical contribution of infinite chains, derived from eq.(1.25). The second one is a Lagrange multiplier, derived from the Grand-Canonical formalism, which ensures that $c_0 = \langle c \rangle$ is a constant under the right size-distribution (notably for chain ends, *via* the functional of $-2\mu\sqrt{c_0}\sqrt{c} = -2\frac{1}{\langle N \rangle}\sqrt{c_0}\sqrt{c}$)[4]. We know that the correlations of ideal (non-interacting) linear polymers with a Flory-distribution should read

$$S(q) = \frac{2c_0}{\mu + q^2 a^2} = c_0 G_\mu^{(0)}(q). \tag{4.6}$$

Here $G_\mu^{(0)}(q)$ is the form factor for ideal chains, noted $F^{(0)}(q)$ in eq.(1.54). For consistency, we will adopt that new notation here. As fluctuations for ideal chains can be very strong, approximating the Hamiltonian with little

[3] Among other reasons.

[4] It is known [15, 7] that in mean-field, $\mu \simeq c_0^{-1/2} \exp(-E/2)$, with E the scission energy *i.e.* the cost of energy to create two chain ends. Therefore, this term may be expressed as $-2\exp(-E/2)\sqrt{c}$, confirming the interpretation of this energy in terms of chain ends.

deviations around c_0 is forbidden. But writing this equation with the real order parameter ψ, normalized in order that $c = c_0\psi^2$, one finds,

$$\begin{aligned} H_{\rm id}^{(0)}[\psi] &= \int a^2 c_0 (\nabla\psi)^2 + \mu c_0 (\psi - \psi_0)^2 \\ &= \frac{2c_0}{V} \sum_{\mathbf{q}>0} (q^2 a^2 + \mu) \delta\psi_{\mathbf{q}} \delta\psi_{-\mathbf{q}} \end{aligned} \tag{4.7}$$

with the Fourier transformation defined by these two relations (to separate the mean-value of ψ from its varying part):

$$\begin{aligned} \delta\psi_{\mathbf{q}} &= \int (\psi(\mathbf{r}) - \psi_0) e^{-i\mathbf{q}.\mathbf{r}} d\mathbf{r} = \psi_{\mathbf{q}} - \psi_0 \, V \, \delta_{\mathbf{q},0} \\ \psi(\mathbf{r}) &= \psi_0 + \delta\psi(r) = \frac{1}{V} \sum_{\mathbf{q}} (\psi_0 \, V \, \delta_{\mathbf{q},0} + \delta\psi_{\mathbf{q}}) \, e^{i\mathbf{q}.\mathbf{r}}. \end{aligned} \tag{4.8}$$

Under Fourier transformation, c_q are becoming convolutions of ψ_q, and the statistical average becomes

$$\langle c_{\mathbf{q}} \, c_{-\mathbf{q}} \rangle = \frac{{c_0}^2}{V^2} \sum_{\mathbf{q}',\mathbf{q}''} \langle \psi_{\mathbf{q}'} \psi_{\mathbf{q}-\mathbf{q}'} \psi_{\mathbf{q}''} \psi_{-\mathbf{q}-\mathbf{q}''} \rangle. \tag{4.9}$$

Using the definitions in eq.(4.8), applying Wick's theorem, which gives $n^{\rm th}$ moments of Gaussian random variables as functions of second moments, this last equation becomes, for $q \neq 0$

$$\begin{aligned} \langle c_{\mathbf{q}} \, c_{-\mathbf{q}} \rangle = \frac{2{c_0}^2}{V^2} \{ & 2V^2 \langle \psi_0^2 \rangle \langle \delta\psi_{\mathbf{q}} \delta\psi_{-\mathbf{q}} \rangle \\ & + \sum_{\mathbf{q}'} \langle \delta\psi_{\mathbf{q}'} \delta\psi_{-\mathbf{q}'} \rangle \langle \delta\psi_{\mathbf{q}-\mathbf{q}'} \delta\psi_{\mathbf{q}'-\mathbf{q}} \rangle \}. \end{aligned} \tag{4.10}$$

The first term of this equation generates the right correlations for the system since $\langle \psi_0^2 \rangle = 1$ and $\frac{4{c_0}^2}{V} \langle \delta\psi_{\mathbf{q}} \delta\psi_{-\mathbf{q}} \rangle = \frac{2c_0}{\mu + q^2 a^2}$. But obviously it remains something that has to be compensated. This extra contribution reads:

$$\delta S(q) = \frac{1}{8} \sum_{\mathbf{q}'} G_\mu^{(0)}(q') G_\mu^{(0)}(q - q') \tag{4.11}$$

Let us give some details of the integration that will drive us to the final expression of the correction in three dimensions. Taking the continuum

limit, the important integral is in fact:

$$\frac{1}{8}\sum_{\mathbf{q}'} G_\mu^{(0)}(q')G_\mu^{(0)}(q-q') = \frac{1}{2}\int \frac{d\mathbf{q}'}{(2\pi)^3}\frac{1}{\mu+q'^2a^2}\,\frac{1}{\mu+(q-q')^2a^2}$$
$$= \frac{1}{32\pi^2 qa^4}\int_{-\infty}^{\infty} dx \frac{x}{x^2+\mu/(q^2a^2)}\ln\left(\frac{(1+x)^2+\mu/(q^2a^2)}{(1-x)^2+\mu/(q^2a^2)}\right) \tag{4.12}$$

with the substitution $q' = qx$. It is possible to solve this integral in the $\mathbb{C}$ plane, listing the singularities. Analyzing this last integral, a possible contour is given in Fig.4.1, which highlights the logarithmic branch cut and the single pole. As a direct application of general theorems, one finds

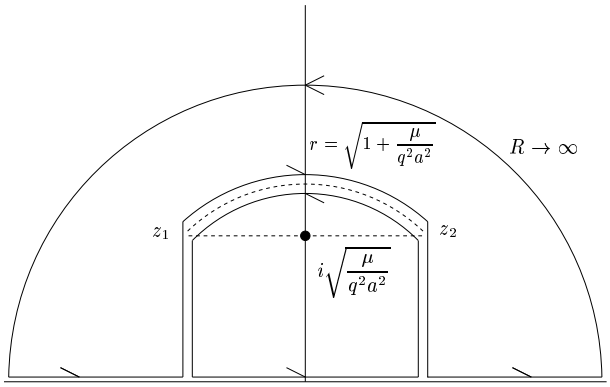

Figure 4.1: One of the possible contour in the $\mathbb{C}$ plane. The dashed line depicts the logarithmic branch-cut, which is an arc of the circle of radius $r = \sqrt{1+\frac{\mu}{q^2a^2}}$ between $z_1 = re^{i(\pi-\alpha)}$ and $z_2 = re^{i\alpha}$, with $\alpha = \arctan\left(\sqrt{\frac{\mu}{q^2a^2}}\right)$. The other singularity is a single pole at $z = \sqrt{\mu/q^2a^2}$.

$$\frac{1}{8}\sum_{\mathbf{q}'} G_\mu^{(0)}(q')G_\mu^{(0)}(q-q') = \frac{1}{16qa^4}\,\frac{2}{\pi}\arctan\left(\frac{qa}{2\sqrt{\mu}}\right). \tag{4.13}$$

This term comes from higher order terms in the δc-expansion of $H_{\mathrm{id}}^{(0)}$, it is therefore small in melts with $G_{\mathrm{z}} \ll 1$ (therefore $v \neq 0$). So it is possible to generate the correct structure factor, through the addition of the quadratic

contribution

$$H_{\rm lr} = \sum_{\mathbf{q}} \frac{1}{16c_0^2V^2(G_\mu^{(0)}(q))^2}\delta c_{\mathbf{q}}\delta c_{-\mathbf{q}} \sum_{\mathbf{q}'} G_\mu^{(0)}(q')G_\mu^{(0)}(q-q') + O\left(\frac{\delta c}{c_0}\right)^3$$
$$= \frac{1}{64\pi c_0^2 a^4}\int \frac{d\mathbf{q}}{(2\pi)^3}\frac{(\mu+q^2a^2)^2}{q}\arctan\left(\frac{qa}{2\sqrt{\mu}}\right)\delta c_q\delta c_{-q} \tag{4.14}$$

that cancels out those extra correlations. Thus the Hamiltonian characterizing the ideal system reads $H_{\rm id} = H_{\rm id}^{(0)} + H_{\rm lr}$. Considering by now the same system with excluded volume interactions, which reduce the fluctuations, the case $\delta c \ll c_0$ or $G_{\rm z} \ll 1$ is now easier to conceive and the quadratic approximation may be allowed. The expression (4.14) just derived holds now for $q\xi \ll 1$ and it is straightforward to show that the new structure factor under these conditions is:

$$S(q) = \left(v + \frac{(\mu+q^2a^2)}{2c_0} + \frac{(\mu+q^2a^2)^2}{64c_0^2qa^4}\frac{2}{\pi}\arctan\left(\frac{qa}{2\sqrt{\mu}}\right)\right)^{-1}. \tag{4.15}$$

With this last formula, it is possible to work out the correlation function in the real space, operating an inverse Fourier Transform. Using the same techniques as before, and noticing that we have two well separated length scales, the correlation length ξ which is the smallest scale, and $a^2/\mu \simeq R_{\rm g}$. So, the Ornstein-Zernike formula $\left(v + \frac{(\mu+q^2a^2)}{2c_0}\right)^{-1}$ defines the first pole where the correction is not relevant, and one finds the classical result of the mean-field treatment,

$$\mathcal{G}_{\rm mf}(r) = \frac{c_0}{2\pi r a^2}e^{-r/\xi_\mu}, \quad \text{with} \quad \xi_\mu^2 = \frac{a^2}{2c_0v+\mu} = \frac{a^2}{2c_0v} + O\left(\frac{1}{\langle N\rangle}\right). \tag{4.16}$$

This contribution is screened on $\xi_\mu \simeq \xi$, the smallest length scale of the problem, and reinforces the idea of Flory. So it is possible to treat the weak logarithmic singularity contained in the structure factor with the contour in Fig.4.2, what is tantamount to evaluating the two integrals along the imaginary axis. Assuming that $q^2 \ll \xi^{-2}$ when this correction is relevant,

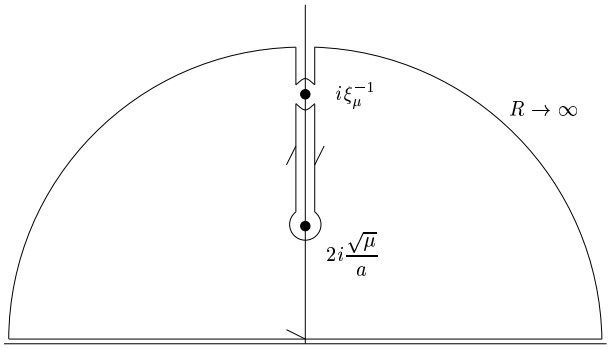

Figure 4.2: One of the possible contour in the $\mathbb{C}$ plane to derive the new correlations. The integral along the $\mathbb{R}$ axis is equivalent to an integral along the $i\mathbb{R}$ axis. The inferior bound fixes the range of the correlations and the polynomial function, while the superior bound gives the negative power laws and the prefactor. Please note that the single pole is in fact in the contour.

these integrals are easy to assess and finally, correlations are

$$\begin{aligned}\mathcal{G}(r) =& \mathcal{G}_{\rm mf}(r) - \frac{3}{16\pi^2 c_0^2 v_\mu^2}\frac{e^{-2\frac{\sqrt{\mu}}{a}r}}{r^6}\{1 + 2\frac{\sqrt{\mu}}{a}r + \frac{11}{6}\frac{\mu}{a^2}r^2 + \frac{\mu^{3/2}}{a^3}r^3 + \frac{3}{8}\frac{\mu^2}{a^4}r^4\} \\ \underset{r\gg\xi}{\simeq}& - \frac{3}{16\pi^2 c_0^2 v_\mu^2}\frac{e^{-2\frac{\sqrt{\mu}}{a}r}}{r^6}\{1 + 2\frac{\sqrt{\mu}}{a}r + \frac{11}{6}\frac{\mu}{a^2}r^2 + \frac{\mu^{3/2}}{a^3}r^3 + \frac{3}{8}\frac{\mu^2}{a^4}r^4\} = \mathcal{G}_{\rm lr}(r)\end{aligned} \tag{4.17}$$

with $v_\mu = v + \frac{\mu}{2c_0} = v + O\left(\frac{1}{\langle N\rangle}\right)$. $\mathcal{G}_{\rm lr}(r)$ subsists over the mean-field correlation length ξ_μ. At small r, saying $\xi \ll r \ll R_{\rm g}$, the first term of the polynomial is dominant and correlations decrease as r^{-6}. Power laws are exponentially cut on scales larger than some $a/(2\sqrt{\mu})$ Noticing the direct relation between correlations and Hamiltonian terms (when functionals are quadratic forms), it is now possible to write the new interaction in the direct space. It yields

$$\begin{aligned}H_{\rm lr} = \int d\mathbf{r}d\mathbf{r}'\delta c(r)\frac{1}{2}\frac{3}{16\pi^2 c_0^2}\frac{e^{-2\frac{\sqrt{\mu}}{a}|r-r'|}}{|r-r'|^6}\delta c(r') \\ \{1 + 2\frac{\sqrt{\mu}}{a}|r-r'| + \frac{11}{6}\frac{\mu}{a^2}|r-r'|^2 + \frac{\mu^{3/2}}{a^3}|r-r'|^3 + \frac{3}{8}\frac{\mu^2}{a^4}|r-r'|^4\}.\end{aligned} \tag{4.18}$$

It is to be noted that monomers repel each other on large scales. Obviously, the limit $\mu \to 0$ gives the right correlation for infinite chains [64]

$$\mathcal{G}_{\rm lr}(r) = -\frac{3}{16\pi^2\, c_0^2\, v^2}\frac{1}{r^6} \tag{4.19}$$

or in the reciprocal space

$$S(q) = \left(v + \frac{q^2 a^2}{2c_0} + \frac{1}{64}\frac{q^3}{c_0^2}\right)^{-1}. \tag{4.20}$$

It might be interesting to visualize how the correlations of finite chains in eq.(4.17) differ from infinite chains eq.(4.19). Calling $x = r\sqrt{\mu}/(\sqrt{3}a) = r/R_{\rm g,Z}^{(0)}$, these two formulas only differ by the exponentially cut polynomial (see Fig.4.3)

$$f(x) = \left(1 + 2\sqrt{3}x + \frac{11}{2}x^2 + 3\sqrt{3}x^3 + \frac{27}{8}x^4\right) e^{-2\sqrt{3}x}. \tag{4.21}$$

As expected, long-range correlations vanish at about $3R_{\rm g,Z}^{(0)}$. Finite-size

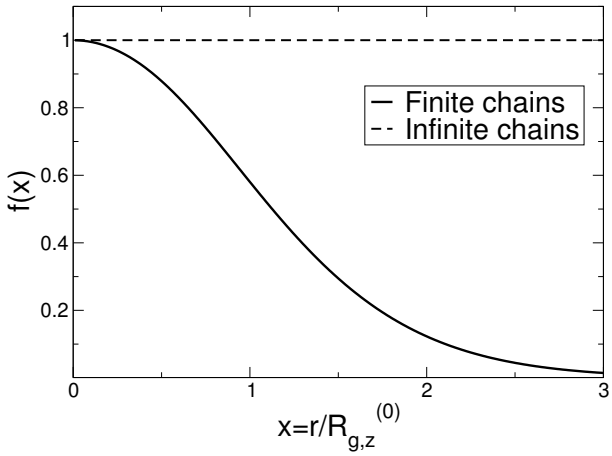

Figure 4.3: This plot shows the variation of the exponentially cut polynomial associated to the $1/r^6$ law. Long-range correlations vanish at $\simeq 3R_{\rm g,Z}^{(0)}$. Finite size effects moderately affect the pure power law at small distances since $f(x) \simeq 1 - x^2/2 + O(x^4)$.

effects moderately affect the pure power law r^{-6} at small distances, since when $x \ll 1$, $f(x) \simeq 1 - \frac{x^2}{2} + O(x^4)$.

Therefore, to summarize this section, the traditional Hamiltonian of an ideal system does not reproduce the correct structure factor for linear chains. One has to correct it with a long-range repulsion between monomers, that holds on the coil size. It should also be noted the striking fact that the RPA written with the corrected form factor (eq.(4.1)) and this derivation (eq.(4.20)) only differ by a factor 2 in the correction. In the next section, an alternative derivation will highlight the deep origin of this interaction: it is related to the closed conformations (cycles).

4.2 Fluctuation-Induced Interactions and Ring Conformations

Let us first consider a concentrated system of *interacting* polymers. The Hamiltonian of the system can be separated in two terms [64]: a local functional of the concentration and its gradient and a non-local term $H_{\rm nloc}$ (to be determined). As seen in the preceding section, this last term is small under the conditions $G_{\rm z} \ll 1$ or if the cell size of coarse-graining is large enough compared to ξ. Under one of these conditions, one can apply perturbation methods [48] and deduces immediately the free energy $F \simeq F^{(0)} + \langle H_{\rm nloc} \rangle$. The averaging is established on the statistics generated by $H^{(0)} = H_{\rm id} + H_{\rm int}$, the sum of the conformational entropic part and the volume interaction. Because we are dealing with weak deviations from the mean-field result, $\langle H_{\rm nloc} \rangle \simeq H_{\rm nloc}[\overline{c}]$ is allowed. Thus it is possible to write

$$F \simeq F^{(0)} + H_{\rm nloc}[\overline{c}] \simeq H^{(0)}[\overline{c}] + F^{(\rm fluct)} + H_{\rm nloc}[\overline{c}]. \tag{4.22}$$

$H^{(0)}[\overline{c}]$ is the mean-field free energy (saddle point), $F^{(\rm fluct)}$ is the classical fluctuation correction [17] to the mean-field treatment. This term is local because correlations are screened on ξ (there are no soft modes when $v \neq 0$). $F^{(0)}$ is of course also local, as a simple functional of c and its gradient. So the entire long-range effects are featured in $H_{\rm nloc}$.

In the previous section, it has been established that this long-range correcting Hamiltonian does not depend on v. Here is the point. These long-range effects come from the soft modes (on the coil size) allowed in the ideal system of reference. In this case, there are no interactions and the free energy reads therefore $F_{\rm id} \simeq H^{(0)}[\overline{c}] + F_{\rm id}^{\rm fluct} + H_{\rm nloc}[\overline{c}]$. Moreover, in the Lifshitz-Edwards theory, $F_{\rm id}$ is *exactly* $H^{(0)}[\overline{c}]$. Thus, the non-local contribution $H_{\rm nloc}$ should compensate the fluctuation correction $F_{\rm id}^{\rm fluct}$ in the ideal system

More quantitatively, consider an ideal system under Flory distribution, with an external field U (that may create inhomogeneities in $c(\mathbf{r})$). As a first step, let us derive the Edwards equation for Green functions in the Grand Canonical Ensemble. For a N-chain, as mentioned in 1.2, the "N"-Green function is the solution of the system:

$$\begin{aligned} \frac{\partial}{\partial N} G_N &= -\hat{L} G_N \\ G_0(\mathbf{r}, \mathbf{r}') &= \delta(\mathbf{r} - \mathbf{r}'). \end{aligned} \tag{4.23}$$

Defining the Green function in the Grand-Canonical Ensemble G as the sum over the "N"-Green functions with the weight $e^{-\mu N}$

$$G(r, r') = \int_0^\infty G_N(r, r') e^{-\mu N} dN, \tag{4.24}$$

the system above becomes

$$\mu G - \delta(\mathbf{r} - \mathbf{r}') = -\hat{L} G, \tag{4.25}$$

where $\hat{L} = -a^2 \nabla^2 + U(r)$. The function G defines the mean concentration profile

$$\overline{c}(r) = \psi^2(r), \qquad \psi(r) = \text{const} \int G(\mathbf{r}, \mathbf{r}') d\mathbf{r}'. \tag{4.26}$$

As follows from eq.(4.25),

$$(\hat{L} + \mu)\psi = \text{const}. \tag{4.27}$$

The condition $U \to 0$ and $\psi \to \psi_0 = \sqrt{c_0}$ as $r \to \infty$ define const $= \mu\psi_0$ in eq.(4.27). The ideal Hamiltonian in the Grand-Canonical Ensemble consistent with eq.(4.27) is

$$H_{\text{id}}^{(0)} = \int \left\{ a^2 (\nabla\psi)^2 + \mu(\psi - \psi_0)^2 + U(\mathbf{r})\psi^2 \right\} d\mathbf{r} \tag{4.28}$$

and ψ is detemined *via* the equation

$$\overline{c}(r) = \psi^2(r), \qquad \{\hat{L} + \mu\}\psi \equiv \{-a^2\nabla^2 + \mu + U(\mathbf{r})\}\psi = \mu\psi_0. \tag{4.29}$$

With the right ψ, F_{id} is exactly $H_{\text{id}}^{(0)}[\psi^2]$ given above. So we know that the long-range contribution has to compensate the fluctuation correction

of the ideal system. In the quadratic approximation, the increment of the Hamiltonian generated by the fluctuation[5] $c'(\mathbf{r}) = c(\mathbf{r}) - \overline{c}(\mathbf{r})$ is

$$\begin{aligned}\Delta H[c'(\mathbf{r})] &= \frac{1}{2}\int c'(\mathbf{r})\left.\frac{\delta^2 H}{\delta c'(\mathbf{r})\delta c'(\mathbf{r}')}\right|_{\overline{c}} c'(\mathbf{r}')\,d\mathbf{r}d\mathbf{r}' \\ &= \frac{1}{2}\int c'(\mathbf{r})\mathcal{G}_0^{-1}(\mathbf{r},\mathbf{r}')c'(\mathbf{r}')\,d\mathbf{r}d\mathbf{r}'\end{aligned} \tag{4.30}$$

where $\mathcal{G}_0$ is the pair correlation function $\langle c'(\mathbf{r})c'(\mathbf{r}')\rangle$. Therefore, the long-range free energy term reads

$$F_{\rm lr}[\overline{c}] \simeq H_{\rm nloc}[\overline{c}] \simeq -F_{\rm id}^{\rm fluct} = \frac{1}{2}\ln\det\mathcal{G}_0 = \frac{1}{2}{\rm Tr}\ln\mathcal{G}_0 \tag{4.31}$$

where $\mathcal{G}_0$ is the pair correlation function, det and Tr are the classical determinant and trace of continuous operators, and unuseful constants are omitted. For non-interacting chains under a Flory-distribution, correlations are given by the relations:

$$\mathcal{G}_0(r,r') = 2\psi(r)\psi(r')G(r,r') \tag{4.32}$$

$$G(r,r') = \int_0^\infty G_N(r,r')e^{-\mu N}dN \tag{4.33}$$

and G_N is of course the two-point correlation of an N segment, associated to the operator $\hat{G}_N = e^{-N\hat{L}}$. Operating the integral on N, one finds $\hat{G} = (\hat{L}+\mu)^{-1} = (\hat{L}_\mu)^{-1}$ and without unuseful constants, fluctuation-induced effects read

$$F_{\rm lr} = -\frac{1}{2}{\rm Tr}\ln(\hat{L}+\mu) = -\frac{1}{2}{\rm Tr}\ln(\hat{L}_\mu). \tag{4.34}$$

Using the identity

$$-\ln A = \int_0^\infty \frac{dt}{t}\left\{e^{-At} - e^{-t}\right\} \tag{4.35}$$

this result becomes (without the constant)

$$\begin{aligned}F_{\rm lr} &\simeq \frac{1}{2}{\rm Tr}\int_0^\infty \frac{dN}{N}e^{-N(\hat{L}+\mu)} \\ &\simeq \frac{1}{2}\int d\mathbf{r}\int_0^\infty \frac{dN}{N}G_N(r,r)e^{-\mu N} \\ &= \sum_N Z_N\end{aligned} \tag{4.36}$$

[5]The quantity c' is very different from the (statistically averaged) deviation from the mean concentration $\delta c = \overline{c}(\mathbf{r}) - c_0$, usually used in the thesis.

with Z_N, the statistical weight of a ring of N monomers and Tr the trace operator. Knowing that the grand partition function of noninteracting (living) ideal rings can be factorized as[6]

$$\Xi_{\rm ring} = \prod_{N=0}^{\infty} \left(\sum_n \frac{Z_N^n}{n!} \right) = \prod_{N=0}^{\infty} \exp(Z_N), \tag{4.37}$$

the long-range free energy term is clearly identified as the opposite of the excess free energy of cyclic conformations, $F_{\rm lr} \simeq -F_{\rm ring}$ in our system of linear polymer, because the Hamiltonian considered does not distinguish closed and linear conformations. Self-Organized Criticality has since a long time been recognized as resulting from interactions between soft-modes [51]. These long-range "anomalous" correlations described here have explicitly been recognized as an effect of the $n-1=-1$ Goldstone mode, using the polymer/magnet analogy [64], or as an *anti-Casimir effect* which creates repulsion between two plates immersed in a polymer matrix (because the $n-1=-1$ Goldstone mode creates *anti*-correlations, with a minus sign).

4.3 Applications

4.3.1 Weakly Inhomogeneous Systems

As an application, let us estimate the energy of long-range interactions when the concentration is weakly perturbed around c_0, $\delta c = \overline{c}(r) - c_0 \ll c_0$ by something (let us say dilute mesoscopic particles in a polymer matrix, for instance). One can self-consistently deduce a relation between the potential and the profile far enough from the origin of the inhomogeneities. In our case, following the Lifshitz-Edwards equation for $\psi = \sqrt{\overline{c}}$ given above, it gives

$$U(r) \simeq \frac{a^2 \nabla^2 \delta c}{2c_0} - \frac{\mu \delta c}{2c_0}. \tag{4.38}$$

Then we can write $L_\mu = L_\mu^{(0)} + \delta L_\mu$, where $L_\mu^{(0)} = -a^2\nabla^2 + \mu$ and $\delta L_\mu(r,r') = U(r)\delta(r-r')$. Expanding L_μ in eq.(4.34) as a series of δL_μ, and noting that the linear term does not contribute, long-range effects give

$$F_{\rm lr} \simeq \frac{1}{4} {\rm Tr} \left(\left(\delta L_\mu G^{(0)} \right)^2 \right) \tag{4.39}$$

[6] Rings with the same polymerization degree cannot be distinguished, $\frac{Z_N^n}{n!}$ is the (canonical) partition function of a system of n identical N-rings.

with $G^{(0)} = [L_\mu^{(0)}]^{-1}$ (in the reciprocal space, it is $\frac{G_\mu^{(0)}(q)}{2c_0}$). It therefore reads

$$\begin{aligned} F_{\rm lr} &= \frac{1}{4}\int d\mathbf{r}d\mathbf{r}'\{U(r)G^{(0)}(r,r')U(r')G^{(0)}(r',r)\} \\ &= \frac{1}{4}\int \frac{d\mathbf{q}}{(2\pi)^3}\left(\frac{q^2a^2+\mu}{2c_0}\right)^2 \delta c_{\mathbf{q}}\delta c_{-\mathbf{q}} \int \frac{d\mathbf{q}'}{(2\pi)^3}\frac{1}{\mu+q'^2a^2}\frac{1}{\mu+(q-q')^2a^2} \\ &= \frac{1}{4}\int d\mathbf{r}d\mathbf{r}'\,\frac{\delta c(r)\delta c(r')}{4\,c_0^2}\{-a^2\nabla^2+\mu\}^2 G^{(0)2}(r,r') \end{aligned} \tag{4.40}$$

It is exactly the same result as in eq.(4.18), which corrected the structure factor in the melt of linear living polymers and raised to the long-range term

$$\begin{aligned} F_{\rm lr} \simeq \int d\mathbf{r}d\mathbf{r}'\delta c(r)\frac{1}{2}\frac{3}{16\pi^2\,c_0^2}\frac{e^{-2\frac{\sqrt{\mu}}{a}|r-r'|}}{|r-r'|^6}\delta c(r') \\ \{1+2\frac{\sqrt{\mu}}{a}|r-r'|+\frac{11}{6}\frac{\mu}{a^2}|r-r'|^2+\frac{\mu^{3/2}}{a^3}|r-r'|^3+\frac{3}{8}\frac{\mu^2}{a^4}|r-r'|^4\}. \end{aligned} \tag{4.41}$$

One has to keep in mind that here are measured deviations from mean-field methods in the ground state dominance approximation, allowing $F_{\rm lr} \simeq H_{\rm lr}$. The last line of eq.(4.40) ease the calculation of these correlations at any dimension.

4.3.2 Solvent/Solvent Interfaces.

In the light of these new correlations in concentrated polymer solution, it is possible to establish a very toy model describing an interface between two dense solutions of a linear living polymer in two solvents (the excluded volume in each solvent is supposed to be almost the same). The affinity of a monomer for one solvent rather than the other is here expressed by a molecular field (per monomer) represented as an external step potential φ, which creates inhomogeneities and reads (Fig.4.4)

$$\varphi(z) = \frac{U}{2} - U\theta(-z) = \begin{cases} +\frac{U}{2} & \text{if } z>0 \\ -\frac{U}{2} & \text{else.} \end{cases}$$

where θ is the Heaviside step function. Supposing weak deviations in the

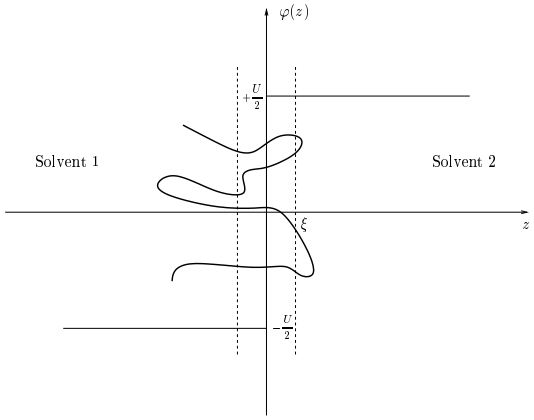

Figure 4.4: A conformation of a polymer in the melt near a solvent/solvent interface. Monomers are going rather into solvent 1 than into solvent 2. U is the cost of energy for a monomer to go from solvent 1 to solvent 2.

system, linear response can be applied. In the reciprocal space, using the response function given by eq. (4.15), it reads

$$\delta c_{\mathbf{q}} = -S(\mathbf{q})\varphi(\mathbf{q}) \tag{4.42}$$

where $\delta c_{\mathbf{q}}$ and $\varphi(\mathbf{q})$ are respectively Fourier transforms of the profile and of the potential. Because of the symmetry of the problem, it is enough to calculate δc from eq.(4.42) in the right-hand side of the system $z > 0$, and deduce the left-hand side. The potential reads $\varphi(\mathbf{q}) = -iU(2\pi)^2\delta(q_x)\delta(q_y)\mathcal{P}\frac{1}{q_z}$ in the reciprocal space, where $\mathcal{P}$ is the principal value and q_x, q_y and q_z are respectively components of the wave-vector along x, y and z-axes. As the system is homogeneous along the parallel axes Ox and Oy, let us now substitute $q \leftarrow q_z$. The linear response therefore reads

$$\delta c(z) = \frac{2c_0}{a^2}\mathcal{P}\int_{-\infty}^{\infty}\frac{dq}{2\pi}iU\,\frac{e^{iqz}}{q\left\{q^2+\xi_\mu^{-2}+\frac{(\mu/a^2+q^2)^2}{32c_0qa^2}\frac{2}{\pi}\arctan\left(\frac{qa}{2\sqrt{\mu}}\right)\right\}} \tag{4.43}$$

in the direct space. There we use eq.(4.15) valid for $q\xi \ll 1$. Therefore eq.(4.43) is valid for $|z| \gg \xi$. It is possible to evaluate it with the contour shown in Fig.4.5. The different contributions are clearly identified as specific singularities in the contour. As usually, the mean-field solution comes out from the single pole $i\xi_\mu^{-1}$, the bulk limit is found in the large length-scale, around the singularity at the origin, while the long-range terms emerge from

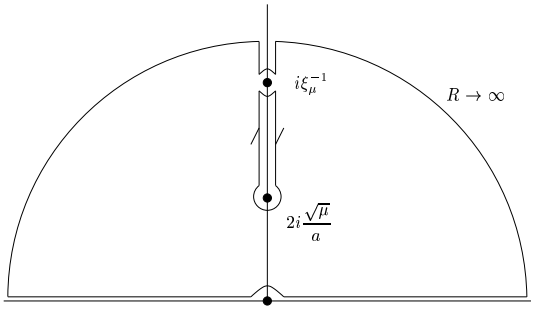

Figure 4.5: One of the possible contour in the $\mathbb{C}$ plane to evaluate the new profile. The mean-field contribution comes from the single pole $i\xi_\mu^{-1}$, the bulk limit is given by the singularity at the origin and the effect of the long-range correlations comes from the integrals along the imaginary axis.

the integrals along the Imaginary axis. It yields, for $z > 0$,

$$\delta c(z) = \delta_{\rm mf} c(z) + \delta_{\rm lr} c(z) \qquad \text{with} \qquad \delta_{\rm mf} c(z) = -c_0 \frac{\xi_\mu^2}{a^2} U(1 - e^{-z/\xi_\mu}) \tag{4.44}$$

the long-range contribution being

$$\delta_{\rm lr} c(z) = -\frac{U\xi_\mu^4}{16\pi a^4} \left(\left(\frac{2}{z} \left(\frac{\sqrt{\mu}}{a} + \frac{1}{z} \right)^2 + \frac{\mu^{3/2}}{2a^3} \right) e^{-\frac{2z\sqrt{\mu}}{a}} + z \frac{\mu^2}{a^4} \mathrm{Ei}(-\frac{2z\sqrt{\mu}}{a}) \right) \tag{4.45}$$

with the Exponential Integral function $E_{\rm i}(z) \equiv -\mathcal{P} \int_{-z}^{\infty} e^{-t} \frac{dt}{t}$. The first term is obviously the mean-field relaxation from the left to the right bulk density. It is quickly carried out around the origin. The lack of monomer on the right-hand side is therefore $\delta c_{\rm bulk2} = c_{\rm bulk2} - c_0 = -\frac{U c_0}{\mu + 2 c_0 v}$. Please note that this derivation is valid if $U \ll v c_0$. The second term is of course due to the long-range interactions. These effects holds on $R_{\rm g}$ and creates algebraic tails. In the intermediate region $\xi \ll z \ll R_{\rm g}$, the tails scale as $\frac{1}{z^3}$. Taking $\mu = 0$, the deviation for infinite chain is immediate from eq.(4.45), it is:

$$\delta_{\rm lr} c(z) = -\frac{U\xi^4}{8\pi a^4} \frac{1}{z^3}. \tag{4.46}$$

Therefore, to conclude, the only mean-field treatment creates a monotonous interface on the scale ξ, while the long-range term creates variations and algebraic queues which subsist on $R_{\rm g}$ as represented on the schematic view of Fig.4.6. Let us now have simple considerations with a small difference

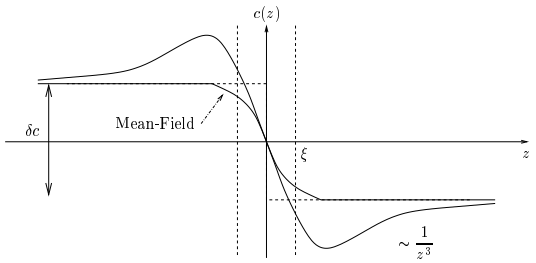

Figure 4.6: Schematic profile at a solvent/solvent interface.

of excluded volume $\delta v = v_2 - v_1$. The molecular field in the right side of the system would therefore include the excluded volume interaction which reads $(v_1 + \delta v)(c_0 + \delta c(z))$. As the deviation from c_0 is small, the constant molecular field may be enough to treat this slight difference, saying the effective molecular field $U_{\text{eff}} = U + \delta v c_0$. At the lowest order, it does not change anything to the preceding statements.

4.3.3 Influence on the Surface Tension

It is possible to imagine the effects of these correlations on the surface tension near an impenetrable wall. Actually in a melt of macromolecules of typical size R_g, one can evaluate the surface energy. Before considering these long range effects, it has been established that the dominant term of interfacial energy after a mean-field treatment is proportional to $\frac{a^2 c_0}{\xi}$ (see section 1.2.8). Let us have qualitative considerations at the sight of eq.(4.36). Firstly, it has been shown in chapter 1.2 [19, 35], that at the mean-field level, the influence of a wall only holds on a layer of thickness ξ (depleted or adsorbed depending on the nature of the interaction between the wall and the monomers). Therefore, further than some ξ, the mean-field concentration profile is flat, suggesting systematic reflective boundary conditions when studying properties far from the wall $\nabla G_N \cdot \hat{\mathbf{z}}|_{z=0} = 0$. Furthermore, at an interface where the conformations might be reflected (see Fig.4.7), not only phantom cycles from the right-hand side, but also the reflected conformations forming extra cycles have to be taken into account. Compared to the bulk case, these reflected loops induce extra repulsion in a layer of thickness R_g, which naturally increase the surface tension and imply mass-corrections. Equation (4.36) enables to be more quantitative. Actually we consider a semi-infinite system as in Fig 1.10. In references [46, 69, 49, 30], propagators are assessed, taking into account the attraction or the depletion layer (according to the

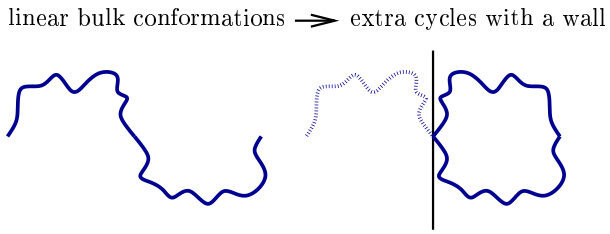

Figure 4.7: Loops involved near the wall are naturally the closed conformations which would exist in the bulk but also the reflected linear conformations of the bulk which form extra cycles in the presence of an impenetrable wall (as represented in this figure). These reflected conformations lead to extra repulsion which increases the surface tension.

nature of the interaction between the monomers and the wall). Both cases show that over some ξ, the propagators behave as if they would verify the reflective boundary condition $\nabla G_N \cdot \hat{\mathbf{z}} = 0$ at the wall. They read in both cases

$$G_N(r,r') \underset{r,r' \gtrsim \xi \text{ or } N > g_0}{=} \left(\frac{1}{4\pi N a^2}\right)^{3/2} * \exp\left(-\frac{(x-x')^2}{4Na^2}\right) * \exp\left(-\frac{(y-y')^2}{4Na^2}\right) * \left\{\exp\left(-\frac{(z+z')^2}{4Na^2}\right) + \exp\left(-\frac{(z-z')^2}{4Na^2}\right)\right\}. \tag{4.47}$$

This last equation shows that this boundary condition boils down to taking into account the mirror-conformations [30] (see Fig.4.7). Thus one can deduce from eq.(4.36) the influence of these long-range correlations on the surface tension. Let us consider the Wilhelmy geometry (see Fig.4.8). The surface tension between the polymer solution and the wall can be seen as the difference between the energy of the polymeric system with an impenetrable wall and half the bulk energy (without any hindrance). The surface tension

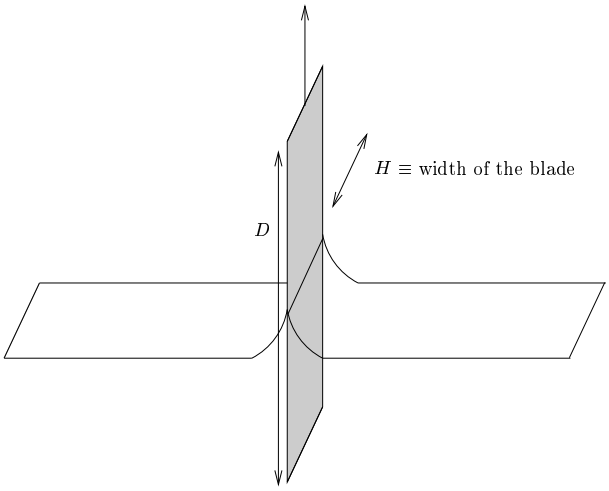

Figure 4.8: The geometry considered to assess the surface tension is well represented by Wilhelmy's method to measure surface tension.

due to the long range correlations thus reads

$$\begin{aligned}
\gamma_{\rm lr} &\simeq \left(\frac{F_{\rm lr}}{A}\right)_{\rm wall} - \frac{1}{2}\left(\frac{F_{\rm lr}}{A}\right)_{\rm bulk} \\
&\simeq \frac{1}{2}\int_{\xi}^{\infty} dz \int_{g_0}^{\infty} \frac{dN}{N}\{G_{N,\rm wall}(r,r) - G_{N,\rm bulk}(r,r)\}e^{-N\mu} \\
&\simeq \frac{1}{2}\int_{\xi}^{\infty} dz \int_{g_0}^{\infty} \frac{dN}{N} e^{-N\mu}\left(\frac{1}{4\pi N a^2}\right)^{3/2} \exp\left(-\frac{z^2}{Na^2}\right) \\
&\simeq \int_{g_0}^{\infty} \frac{1}{32\pi N^2 a^2} e^{-N\mu} dN
\end{aligned} \tag{4.48}$$

where $g_0 = \frac{\xi^2}{a^2}$ is the mean-field correlation blob size, used here to remove divergences coming from the small cycles. Next, the contribution of the reflected rings reads

$$\begin{aligned}
\gamma_{\rm lr} &\simeq \frac{cste}{g_0 a^2} + \frac{1}{32\pi a^2}\mu\left\{\log(\mu\, g_0) + C - 1\right\} \\
&= \frac{cste}{g_0 a^2} - \frac{1}{32\pi a^2}\frac{1}{\langle N\rangle}\left\{\log\left(\frac{\langle N\rangle}{g_0}\right) + 1 - C\right\}
\end{aligned} \tag{4.49}$$

with C the Euler constant ($C = \lim_{m\to\infty}\{\sum_{k=1}^{m}\frac{1}{k} - \log(m)\} \simeq 0.577216...$), and the first dominant constant term coming from (and depending on) the

lower bound. This term scales as ξ^{-2}, as γ_{fluct} does, (see section 1.2.8). Of course, as $R_g \gg \xi$, the sign of the $\langle N \rangle$-dependent part of this long range contribution is negative, so that the surface tension increases with the mean polymerization degree $\langle N \rangle$ (the same tendency is derived in [60, 31], from the correction to the ground state approximation for finite chains).

4.4 Conclusion

In this chapter, long-range correlations, induced by fluctuations have been derived for a system of linear polymer with a Flory-distribution. They are directly related to the extra non-local monomer correlations imposed by the structure of long linear chains. The effect is taken into account by extra conformational free energy terms. Two effects of these collective correlations have been analyzed near interfaces:

- in the case of chains near an interface between two slightly different solvents, instead of common mean-field effects which confine interfacial properties in a small layer of size ξ, these interactions induce transitional effects which hold on the macroscopic size R_g and create algebraic tails in the density profile for instance. Qualitatively similar effects are anticipated near a solid wall.
- in the case of an impenetrable wall, because of the reflected ring conformations, extra repulsions induce positive contributions to the surface tension, and put forward an increase of the surface tension with chain length.

One step further, we can assume that these effects may also play a role in colloidal suspensions stabilization for instance [64]. Actually, considering two small neutral particles in a matrix of infinite polymers, separated by a distance D far greater than their own size $(V_1)^{1/3}$ and $(V_2)^{1/3}$, the polymer-induced interactions would approximately read

$$\begin{aligned} F_{\text{lr}} \simeq \simeq & \frac{3}{16\pi^2}\frac{V_1 V_2}{D^6}\{1 + 2\frac{\sqrt{\mu}}{a}D + \frac{11}{6}\frac{\mu}{a^2}D^2 + \frac{\mu^{3/2}}{a^3}D^3 + \frac{3}{8}\frac{\mu^2}{a^4}D^4\}e^{-2\frac{\sqrt{\mu}}{a}D} \\ & \underset{\mu \to 0}{\simeq} \frac{3}{16\pi^2}\frac{V_1 V_2}{D^6}. \end{aligned} \tag{4.50}$$

That interaction is not only long-range, scaling as the Van der Waals forces as $\frac{1}{D^6}$, but it is also repulsive, so it may screen a part or the whole Van der Waals attraction responsible for coagulation of colloids.

Chapter 5

Conclusions

We investigated in this thesis the physics of dense solutions of long linear polymers. In such systems, fluctuations are weak and were previously expected to be negligible. This assumption is known as the Flory theorem and is based on a mean-field view: a unit of a chain in the melt perceives the surrounding units as a constant background (without fluctuations), the volume interactions are screened (the molecular field vanishes) and a chain should adopt Gaussian conformations. In such systems static properties related to Gaussian statistics are thus expected. Among others, the size of a chain should scale as $N^{1/2}$, and the small-angle neutron scattering spectrum should exhibit a plateau in a Kratky representation ($q^2 I(q)$ *versus* q) as a signature of its Hausdorff dimension. Edwards developed a quantitative self-consistent theory which describes how the excluded volume interactions are screened in dense solutions (the Random Phase or Simple Tree Approximation). That theory explicitly puts forward an effective potential which consists of a strong repulsive part of very short range and a weak attractive counterpart of interaction range ξ, the mean-field correlation length. In that scheme, the effective interaction between two monomers whose separation r is larger than ξ is expected to be very weak, and exponentially cut on ξ. The effective Fixman interaction parameter scales as $1/\sqrt{N}$ in three dimensions confirming the weakness of the effective interaction (when summed over all the pairs of a chain). Nevertheless, we checked how some quantities are perturbed from the Gaussian statistics.

First, we evaluated the correlations between two Gaussian bonds of an infinite chain in a melt of flexible polymers (section 2.1). Even neighboring bonds should *a priori* be uncorrelated in a Gaussian chain. But, calling $g = \xi^2/a^2$ the number of units in a correlation blob, this calculation shows

that even over the blob, for bonds separated by $s \gg g$ monomers, these correlations decrease as $s^{-3/2}$ with a prefactor independent of the interaction. That correction is clearly identified in numerical simulations of J. P. Wittmer. That power law underlines the difficulty of defining a persistence length in polymer melts. This calculation also puts forward an orientation effect associated to the first Legendre polynomial, which extends on the coil size rather than ξ. Although weak for $s > g$, it is non-local.

Then we turned to living polymers: we wanted to know how the screened potential may affect the equilibrium molecular weight distribution of ideal living polymers. (section 2.2). Using the potential adapted to the correct polydispersity, we derived the perturbative correction to the partition function of an N-chain, which comes down to assessing the Gaussian averaging of the effective potential summed on the entire chain. The result does not depend on the strength v of direct monomer interaction as well. One of the two terms of the correction may be large if $N \gtrsim \langle N \rangle^2$, *i.e.* for rare chains really much longer than the mean-size. There we defined a function which measures the deviations of the moments from the ideal Flory-distribution. The analytical results for this function are in good agreement with the dense systems of living polymers simulated by J. P. Wittmer.

Afterwards, in the light of some experimental results which showed that, so far, no neutron scattering result may be considered as a clear evidence of Flory's prediction, we corrected the form factor to first order. We used the Flory distribution in order to include some size effects in the correction. We predict a non-monotonic correction to the ideal chain scattering function, crossing from positive in the Guinier regime, to negative in the Kratky regime. As for other intramolecular quantities, because of the perturbative treatment, the size-related corrections scale as $\langle N \rangle^{-1/2}$ in the asymptotic regimes. But another interesting term emerges from this calculation which enables to write the form factor of an infinite chain in the melt in the very speaking form

$$\frac{1}{F(q)} = \frac{q^2 b^{*2}}{12} + \frac{1}{32}\frac{q^3}{c_0} \qquad \text{for} \quad q\xi \ll 1.$$

The correction depends neither on the excluded volume parameter v, nor on the statistical segment. It should thus hold even in the strongly fluctuating semidilute regime. A very similar term comes out from the renormalization group calculations of L. Schäfer. It is identified as coming from some residual interactions between blobs. It contributes as an anti-correlation term decreasing as r^{-2} in the intramolecular correlations in direct space. That systematic deviation from the Debye formula shows that even for infinitely

long and flexible polymer chains, no Kratky plateau should be expected in the form factor measured from a dense solution or melt. The agreement between the predictions and Monte-Carlo simulations is quite good.

In the next part, we turned to collective properties in melts of long *linear* polymers. From the simple observation that the local mean-field Hamiltonian of ideal chains does not generate the right density correlation functions for *linear* chains, we derived the first correction for living polymers. That correction consists in a long-range repulsion. Then we showed that in weakly fluctuating systems of infinite chains, it yields a q^3-term to the inverse structure factor loosely related to the q^3-correction to the inverse form factor. In addition to the classical mean-field density correlations screened on the correlation length, this q^3-term leads to extra long-range correlations, scaling as r^{-6} . For finite chains, the corresponding expressions are more complicated, but those extra long-range correlations also scales as r^{-6} at small distances and are exponentially cut over $R_{\rm g}$.

Afterwards, the relation was established between these long-range interactions and the fluctuation-induced correction to the mean-field approach. This formal derivation highlights the origin of these long range repulsions: it explicitly comes from the removal of the excess free energy of the ring conformations. The end of that part consists in the description of some effects of these long-range correlations. First, we treated a very toy model of an interface between two dense solutions of living polymers with different solvents. The model consists in a potential step per monomer, and it is solved in the framework of linear response. In addition to the mean-field monotonous profile confined in a layer of size $\simeq \xi$, we derived long-range variations and algebraic tails dominated by z^{-3}, for intermediate distances from the interface $\xi \ll z \ll R_{\rm g}$. These tails hold on the coil size.

And finally, we assessed the correction to the polymer-induced surface tension at an impenetrable wall in the light of these new correlations. We first sketched that independently of the specific interaction between the wall and the monomers, the reflective boundary condition applies when the major effect estimated is located further than some ξ from the wall. Therefore the non-local free energy here comes from "direct" and "reflected" loops. As a correction to the dominant term $\gamma_{\rm mf} \simeq a^2 c_0/\xi$, we derived a fluctuation correction as ξ^{-2} from a lower cut-off and a size-dependent part of the surface tension increasing as $-1/\langle N\rangle$ and $-(1/\langle N\rangle)\log\langle N\rangle$.

Let us give some direct extensions to this work:

- The approach used to correct the intramolecular properties may be extended to quasi two-dimensional systems. For instance for thin films

of width $H \lesssim \xi$ to avoid segregation (allowing interpenetration) and weakly fluctuating systems $G_z^2 = \frac{1}{4\pi c_0 a^2} \ll 1$ where c_0 is the projected concentration ($c_0 b^2$ allowed to be greater than 1).

- The density profile near an impenetrable wall can be accurately estimated. We anticipate a z^{-3} tail in the intermediate range $\xi \ll z \ll R_g$.
- The effects of these interactions on polymer/polymer interfaces in the strong segregation limit may be evaluated.
- For concentration profiles and surface tension, the effects described here should be compared to the effects due to end points mentioned earlier [62], when both exists.

Appendix A

Some properties of the Form Factor

Here the spatial dimension is $d = 3$. The form factor is a single-object property. It is the intramolecular part of the density correlations. It is proportional to the scattered intensity in the case of solution of non interacting objects, that is why it is the cornerstone of our discussion about the Flory theorem. This quantity is extensively discussed in [37, 24]. Nevertheless, let us remind some properties which could be useful for the arguments of thesis.

A.1 Definition and Normalization

The normalization chosen in section 1.2 and in chapter 3 is not the most common one. Indeed for an object with N scattering centres we defined

$$\begin{aligned} F_N(\mathbf{q}) &= \frac{1}{N}\sum_{i=1}^{N}\sum_{j=1}^{N}\langle \exp(-i\mathbf{q}\mathbf{r}_{ij})\rangle \\ &= N\,P_N(\mathbf{q}), \end{aligned} \tag{A.1}$$

where $P_N(\mathbf{q})$ is the form factor with the more natural normalization $P_N(0) = 1$. Let us generalize P_N to P, in the continuous limit. It reads

$$P(\mathbf{q}) = \frac{\int d\mathbf{r}\, \exp(-i\mathbf{q}\mathbf{r})\mathcal{G}_{\text{intra}}(\mathbf{r})}{\int d\mathbf{r}\, \mathcal{G}_{\text{intra}}(\mathbf{r})} \tag{A.2}$$

where $\mathcal{G}_{\text{intra}}$ is the pair correlation function of one object ("intra" when talking about solutions)[1]. For a compact homogeneous body, it is

$$\mathcal{G}_{\text{intra}}(\mathbf{r}) = \int \{\rho(\mathbf{r}')\rho(\mathbf{r}+\mathbf{r}')\} d\mathbf{r}', \tag{A.3}$$

with $\rho(\mathbf{r}) = 1/V_{\text{body}}$ if $\mathbf{r}$ is inside the body and 0 otherwise (V_{body} is the total volume of the body). This last equation shows that it comes down to assessing the common volume of the object and its copy, translated by the vector $\mathbf{r}$ [24]. Please note also that $\int d\mathbf{r}\, \mathcal{G}_{\text{intra}}(\mathbf{r}) = V_{\text{body}}$ for a compact body and N for a macromolecule. Of course, equations (A.1)and (A.3) are equivalent. Under spherical symmetry, when $\mathcal{G}_{\text{intra}}$ is only a radial function of $r = |\mathbf{r}|$ (when there is no orientational ordering, it is always the case for us) the orientational averaging of $\exp(-i\mathbf{qr})$ may be carry out first. Calling $n(r) = 2\pi r^2 \mathcal{G}_{\text{intra}}(r)$ the spherical pair correlation function[2], it yields

$$P(q) = \frac{1}{\int_0^\infty n(r)dr} \int_0^\infty n(r) \frac{\sin(qr)}{qr} dr \tag{A.4}$$

and for small q,

$$P(q) = 1 - \frac{q^2 R_{\text{g}}^2}{3}, \tag{A.5}$$

with the radius of gyration being

$$R_{\text{g}}^2 = \frac{1}{\int_0^\infty n(r)dr} \int_0^\infty n(r) r^2 dr \quad \text{or} \quad R_{\text{g}}^2 = \frac{1}{2N^2} \sum_{i,j=1}^{N} \langle \mathbf{r}_{ij}^2 \rangle \tag{A.6}$$

for a macromolecule. For objects whose internal shapes do not fluctuate, it is also useful to remind that the form factor is only $P(q) = \rho_q \rho_{-q}$, with ρ_q designating the Fourier transform of the (internal) density of the body. Let us now derive the form factor of easy shapes which could help for a better understanding of neutron scattering experiment.

A.2 Form Factor of a Sphere

As a first academic example, let us consider an homogeneous sphere of density $\rho(r) = \frac{3}{4\pi R^3} = \frac{1}{V_{\text{sphere}}}$ for $r \leq R$ as in Fig.A.1. The Fourier transform of

[1] Our choice was driven by the direct relation between the form and the structure factor in a system of non-interacting chains of mean unit concentration c_0, $S(\mathbf{q}) = c_0 F(\mathbf{q})$. This definition is easier to manipulate in the case of polydispersity, when averaging are ambiguous.

[2] After orientational averaging.

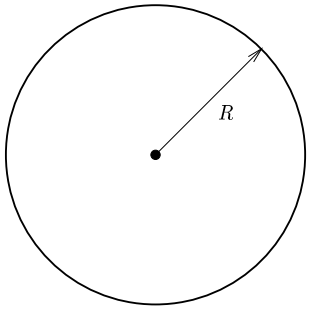

Figure A.1: An homogeneous sphere of radius of density $\rho = \frac{3}{4\pi R^3} = \frac{1}{V_{\text{sphere}}}$ for $r \leq R$.

the density is easy to assess because of the symmetry, and reads

$$\rho_q = \int_0^R 2\pi r^2 dr \int_{-1}^1 e^{-iqru} du = \frac{3}{q^3R^3}(\sin(qR) - qR\cos(qR)) \tag{A.7}$$

which yields immediately the form factor, because of the symmetries

$$P(q) = \frac{9}{q^6R^6}(qR\cos(qR) - \sin(qR))^2 \underset{qR\ll 1}{\simeq} 1 - \frac{q^2R^2}{5}. \tag{A.8}$$

The small-q regime $qR \ll 1$ gives the radius of gyration of this sphere, $R_{\text{g}}^2 = \frac{3R^2}{5}$.

A.3 Form Factor of a Rigid Rod: Effect of the Thickness

The case of the rigid rod features many experimental informations: it gives the right asymptotic scaling law involved in the evaluation of the persistence 3 length, and it is useful to analyze the effect of the thickness of the chain. So, before any orientational averaging, the Fourier transform of the density of an infinitely thick rod reads (see also Fig.A.2)

$$\rho_{\mathbf{q}} = \rho_{\mathbf{q}}(q, \cos\theta) = \frac{1}{L}\int_{-L/2}^{L/2} \exp\left(-iqr\cos\theta\right) dr = \frac{2}{qL\cos\theta}\sin\left(\frac{qL\cos\theta}{2}\right). \tag{A.9}$$

The square of this last expression after orientational averaging yields

$$P_\infty(q) = \frac{2}{qL}\int_0^{qL}\frac{\sin u}{u}du - \frac{\sin^2\left(\frac{qL}{2}\right)}{\left(\frac{qL}{2}\right)^2}. \tag{A.10}$$

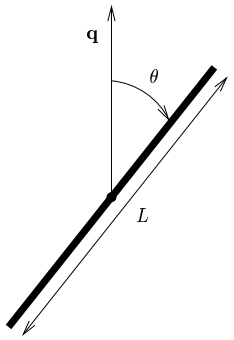

Figure A.2: An homogeneous rigid rod of linear density $\rho = \frac{1}{L}$ (when the radius of gyration of the cross section is negligible, *i.e.* $R_c \ll L$).

For $qL \ll 1$, the Guinier regime gives the radius of gyration of the rod

$$P(q) \underset{qR \ll 1}{\simeq} 1 - \frac{q^2 L^2}{36} \qquad \Rightarrow \qquad R_g = \frac{L^2}{12} \tag{A.11}$$

while in the intermediate regime where $qL \gg 1$, the form factor is $P(q) \simeq \frac{\pi}{qL}$, interpreting the increasing part of the curve in the Kratky plot $q^2 P(q)$, when scanning scales smaller than l_p, the persistence length (see Fig.A.3). Let us

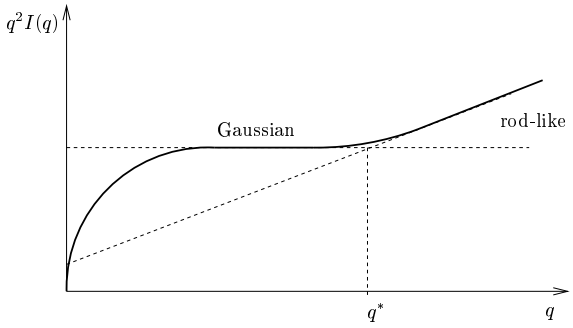

Figure A.3: Schematic visualization of the rod-like effect for a Gaussian chain in the Kratky graph. This effect is perceptible over the crossover wave vector $q^* \sim l_p^{-1}$.

now consider a cylindrical rod with a finite thickness characterized by its radius of gyration R_c small compared to L. If this last inequality is verified, neglecting the phase difference (interferences) between the centre and any other point of a slice is a good approximation (see Fig.A.4). It enables

therefore to factorize the form factor as $P(q) = P_\infty(q) * P_c(q)$ where $P_c(q)$ is the form factor of the cross-section and $P_\infty(q)$ is the form factor of the infinitely thin rod (eq.A.10). One step further, if $qR_c \ll 1$, let us assume that

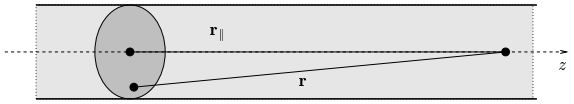

Figure A.4: Interferences of two points in the same section are negligible when integrating on $r_\parallel$ if $L \gg R_c$, with R_c the radius of gyration of the cross section. Therefore the surface and the linear part of the form factor can be factorized.

the whole range of wave vectors are in the Guinier regime for the section, in such a way that $P_c(q) \simeq 1 - \frac{q^2 R_c^2}{3} \simeq \exp\left(-\frac{q^2 R_c^2}{3}\right)$ and the contribution of the rod in the intermediate regime ($qL \gg 1$) reads:

$$P(q) = \frac{\pi}{qL} \exp\left(-\frac{q^2 R_c^2}{3}\right) \tag{A.12}$$

These two effects may compensate[3], as described in [54, 55, 37]. Curves as in Fig.A.3 may be flattened, without describing Gaussian statistics.

A.4 Scaling Law for the Form Factor of Macromolecules

Roughly speaking, an object is fractal if it verifies a relation of self-similarity, which connects its mass M to its size R via a power law $M(R) \sim R^{d_H}$. d_H is the Hausdorff fractal dimension [8]. Typically in the case of a polymer, the mass is proportional to the number of units. Because of the definition of the critical exponent ν as $R \sim N^\nu$ or $R_g \sim N^\nu$, the Hausdorff dimension is $1/\nu$. Consider a solution of N_p macromolecules of polymerization degree N and mean concentration of monomers c_0 in the volume V, we want to know how behaves the scattered intensity (from neutron experiments) on the scales $\frac{1}{R_g} \ll q \ll \frac{1}{b}$ (b is the statistical segment) dominated by the chain statistics [24, 37] (and not by intermolecular interactions). Therefore, the intensity scales as:

$$I(q) \sim N_p N P_N(qR_g) \sim c_0 V N P_N(qR_g) \sim c_0 V N (qR_g)^\alpha. \tag{A.13}$$

[3] More subtle features are described in [54]

As on such scales, the intensity should not depend on the polymerization degree [19], the q-dependency scales as $\alpha = -1/\nu$. It yields in this range of wave vectors

$$P_N(q) \sim q^{-1/\nu}. \tag{A.14}$$

Therefore, in the large-q regime, one expects

$$\begin{aligned} P_N(q) &\sim \frac{1}{q} && \text{for a rod-like macromolecule,} \\ P_N(q) &\sim \frac{1}{q^2} && \text{for a Gaussian chain,} \\ P_N(q) &\sim \frac{1}{q^{5/3}} && \text{for a self-avoiding chain.} \end{aligned} \tag{A.15}$$

Appendix B

Thermodynamics of Binary Polymer Mixtures: The Flory-Huggins Model

This section is devoted to some results of the Flory-Huggins theory. This mean-field theory is a simple lattice model (see Fig.B.1) for polymer mixtures and solutions[1]. Consider the mixing of two species, A and B, and assume for the moment that the two form one (mixed) homogeneous single phase. It is assumed that there is no volume change on mixing so that the volume V_A of species A is mixed with volume V_B of species B to give a mixture of volume $V_A + V_B$. The mixture is macroscopically homogeneous and the two components fill the entire lattice.

Therefore, only one volume fraction is relevant since

$$f_A = \frac{V_A}{V_A + V_B} = f \quad \text{and} \quad f_B = \frac{V_B}{V_A + V_B} = 1 - f. \tag{B.1}$$

The lattice site volume v_0 is defined by the smallest units (solvent molecules or monomers) and larger molecules occupy several connected sites. The number of sites in $V_A + V_B$ is $N = (V_A + V_B)/v_0$. Molecules of species A or B have also respectively a molecular volume (the volume per molecule) $v_A = N_A v_0$ and $v_B = N_B v_0$, with N_A and N_B the numbers of sites occupied by each species (an effective degree of polymerization). In the next section, well-known results of this model are briefly given.

[1] More details may be found in many textbooks, see for instance [37, 56, 19, 32] among others.

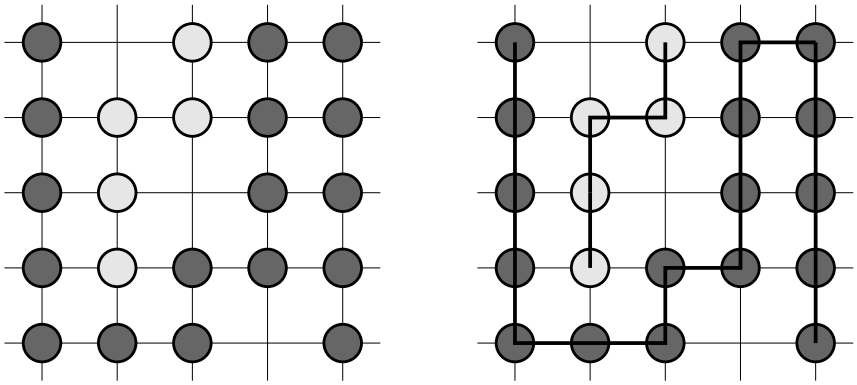

Figure B.1: The Flory-Huggins lattice model is a mean-field theory based on thermodynamics of classical mixtures (left-hand side of the figure), trying to take into account the connectivity (right-hand side).

B.1 The Entropy of Mixing

In the mean-field approximation (where fluctuations are ignored), one macromolecule sees all the other surrounding chains as a background. Before mixing, the A-monomers occupy Nf sites. Therefore, the number of translational states[2] for a macromolecule is $\Omega_{\mathrm{A}} = Nf$, and it is $\Omega_{\mathrm{AB}} = N$ after mixing[3]. Therefore, for a single macromolecule of species A, the entropy change on mixing is

$$\Delta S_{\mathrm{A}} = \log\left(\frac{\Omega_{\mathrm{AB}}}{\Omega_{\mathrm{A}}}\right) = -\log f \qquad (>0). \tag{B.2}$$

Of course, the same argument holds for the B-species. As a consequence, the total entropy of mixing of the system reads

$$\Delta S_{\mathrm{mix}} = -\left(\frac{Nf}{N_{\mathrm{A}}}\log(f) + \frac{N(1-f)}{N_{\mathrm{B}}}\log(1-f)\right) \qquad (>0). \tag{B.3}$$

It enables to deal with the intrinsic quantity of the lattice model, saying the entropy of mixing per site, which reads

$$\Delta \overline{S}_{\mathrm{mix}} = -\left(\frac{f}{N_{\mathrm{A}}}\log(f) + \frac{(1-f)}{N_{\mathrm{B}}}\log(1-f)\right) \qquad (>0). \tag{B.4}$$

[2]The number of translational states is the number of independent positions available for the center of mass of a macromolecule for instance.

[3]Please note that the mean-field is strongly used here.

This last equation predicts enormous differences between the entropies of mixing in the case of regular solutions ($N_{\mathrm{A}} = N_{\mathrm{B}} = 1$) and macromolecular blends [56] and shows how constraints (here the connectivity) can reduce the number of possible states. Nevertheless, even if this entropy is reduced, it always promotes mixing. Please note finally the main hypotheses assumed: firstly, only translational entropy is engaged, supposing that the conformational energy is the same in the pure and the mixed states (what is wrong because the only excluded volume of a chain is quite different in a pure phase and in a solution).

B.2 The Flory-Huggins Energy of Mixing

Because of the assumption of mixing under constant volumes, the relevant potential here is the Helmholtz free energy of mixing. The energetic term remains to be evaluated. The easiest version of the Flory-Huggins model is made up of a lattice (all types of monomer having the same volume v_0=the volume of a site), and pairwise interaction energies $u_{\mathrm{AA}}, u_{\mathrm{BB}}, u_{\mathrm{AB}}$ between adjacent lattice sites occupied. Therefore the averaged interaction energy between an A-monomer (B-monomer) and one of his nearest neighbor is $U_A = u_{\mathrm{AA}} f + u_{AB}(1-f)$ (respectively $U_A = u_{\mathrm{AB}} f + u_{BB}(1-f)$). Noting z the connectivity of the lattice and being aware of counting only once each pairwise interaction, the total interaction energy is:

$$U = \frac{zN}{2}\{U_{\mathrm{A}} f + U_{\mathrm{B}}(1-f)\}. \tag{B.5}$$

The energy of the same system before mixing (ignoring interfacial effects) is $U_0 = \frac{zN}{2}\{u_{\mathrm{AA}} f + u_{\mathrm{BB}}(1-f)\}$. The energy change on mixing per lattice site now reads

$$\Delta\overline{U}_{\mathrm{mix}} = \frac{U - U_0}{N} = f(1-f)\frac{z}{2}\{2u_{\mathrm{AB}} - u_{\mathrm{AA}} - u_{\mathrm{BB}}\} = \chi f(1-f), \tag{B.6}$$

with χ the Flory interaction parameter which characterizes the difference of interactions in the mixture and in the separated phases

$$\chi = \frac{z}{2}\{2u_{\mathrm{AB}} - u_{\mathrm{AA}} - u_{\mathrm{BB}}\}. \tag{B.7}$$

The free energy per site is therefore a function of the only parameter f and reads

$$\Delta\overline{F}_{\mathrm{mix}} = \left\{ \frac{f}{N_{\mathrm{A}}} \log f + \frac{1-f}{N_{\mathrm{B}}} \log(1-f) + \chi f(1-f) \right\} \tag{B.8}$$

which is a form of mean-field free energy which exhibits first order transition from mixed to segregated phases [48, 56]. Classical relations of thermodynamics rule the phase diagrams of such systems [17, 48].

B.3 Stability of a Mixture of Deuterated and Hydrogenated Polystyrene dPS/PS

From thermodynamics, we know that a necessary condition of stability of a mixture is to be on the right side of the spinodal, which comes down to saying that the free energy of the mixture is lower than the free energy of the segregated system. As a consequence, $\Delta\overline{F}_{\rm mix}$ has to be convex, verifying in the case of a mixture of deuterated and hydrogenated polystyrene with the same effective degree of polymerization N_0

$$\frac{\partial^2 \Delta\overline{F}_{\rm mix}}{\partial f^2} = \frac{1}{v_0} S^{-1}(q=0) = \frac{1}{N_0 f} + \frac{1}{N_0(1-f)} - 2\chi > 0. \tag{B.9}$$

Therefore to insure the stability of the mixture, one has to verify

$$\frac{1}{2\chi N_0} > \max_{\{f\in[0,1]\}} f(1-f) = 0.25 \quad \Rightarrow \quad \chi N_0 < \chi_{\rm c} N_0 = 2. \tag{B.10}$$

This condition is necessary and also sufficient here, because it defines the critical Flory parameter $\chi_{\rm c} = 2/N_0$ where the binodal and the spinodal meets [48, 56] (for any binary mixture in fact). This relation highlights the difficulty in making homogeneous polymer blends. As already mentioned, in the case of a blend of PS and dPS, with fully deuterated PS, $\chi = 1.5.10^{-4}$.

This result is derived in the mean-field approximation, therefore it is clearly valid in dense systems. It may be understood as this scaling argument: in a dense system, each monomer is in contact with another one. The probability that this monomer is from the other species is 1/2, therefore the critical interaction parameter may be seen as the value verifying

$$\frac{\chi N_0}{2} \simeq 1 \Rightarrow \chi_{\rm c} = \frac{2}{N_0}. \tag{B.11}$$

We emphasize in chapter 3 that the corrections to the form factor for instance, stand up to dilution. So, can we avoid segregation and enlarge the effective intermediate regime by dilution?[4] It comes down to wondering what eq.(B.11) becomes in the semidilute regime. Now there are N_0/g contacts

[4]This point was raised by François Boué during the defence.

per chain, between blobs of g monomers. For two blobs in contact, there are $g^2 p(r=b)$ monomer/monomer contacts, $p(r=b)$ being the probability of contact. In [27, 24], it is shown that

$$p(r) \underset{r\sim 0}{\simeq} \frac{1}{g^{\nu d}} \left(\frac{r}{g^{\nu}}\right)^{\theta_2} \Rightarrow g^2 p(r=b) \simeq g^{2-\nu d-\nu\theta_2} \tag{B.12}$$

where θ_2 is known as the contact exponent, related to the vertex exponents σ_4 and σ_2. Equation (B.11) reads in the fluctuating regime

$$\frac{N_0}{g}\frac{\chi_c}{g^{\chi_s}} = 2 \quad \text{with} \quad \chi_s = \nu d + \nu\theta_2 - 2. \tag{B.13}$$

For $d=3$, this exponent is approximated by $\chi_s \simeq 0.18$ in [23] or in [43], $\chi_s \simeq 0.225$ in [11] or in [42], or $\chi_s \simeq 0.24$ in [38], depending on the Padé approximations used in the renormalization processes. Because

$$\chi N_0 \underset{\chi\simeq\chi_c}{\simeq} g^{1+\chi_s} \gg 1,$$

eq.(B.13) shows that dilution enables to use longer chains. But is the effective intermediate regime enlarged? This regime is given by the relation $\xi \ll q^{-1} \ll R_g$, it is therfore regulated by the ratio $R/\xi \simeq \sqrt{N_0/g}$. In the limit defined by equation (B.13), this ratio scales as

$$\frac{R}{\xi} \simeq \sqrt{\frac{N_0}{g}} \simeq \sqrt{\frac{2}{\chi}} (\chi N_0)^{\frac{\chi_s}{2(1+\chi_s)}} \simeq \sqrt{\frac{2}{\chi}}\, g^{\chi_s/2} \tag{B.14}$$

with $\chi_s/\{2(1+\chi_s)\} \simeq 0.092$ and $\chi_s/2 = 0.1125$ for $\chi_s = 0.225$. It has to be compared to $\sqrt{N_0/g} = \sqrt{2/\chi}$ in mean-field (see eq.(B.11)). Although $\chi N_0 \simeq g^{1+\chi_s} \gg 1$, the weakness of the exponent χ_s shows that dilution does not significantly extend the intermediate regime.

B.4 Scattering Function of a Polymer Mixture: Benoît's Argument.

From the classical RPA relation eq.(1.30), for a system of monodisperse N_0-polymers with a mean concentration of units c_0, taken at zero angle, one finds

$$\frac{1}{S(0)} = \frac{1}{c_0 F_N(0)} + v = \frac{1}{c_0 N_0} + v. \tag{B.15}$$

These equations make think that the scattering function at zero angle may be extended at any angle replacing the polymerization degree by the corresponding intramolecular correlation function. This heuristic argument put forward by H. Benoît enables to find back very quickly the RPA results, notably for polymer binary mixtures. Indeed, following thermodynamics and eq.(B.8), the scattering function taken at zero angle reads

$$\frac{1}{v_0}\,S^{-1}(q=0) = \frac{\partial^2 \Delta \overline{F}_{\rm mix}}{\partial f^2} = \frac{1}{f\,N_{\rm A}} + \frac{1}{(1-f)\,N_{\rm B}} - 2\chi, \tag{B.16}$$

and the extension of this formula gives the RPA result

$$S^{-1}(q) = \frac{1}{f\,c_0\,F_A(q)} + \frac{1}{(1-f)\,c_0\,F_{\rm B}(q)} - 2\chi. \tag{B.17}$$

This formula is one of the basics of neutron scattering experiments. In a mixture of PS/dPS for instance, supposing χ negligible, the species being sufficiently close chemically, one expects a direct measurement of the form factor *via* the formula already mentioned $S(q) \propto f(1-f)F(q)$.

Appendix C

First Corrections to the Statistical Segment.

C.1 First Corrections for Infinite Chains

After having derived the screening of the volume interaction eq.(1.35) in dense systems of polymers with a concentration c_0, Edwards assessed the first order correction to the end-to-end distance in the high molecular weight limit, namely $\lim_{N\to\infty} R_e^2(N)/N$ [25]. He used first order perturbations [48] in order to see the effect of screening, dealing with the one-loop diagrams of Fig.C.1. Here we want to assess the the end-to-end distance of an m-segment in an infinite chain in the framework of Edwards shielding. Because of the very general definition $G_m(q) = \langle e^{-i\mathbf{q}\cdot\mathbf{r_m}}\rangle$, that distance reads

$$\langle r_m^2\rangle = -\nabla_{\mathbf{q}}^2 G_m(q)\big|_{\mathbf{q}=0}\,. \tag{C.1}$$

In many sections, as in chapter 3, many references are made to the clas-

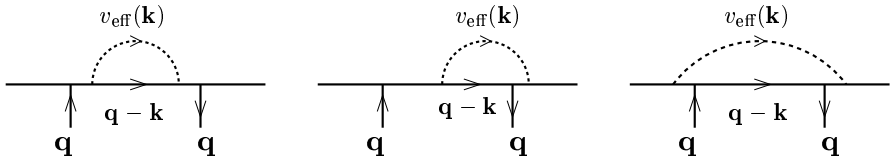

Figure C.1: Non-zero contributions to the first-order perturbations.

sical Edwards renormalization of the statistical segment. This correction comes from the singularity at $i\xi^{-1}$ (large-q). It always appears with the

lowest order in G_z from the top-left diagram. As the Gaussian unperturbed correlation is $G_s^{(0)}(q) = \exp(-q^2 s a^2)$, this diagram reads in fact

$$\delta\langle r_m^2\rangle = \int_0^m ds \int \frac{d\mathbf{q}}{(2\pi)^3} v_{\text{eff}}(q) \left(mb^2 + \nabla_{\mathbf{q}}^2\right) G_m^{(0)}(q)(m-s). \tag{C.2}$$

Operating a Laplace transformation *via* the operator $\mathcal{L}$, one finds

$$\mathcal{L}\delta\langle r_m^2\rangle = \int_{-\infty}^{\infty} dq \frac{1}{2\pi^2} \frac{vq^2}{q^2+\xi^{-2}} \frac{q^4b^4}{9} \frac{1}{\tau^2} \frac{1}{(\tau + q^2b^2/6)^3}. \tag{C.3}$$

It yields, for $m \gg 1$ (or $\tau \ll 1$),

$$\langle r_m^2\rangle = mb^2\left(1 + \frac{12v\xi}{\pi b^4}\right) = mb^2\left(1 + \frac{\sqrt{12}}{\pi} G_z\right) \tag{C.4}$$

defining a new statistical segment $b^* = b(1 + (\sqrt{12}/\pi)\, G_z)^{1/2}$ in dense systems. Nevertheless, eq.(C.3) shows that a size correction, somewhat universal, independent of the interaction, is coming with the same order in all the diagrams from the pole $i\frac{\sqrt{6}}{b}\tau$. Separating the contribution of each diagram with the same order as in Fig.C.1, it yields

$$\begin{aligned}\langle r_m^2\rangle &= mb^2\left(1 + \frac{\sqrt{12}}{\pi} G_z - (45-18-3)\frac{\sqrt{6}}{\pi^{3/2}} \frac{1}{12c_0b^3} \frac{1}{\sqrt{m}}\right) \\ &= mb^2\left(1 + \frac{\sqrt{12}}{\pi} G_z - \frac{2\sqrt{6}}{\pi^{3/2}} \frac{1}{c_0b^3} \frac{1}{\sqrt{m}}\right).\end{aligned} \tag{C.5}$$

putting forward a finite-size effect which scales as the screened interaction summed on the entire chain, $U_{\text{eff}} \sim 1/\sqrt{m}$, because of the perturbative treatment (see section 2.1). It is to mention that if this potential would describe any size-distribution, and especially the monodisperse case[1], the end-to-end distance δR_e^2 would imply only the top-left diagram, and therefore would be more strongly corrected by the term $\propto 45$ in the first line of eq.(C.4), than any internal segment[63, 67].

C.2 Evaluation of the Error due to Polydispersity

The aim of this section is to compare the size effects due to different distributions considered in this thesis. Indeed, the effective potential is explicitly

[1]It is mentioned in chapter 3 that it is not the case.

related to the distribution (see section 1.2.6)

$$\frac{1}{v_{\rm eff}(q)} = \frac{1}{v} + c_0 F_0(q). \tag{C.6}$$

One may wonder how would be the results if the size effects would not have been included in the potential. To have a quantitative idea of the effect of polydispersity, we assessed the end-to-end distance R_e^2 for N-chains and for system of living chains of size $\langle N\rangle$ in a melt. As expressed in eq.(C.2), that correction systematically reads

$$R_e^2 = Nb^2(1 + \frac{12v\xi}{\pi b^4} - \Delta) \qquad \text{with} \qquad \Delta \propto \frac{1}{\sqrt{N}} \tag{C.7}$$

and only Δ depends on the distribution. These calculations were done with the simplified potential

$$v_{\rm eff}(q) \underset{q\xi\ll 1}{\simeq} \frac{1}{c_0 F_0(q)} \tag{C.8}$$

which takes into account the distribution. We discard here the ultraviolet divergence due to eq.(C.8). That divergence corresponds in fact to Edwards renormalization of the statistical segment (and is already taken into account in eq.C.7). For finite monodisperse chains, it yields:

- using the infinite chains potential $v_{\rm eff}(q) = \frac{vq^2a^2}{2c_0}$, our reference Δ_N^0 reads

$$\Delta_N^0 = \frac{15}{4\,\pi^{3/2}}\,\frac{\sqrt{6}}{\sqrt{N}}\,\frac{1}{\phi\, b^3}\ . \tag{C.9}$$

  The index N refers to monodisperse systems (N is fixed). This term is one of the contribution of eq.(C.5) (coming from the top-left diagram of Fig.C.1).

- using the correct potential $v_{\rm eff}(q) = 1/(Nc_0 f_{\rm D}(q^2R_{\rm g}^2))$ with $f_{\rm D}$ the Debye function (see eq.(1.19)), and performing numerically the integration, one finds

$$\Delta_{\rm N}^N \simeq \Delta_N^0(1 - 0.16). \tag{C.10}$$

  Therefore the deviation due to finite-size effects is about 16%. The remarkably slow convergence of that integral at high-q is to be noted.

The same (separated) corrections to the N-averaged $R_{\rm e}$ (different from eq.(3.11)) for living polymers are derived now. It yields:

- using the infinite chains potential

$$\begin{aligned}\Delta_\mu^0 &= \frac{1}{\pi}\sqrt{6}\,\frac{15}{8}\,\frac{1}{\phi\, b^3}\mu^{1/2} \\ &= \frac{1}{\pi}\sqrt{6}\,\frac{15}{8}\,\frac{1}{\phi\, b^3}\,\frac{1}{\sqrt{\langle N\rangle}}\,.\end{aligned} \tag{C.11}$$

- using now the correct potential (from the right correlation function $F^{(0)}(q) = 2/(\mu + q^2a^2)$)

$$\Delta_\mu^\mu = \Delta_\mu^0(1 - \frac{1}{5}). \tag{C.12}$$

  Here the deviation due to finite-size effects on the potential is exactly 20%.

As a consequence, probably each correction assessed without taking into account the distribution (*i.e.* using the infinite chains potential) is approximated by about 20% from the right result.

Other close considerations were pointed out in section 3.2.3, where we wanted to adapt corrections for polydisperse systems to monodisperse ones (*i.e.* using the incorrect potential, but including size-effects). Two technical choices might be adopted to relate these results. The first easy choice was just to substitute $N \leftarrow \langle N\rangle$. The other choice was to perform exactly the Laplace transform which gives back the right distribution as it is done in section 3.2.3. In fact the difference between these two ways is systematic: we always want to transform a $\mu^{1/2}$ correction, therefore it always involves the inverse Laplace transform $\mathcal{L}^{-1}(\frac{1}{\mu^2}\mu^{1/2}) = N(\frac{2}{\sqrt{\pi}}1/\sqrt{N}) \simeq N(1.121/\sqrt{N})$. Thus the difference between these methods, *i.e.* substituting $N = \langle N\rangle$ or performing the inverse Laplace transform is approximately 10%.

To end this discussion, it must be clearly underline that taking into account any finite-size correction on the potential is far better than discarding it. For instance, for the end-to-end distance

$$\frac{1}{N}\mathcal{L}^{-1}\left(\frac{\Delta_\mu^\mu}{\mu^2}\right) = \Delta_N^0(1 - \frac{1}{5}). \tag{C.13}$$

This result is only 4% different from the result Δ_N^N correctly assessed. Therefore that inversion from living to monodisperse polymers (with any method) seems fairly precise.

Appendix D

Diagrams for the Form Factor of an Infinite Chain

D.1 Construction of the Diagrams

We write here the derivation of the three contributions to the perturbation [48] of the correlation function $\delta G_S(q) = G_S(q) - G_S^{(0)}(q) = -\langle U G_S^{(0)}(q)\rangle_0 + \langle U\rangle_0 G_S^{(0)}(q)$ (Fig.3.3). Let us note $\delta^{\mathrm{l}} G_S(q)$ the top-left diagram's amount, $\delta^{\mathrm{m}} G_S(q)$ for the central one and $\delta^{\mathrm{r}} G_S(q)$ for the top-right one. For the top-left diagram, summing on all pairs of the S-segment, as shown in Fig.D.1, the perturbation formula yields[1]

$$\begin{aligned}
\delta^{\mathrm{l}} G_S(q) \equiv G_S(q) &\sum_{s_2=0}^{S} \int \frac{d^3\mathbf{k}}{(2\pi)^3} G_{s_2}(k) \frac{v_{\mathrm{eff}}(\mathbf{k})}{2} \\
&- \sum_{s_2=0}^{S} \sum_{\substack{s_1+s_3 \\ = S-s_2}} \int \frac{d^3\mathbf{k}}{(2\pi)^3} G_{s_1}(q) G_{s_2}(q-k) G_{s_3}(q) \frac{v_{\mathrm{eff}}(\mathbf{k})}{2} \\
= \sum_{s_2=0}^{S} &\int \frac{d^3\mathbf{k}}{(2\pi)^3} (S-s_2) G_S(q) G_{s_2}(k) v_{\mathrm{eff}}(\mathbf{k}) \\
&- \sum_{s_2=0}^{S} \int \frac{d^3\mathbf{k}}{(2\pi)^3} (S-s_2) G_{S-s_2}(q) G_{s_2}(q-k) v_{\mathrm{eff}}(\mathbf{k}).
\end{aligned} \tag{D.1}$$

To exploit the convolutions, we use the Laplace Transforms $\delta G_\tau(q)$ and this

[1] Please note that this type of equation is the starting point of all the corrections to correlations assessed in this thesis.

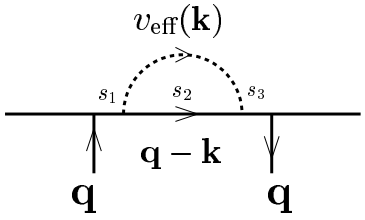

Figure D.1: The segment is divided in 3 parts of s_1, s_2 and s_3 units, verifying $s_1 + s_2 + s_3 = S$.

contribution becomes:

$$\delta^{\mathrm{l}} G_\tau(q) = \int \frac{d^3\mathbf{k}}{(2\pi)^3} \frac{1}{(\tau + q^2a^2)^2} [\frac{1}{\tau + (q^2+k^2)a^2} - \frac{1}{\tau + (q-k)^2a^2}] v_{\text{eff}}(\mathbf{k}). \tag{D.2}$$

In the same way for the other contributions, it yields:

$$\delta^{\mathrm{m}} G_\tau(q) = 2 \cdot \int \frac{d^3\mathbf{k}}{(2\pi)^3} \frac{1}{k^2a^2} \frac{1}{\tau + q^2a^2} [\frac{1}{\tau + (q^2+k^2)a^2} - \frac{1}{\tau + (q-k)^2a^2}] v_{\text{eff}}(\mathbf{k})$$

and

$$\delta^{\mathrm{r}} G_\tau(q) = \int \frac{d^3\mathbf{k}}{(2\pi)^3} \frac{1}{k^4a^4} [\frac{1}{\tau + (q^2+k^2)a^2} - \frac{1}{\tau + (q-k)^2a^2}] v_{\text{eff}}(\mathbf{k}). \tag{D.3}$$

Translational Invariance and Solution

As the chain is infinite, it induces a translational invariance, such that the form factor becomes:

$$F(q) = 2G_{\tau=0}(q) \tag{D.4}$$

So, to get the form factor, equations (D.2) and (D.3) have to be multiplied by the factor 2 (see eq.(D.4)) and to be assessed for $\tau = 0$. They become, because of the parity of the integrands

$$\begin{aligned}
\delta^{\mathrm{l}} G_{\tau=0}(q) &= \frac{v}{4\pi^2 q^4 a^6} \int_{-\infty}^{+\infty} dk \frac{k^4}{k^2 + \xi^{-2}} \left\{ \frac{2}{q^2+k^2} - \frac{1}{2kq} \ln\left(\frac{(q+k)^2}{(q-k)^2}\right) \right\} \\
\delta^{\mathrm{m}} G_{\tau=0}(q) &= \frac{v}{4\pi^2 q^4 a^6} \int_{-\infty}^{+\infty} dk \frac{2q^2k^2}{k^2 + \xi^{-2}} \left\{ \frac{2}{q^2+k^2} - \frac{1}{2kq} \ln\left(\frac{(q+k)^2}{(q-k)^2}\right) \right\} \\
\delta^{\mathrm{r}} G_{\tau=0}(q) &= \frac{v}{4\pi^2 q^4 a^6} \int_{-\infty}^{+\infty} dk \frac{q^4}{k^2 + \xi^{-2}} \left\{ \frac{2}{q^2+k^2} - \frac{1}{2kq} \ln\left(\frac{(q+k)^2}{(q-k)^2}\right) \right\}.
\end{aligned} \tag{D.5}$$

It is possible to solve these integrals in the complex plan, just noticing that there is one pole for $q = i\xi^{-1}$ and the logarithmic branch cut contribution (the circle of module q is the border where $\ln(z) = \ln\left(\frac{(q+k)^2}{(q-k)^2}\right)$ moves to the following Riemann sheet). It is also the limit $\mu \to 0$ of the anchor shaped contour in chapter 3. Observing equations (D.5), it is instant that $\delta^{\mathrm{l}}G_{\tau=0}(q) + \delta^{\mathrm{m}}G_{\tau=0}(q) + \delta^{\mathrm{r}}G_{\tau=0}(q)$ is a perfect square and therefore iq is not a pole. With these contours, one can see easily that:

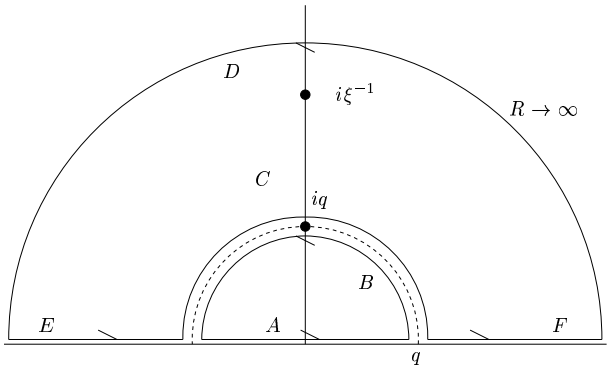

Figure D.2: One of the contour possible to assess the three diagrams. It puts forward the pole at $i\xi^{-1}$ and the logarithmic branch cut.

$$\begin{aligned}\int_{-\infty}^{+\infty} &= \int_E + \int_A + \int_F = \int_E - \int_B + \int_F \\ &= \int_{E+C+F+D} - \int_{B+C} \text{ (with } \int_D \to 0) \\ &= 2\pi i \sum_{q=i\xi^{-1}} \text{Residue} + \text{branch cut contribution}\end{aligned} \tag{D.6}$$

with:

$$\text{branch cut contribution} \equiv \int_0^{\pi} \text{discontinuity}(\theta) d\theta \tag{D.7}$$

Applying this to the first diagram, δ^{l} reads:

- pole $k = i\xi^{-1}$:

$$I_1 = \frac{v}{4\pi q^4 a^6 \xi}\left[\frac{2}{q\xi}\arctan(q\xi) - \frac{2}{1-q^2\xi^2}\right] \tag{D.8}$$

- branch cut contribution:

$$I_2 = -\frac{v\xi^2}{4\pi q a^6}\int_0^\pi d\theta \frac{\exp(4i\theta)}{q^2\xi^2\exp(2i\theta)+1} = 0. \tag{D.9}$$

For the second diagram, δ^{m}, it reads

- pole $k = i\xi^{-1}$:

$$J_1 = \frac{v\xi}{2\pi q^2 a^6}[\frac{2}{1-q^2\xi^2} - \frac{2}{q\xi}\arctan(q\xi)] \tag{D.10}$$

- branch cut contribution:

$$J_2 = -\frac{v\xi^2}{2\pi q a^6}\int_0^\pi d\theta \frac{\exp(2i\theta)}{q^2\xi^2\exp(2i\theta)+1} = 0. \tag{D.11}$$

And for the last diagram, δ^{r}, one finds

- pole $k = i\xi^{-1}$:

$$K_1 = -\frac{v\xi^3}{4\pi a^6}[\frac{2}{1-q^2\xi^2} - \frac{2}{q\xi}\arctan(q\xi)] \tag{D.12}$$

- branch cut contribution:

$$\begin{aligned} K_2 &= -\frac{v\xi^2}{4\pi q a^6}\int_0^\pi d\theta \frac{1}{q^2\xi^2\exp(2i\theta)+1} \\ &= -\frac{v\xi^2}{4qa^6}. \end{aligned} \tag{D.13}$$

The total branch cut contribution is:

$$K_2 = -\frac{v\xi^2}{4qa^6} \tag{D.14}$$

and

$$I_1+J_1+K_1 = \frac{v}{4\pi q^3 a^6}(-q^3\xi^3+2q\xi-\frac{1}{q\xi})(\frac{2}{1-q^2\xi^2}-\frac{2}{q\xi}\arctan(q\xi)). \tag{D.15}$$

As in our problems, ξ is the smallest length scale, we can take the limit $q\xi \ll 1$, this last equation therefore reads

$$I_1 + J_1 + K_1 \underset{q\xi\ll 1}{\approx} -\frac{2v\xi}{3\pi q^2 a^6} \tag{D.16}$$

This is one of the way to derive the form factor given for instance in eq.(3.18)

$$\begin{aligned} F(q) &= \frac{2}{q^2a^2}(1-\frac{v\xi}{3\pi a^4}-\frac{vq\xi^2}{2a^4}) \\ &= F^{(0)}(q)(1-\frac{12v\xi}{\pi b^4}-\frac{9vq\xi^2}{2b^4}) \\ &= F^{(0)}(q)(1-\frac{\sqrt{12}}{\pi}G_{\rm z}-\frac{3}{8}\frac{1}{c_0\,b^3}\,q\,b). \end{aligned} \tag{D.17}$$

One can recognize the Edwards renormalization of the statistical segment (see appendix C). This is a way to derive the form factor given for instance in eq.(3.18). The difference between this two formulas is the factorization of this non relevant renormalization in eq.(3.18) *via* the substitution

$$b^{*2} = b^2\left(1+\frac{\sqrt{12}}{\pi}G_{\rm z}\right) \leftarrow b^2. \tag{D.18}$$

List of Figures

Bibliography

[1] Milton Abramowitz and Irene A. Stegun, *Handbook of mathematical functions*, Dover, New York, 1964.

[2] S. Asakura and F. Oosawa, *Interaction between particles suspended in solutions of macromolecules*, Journal of Polymer Science (1958), 183–192.

[3] D. Ausserré, *Polymer melt confined between two plates*, Journal de Physique France **50** (1989), 3021–3042.

[4] A.R. Khokhlov A.Yu. Grosberg, *Statistical theory of polymeric lyotropic liquid crystals*, Advances in Polymer Science **41** (1981), 53–97.

[5] J. Baschnagel, J. P. Wittmer, and H. Meyer, *Monte Carlo simulation of polymers: coarse-grained models*, Computational Soft Matter: From Synthetic Polymers to Proteins (Jülich) (N. Attig, K. Binder, H. Grubmüller, and K. Kremer, eds.), vol. 23, NIC Series, Jülich, 2004, (available from `http://www.fz-juelich.de/nic-series`), pp. 83–140.

[6] F. S. Bates and G. D. Wignall, *Isotope-induced quantum-phase transitions in the liquid state*, Phys. Rev. Lett. **57** (1986), 1429–1432.

[7] M. Bellour, A. Knaebel, J.-P. Munch, and S.J. Candau, *Scattering properties of salt-free wormlike micellar solutions*, Eur. Phys. J. E **3** (1999), 111–121.

[8] P. Berge, Y. Pomeau, and C. Vidal, *Order within chaos*, Hermann, Paris, 1988.

[9] E. M. Blokhuis and K. I Skau, *Free energy formalism for polymer adsorption*, Journal of Chemical Physics **119** (2003), 3483–3494.

[10] F Boué, M. Nierlich, and L. Leibler, *A convenient neutron scattering method for studying monomer correlations in homopolymer melts*, Polymer **23** (1982), 29–35.

[11] D. Brosetta, L. Leibler, and J.-F. Joanny, *Critical properties of incompatible polymer blends dissolved in a good solvent*, Macromolecules **20** (1987), 1935–1943.

[12] A. Brûlet, F. Boué, and J.P. Cotton, *About the experimental determination of the persistence length of wormlike chains of polystyrene*, Journal de Physuque II **6** (1996), 885–891.

[13] J. W. Cahn, *Critical point wetting*, Journal of Chemical Physics **66** (1977), 492–500.

[14] I. Carmesin and K. Kremer, *The bond fluctuation method: A new effective algorithm for the dynamics of polymers in all spatial dimensions*, Macromolecules **21** (1988), 2819–2823.

[15] M. E. Cates and S. J. Candau, *Statics and dynamics of worm-like surfactant micelles*, J. Phys.: Condens. Matter **2** (1990), 6869–6892.

[16] A. Cavallo, M. Müller, J. P. Wittmer, and A. Johner, *Single chain structure in thin polymer films: corrections to flory's and silberberg s hypotheses*, J. Phys.: Condens. Matter **17** (2005), 1697.

[17] P. M. Chaikin and T. C. Lubensky, *Principles of condensed matter physics*, Cambridge University Press, 1995.

[18] M. Daoud, J. P. Cotton, B. Farnoux, G. Jannink, G. Sarma, H. Benoît, and P. G. de Gennes, *Solutions of flexible polymers: Neutron experiments and interpretation*, Macromolecules **8** (1975), 804–818.

[19] P. G. de Gennes, *Scaling concepts in polymer physics*, Cornell University Press, Ithaca, New York, 1979.

[20] P. G. de Gennes, *Polymer solutions near an interface. 1. adsorption and depletion layers*, Macromolecules **14** (1981), 1637–1644.

[21] P. G. de Gennes, *Polymer solutions near an interface. 2. two plates carrying polymer layers*, Macromolecules **15** (1982), 492–500.

[22] P. G. de Gennes, *Polymers at an interface : a simplified view*, Colloïd Interface Science **27** (1987), 189–209.

[23] J. des Cloizeaux, *Short range correlation between elements of a long polymer in a good solvent*, Journal de Physique **41** (1980), 223–238.

[24] J. des Cloizeaux and G. Jannink, *Polymers in solution : their modelling and structure*, Clarendon Press, 1990.

[25] M. Doi and S. F. Edwards, *The theory of polymer dynamics*, Oxford University Press, 1986.

[26] B. Duplantier, *Geometrical properties of a khunian polymer chain*, J. Stat. Phys. **47** (1986), 1633.

[27] B. Duplantier, *Statistical mechanics of polymer networks of any topology*, Journal of Statistical Physics **54** (1989), 581–680.

[28] S. F. Edwards, *The statistical mechanics of polymers with excluded volume.*, Proc. Phys. Soc. **85** (1965), 613–624.

[29] S. F. Edwards, *The theory of polymer solutions at intermediate concentration*, Proc. Phys. Soc. **88** (1966), 265–280.

[30] E. Eisenriegler, *Polymers near surfaces*, World Scientific Publishing, 1993.

[31] A. V. Ermoshkin and A. N. Semenov, *Interfacial tension in binary polymer mixtures*, Macromolecules **29** (1996), 6294–6300.

[32] P. J. Flory, *Statistical mechanics of chain molecules*, Interscience Publishers, New York, 1969.

[33] M. Fuchs and K. S. Schweizer, *Structure and thermodynamics of colloid-polymer mixtures: A macromolecular approach*, Europhysics Letters **51** (2000), 621–627.

[34] H. Goldstein, *Classical mechanics*, Adisson-Wesley Publishing Company, 1980.

[35] A. Yu Grosberg and A. R. Khokhlov, *Statistical physics of macromolecules*, AIP Press, New York, 1994.

[36] A. Hanke, E. Eisenriegler, and S. Dietrich, *Polymer depletion effects near mesoscopic particles*, Phys. Rev. E **59** (1999), 6853–6878.

[37] J. S. Higgins and H. C. Benoît, *Polymers and neutron scattering*, Oxford University Press, Oxford, 1996.

[38] H.-P. Hsu, W. Nadler, and P. Grassberger, *Scaling of star polymers with 1-80 arms*, Macromolecules **37** (2004), 4658–4663.

[39] C.-C. Huang, H. Xu, F. Crevel, J. Wittmer, and J. P. Ryckaert, *Reaction kinetics of coarse-grained equilibrium polymers: a brownian dynamics study*, 2006.

[40] S. M. Ilett, A. Orrock, W. C. K. Poon, and P. N. Pusey, *Phase behaviour of a model colloid-polymer mixture*, Physical Review E **51** (1995), 804–818.

[41] J. N. Israelachvili, *Intramolecular and surface forces*, Academic Press, 1991.

[42] T. Jian, S. H. Anastasiadis, A. N. Semenov, G. Fytas, K. Adachi, and T. Kotaka, *Dynamics of composition fluctuations in diblock copolymer solutions far from and near to the ordering transition*, Macromolecules **27** (1994), 4762–4773.

[43] J.-F. Joanny, L. Leibler, and R. Ball, *Is chemical mismatch important in polymer solutions?*, J. Chem. Phys. **81** (1984), 4640.

[44] J.-F. Joanny, L. Leibler, and P.G. De Gennes, *Effects of polymer solutions on colloid stability*, Journal of Polymer Science (1979), 1073–1084.

[45] A. Johner, J. Bonet-Avalos, C. C. Van der Linden, A. N. Semenov, and J.-F. Joanny, *Adsorption of neutral polymers: Interpretations of the numerical self-consistent field results*, Macromolecules **29** (1996), 3629–3668.

[46] A. Johner, J.-F. Joanny, and M. Rubinstein, *Chain statistics in absorbed polymer solutions*, Europhysics Letters **22** (1993), 591–596.

[47] A. R. Khoklov and A. N. Semenov, *Liquid-crystalline ordering in the solution of long persistent chains*, Journal of Statistical Physics **38** (1985), 161.

[48] L. D. Landau and I. M. Lifshitz, *Statistical physics*, Pergamon Press, 1959.

[49] C. M. Marques and J.-F. Joanny, *Adsorption of random copolymers*, Macromolecules **23** (1990), 268–276.

[50] E.S. Nikomarov and S.P. Obukhov, *Computational confirmation of scaling predictions for equilibrium polymers*, Sov. Phys. JETP **53** (1981), 328–336.

[51] S. P. Obukhov, *Self organized criticality: Goldstone modes and their interaction*, Physical Review Letters **65** (1990), 1395–1398.

[52] S. P. Obukhov and A. N. Semenov, *Long-range interactions in polymer melts: The anti-casimir effect*, Phys. Rev. Lett. **95** (2005), 038305.

[53] David Pines and P. Nozieres, *The theory of quantum liquids vol.i*, W.A. Benjamin, Inc, New York, 1966.

[54] M. Rawiso, *De l'intensité à la structure en physico-chimie des polymères*, Diffusion de Neutrons aux Petits Angles (F. Nallet J. P. Cotton, ed.), 1999.

[55] M. Rawiso, R. Duplessix, and C. Picot, *Scattering function of polystyrene*, Macromolecules **20** (1987), 630–648.

[56] M. Rubinstein and R. H. Colby, *Polymer physics*, Oxford University Press, 2003.

[57] L. Schäfer, *Excluded volume effects in polymer solutions*, Springer-Verlag, 1999.

[58] L. Schäfer, M. Müller, and K. Binder, *Intra- and interchain correlations in semidilute polymer solutions: Monte carlo simulations and renormalization group results*, Macromolecules **33** (2000), 4568.

[59] M. Schulz, H.L. Frisch, and P. Reineker, *An analytic percus-yevick approach to the rism model of monodisperse, homopolymer melts*, New Journal of Physics **6** (2004), –.

[60] A. N. Semenov, *Theory of long-range interactions*, Journal de Physique II France **6** (1996), 1759–1780.

[61] A. N. Semenov, J. Bonet-Avalos, A. Johner, and J.-F. Joanny, *Adsorption of polymer solutions onto a flat surface*, Macromolecules **29** (1996), 2179–2196.

[62] A. N. Semenov, J.-F. Joanny, and A. Johner, *Polymer adsorption: Mean field theory and ground state dominance approximation*, Theoretical and Mathematical Models in Polymer Research (A. Grosberg, ed.), Academic Press, 1998, pp. 37–81.

[63] A. N. Semenov and A. Johner, *Theoretical notes on dense polymers in two dimensions*, Eur. Phys. J. E **12** (2003), 469.

[64] A. N. Semenov and S. P. Obukhov, *Fluctuation-induced long-range interactions in polymer systems*, J. Phys.: Condens. Matter **17** (2005), S1747.

[65] W. H. Stockmayer, *Problems of the statistical thermodynamics of dilute polymer solutions*, Die Makromolekulare Chemie **35** (1960), 54–74.

[66] J. P. Wittmer et al., -, to be communicated (2006), –.

[67] J. P. Wittmer, H. Meyer, J. Baschnagel, A. Johner, S. P. Obukhov, L. Mattioni, M. Müller, and A. N. Semenov, *Long range bond-bond correlations in dense polymer solutions*, Physical Review Letter **93** (2004), 147801.

[68] J. P. Wittmer, A. Milchev, and M. E. Cates, *Computational confirmation of scaling predictions for equilibrium polymers*, Europhysics Letter **41** (1998), 291–296.

[69] D. T. Wu, G. H. Frederickson, J.-P. Carton, A. Ajdari, and L. Leibler, *Distribution of chain ends at the surface of a polymer melt: Compensation effects and surface tension*, Europhysics Letters **22** (1993), 591–596.

[70] I. Ya. Yerukhimovich, *Divergence of equilibrium molecular weight distribution from the flory distribution due to intra chain interaction*, Vysokomol. soyed. **A19** (1977), 2388–2394.

[71] I. Ya. Yerukhimovich, V. I. Irzhak, and V. G. Rostiashvili, *The concentration dependence of the swelling coefficient of slightly non-gaussian molecules*, Vysokomol. soyed. **A18** (1976), 1470–1476.